β-Carboline as a Privileged Scaffold for Multitarget Strategies in Alzheimer's Disease Therapy

Aurélien Beato, Anthonin Gori, Benjamin Boucherle, Marine Peuchmaur, Romain Haudecoeur

β-Carboline as a Privileged Scaffold for Multitarget Strategies in Alzheimer's Disease Therapy

Aurélien Beato, Anthonin Gori, Benjamin Boucherle, Marine Peuchmaur,* Romain Haudecoeur*

Abstract

The natural β-carboline alkaloids display similarities with neurotransmitters that can be favorably exploited to design bioactive and bioavailable drugs for Alzheimer's Disease (AD) therapy. Several AD targets are currently and intensively being investigated, divided in different hypotheses: mainly the cholinergic, the Amyloid β (Aβ) and the Tau hypotheses. To date, only symptomatic treatments are available involving acetylcholinesterase and NMDA inhibitors. Based on plethoric single-target structure-activity relationship studies, the β-carboline scaffold was identified as a powerful tool for fostering activity and molecular interactions with a wide range of AD-related targets. This knowledge can undoubtedly be used to design multitarget-directed ligands (MTDL), a highly relevant strategy preferred in the context of multifactorial pathology with intricated etiology such as AD. In this review, we first individually discussed the AD targets of the β-carbolines and then we focused on the multitarget strategies dedicated to the deliberate design of new efficient scaffolds.

Introduction

The β-carboline alkaloids represent a large group of natural and synthetic heterocyclic amines derived from tryptophan.[1,2] Probably the most well-studied compounds of this group, harmine **1** and harmaline **2** were originally isolated in the 1840s from the seeds of *Peganum harmala*

L. (Syrian rue), a traditional plant used for various purposes such as an emmenagogue or abortifacient.[3] Since their discovery, numerous β-carboline alkaloids were identified, highlighting the wide distribution of this family mainly in plants but also in animal tissues. These natural products encompass simple β-carbolines and more complex derivatives, such as indoloquinolizidines (*e.g.*, reserpine, mitragynine, yohimbine) and strictosidine- or manzamine-related alkaloids (Figure 1). The β-carboline core is composed of a tricyclic pyrido[3,4-b]indole ring structure, declined in several saturation states: β-carbolines for the unsaturated, fully aromatic scaffold (*e.g.*, harmine **1**); dihydro-β-carbolines (*e.g.*, harmaline **2**) and tetrahydro-β-carbolines or tryptolines (*e.g.*, tetrahydroharmine **3**) for versions with a partially or completely reduced pyridine ring, (the scaffolds are displayed in red, purple and blue, respectively, throughout the review). As such, its structure is reminiscent of human tryptamine-based neurotransmitters, *i.e.* serotonin and melatonin, and this analogy, together with the enhanced rigidity conferred by an additional ring, have been exploited for the design of bioactive compounds for modulating several central nervous system (CNS) targets. Thus, among their broad spectrum of recorded biological activities (*e.g.*, antimicrobial, antitumor, antiviral, antiparasitic properties), synthetic and natural β-carbolines were most often associated with psychopharmacological effects, interacting with a variety of benzodiazepine, serotonin, imidazoline and dopamine receptors, as well as inhibiting brain enzymes. Especially, some β-carbolines were reported as best-in-class inhibitors for several biomolecular targets involved in Alzheimer's diseases (AD), or suspected to play a role.

AD is a chronic neurodegenerative disorder first described by the neuropathologist Alois Alzheimer in 1907, leading to a significant number of deaths. Although mainly occurring in elderly populations, the familial AD can affect younger patients. Clinically, the main cognitive symptoms of AD are progressive short-term memory impairment, disturbances of orientation or neuropsychological disorders (*e.g.*, aphasia, agnosia, apraxis). While the

pathogenesis of AD is still unclear, due to the complex and multifactorial nature of the disease, several hypotheses have been advanced based on pathological or behavioural changes in AD patients.[4–6] Besides the three main hypotheses, namely the cholinergic, amyloid-β (Aβ) and tau protein hypotheses that are regarded as the leading pathological pathways of AD, various other targets have emerged, some of them being interrelated. The cholinergic hypothesis was the first and most studied theory of the disease[4–6] and has led to four out of five anti-AD drugs currently on the market (donepezil, rivastigmine, galantamine and tacrine which are acetylcholinesterase (AChE) inhibitors); the fifth being memantine, a *N*-methyl-D-aspartate receptor (NMDA) inhibitor. This hypothesis is based on the utmost role of the neurotransmitter acetylcholine, its decrease being associated with dementia symptoms. Understandably, research has focused on inhibitors of cholinesterases, serine hydrolase enzymes that can be subdivided into AChE and butyrylcholinesterase (BuChE). The Aβ cascade hypothesis is related to the neurotoxicity and acceleration of the neuronal cell death consecutively to the accumulation of insoluble amyloid plaques.[4,5] These aggregates of Aβ peptides result from the cleavage of the amyloid precursor protein (APP), a transmembrane protein located in neural synapses, by two secretase enzymes, the β-site APP cleaving enzyme 1 (BACE1, or β-secretase) and the γ-secretase. Under normal non-amyloid pathway, APP is sequentially cleaved by α- and γ-secretases leading to soluble and non-toxic APP derivatives. Conversely, β- and γ-secretases cleavage produces among other products an $A\beta_{42}$ monomer derivative (the most neurotoxic form of Aβ) known to accumulate in the extracellular environment, ending in amyloid plaques formation and local inflammatory response. The tau hypothesis pinpoints the hyperphosphorylation of tau protein as one of the main pathological pathway of AD.[4,5] This hyperphosphorylation process is a consequence of both the overactivation of kinases[6] (*e.g.*, mitogen-activated protein kinase (MAPK), cyclin-dependent kinase-5 (CDK-5), glycogen synthase kinase-3β (GSK-3β) or dual specificity tyrosine-

phosphorylation-regulated kinase 1A (DYRK1A)) and the inactivation of protein phosphatase or protein tyrosine phosphatase-A. Apart from these three main theories, AD is also related to other pathological hypotheses[5,6] such as the oxidative stress associated with the search of monoamine oxidases (MAO-A and B) inhibitors or metal chelators, and the excitotoxic theory involving for instance phosphodiesterases (PDE), NMDA and gamma-aminobutyric acid (GABA) receptors.

As the pathogenic mechanisms of AD are thus nebulous and multifactorial, with intricated etiology, current drug discovery researches are moving to multitarget strategies with a view to affect several nodes of the complex neurodegenerative network simultaneously. Different approaches have been described to alter the function of several targets at once, among them the multitarget-directed ligands (MTDL) aimed at hybridize pharmacophoric moieties mostly already known as bioactive molecules.[7–9] In this line, the tacrine and donepezil scaffolds inspired the design of numerous MTDL. The unique place of natural compounds, such as resveratrol or coumarin, in this strategy has also been repeatedly emphasized.

Similarly, the β-carboline scaffold is at the forefront of the targeting of the myriad of biomolecules involved in AD. Harmine (**1**) is a reference inhibitor of MAO-A and tau-phosphorylation kinase DYRK1A. Tadalafil (**8**, Figure 1) has been marketed in 2003 as an excellent (and selective) anti-phosphodiesterase-5 (PDE5) agent. Extended β-carbolines were identified as single-digit nanomolar AChE and histone deacetylase (HDAC) inhibitors, and $GABA_A$ receptor modulators. Therefore, with the emergence of multitarget strategies against AD, the β-carboline scaffold is naturally well-positioned to become a dedicated platform able to concurrently reach a variety of neurological biomolecules and processes.

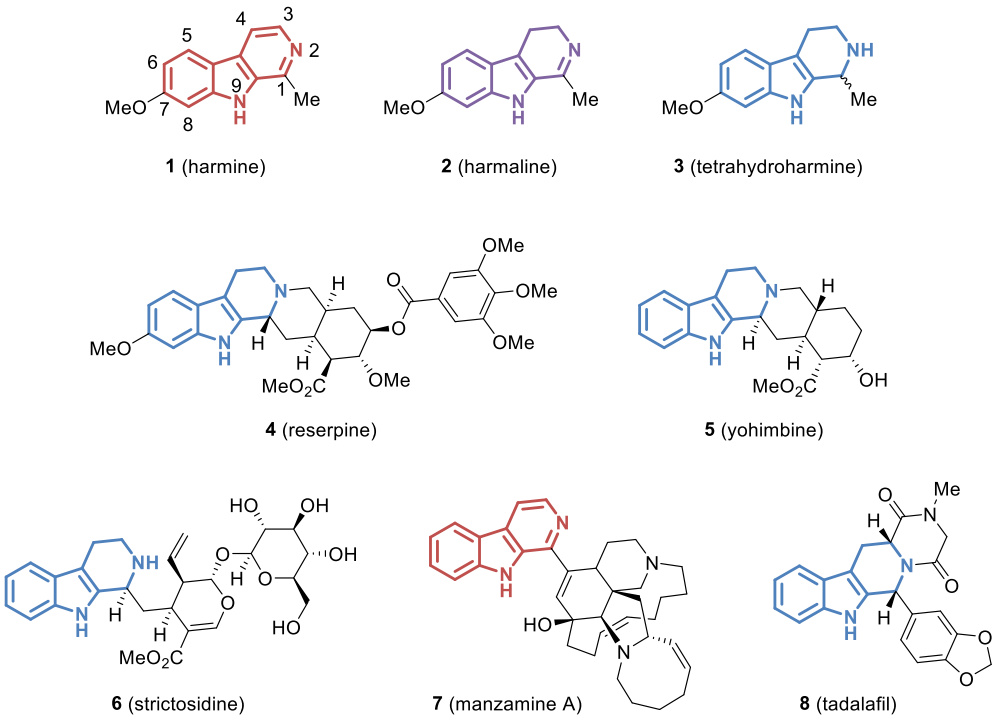

Figure 1. Numbering of the β-carboline scaffold. Structure of representative β-carbolines in various oxidation states (**1**–**3**), and derivatives from natural sources (**4**–**7**) and drug discovery (**8**).

Thus, we present herein an overview of the β-carboline derivatives (with associated structure-activity relationship (SAR) studies) that have been reported for their ability to inhibit or interfere with the main hypotheses, processes and targets in the frame of AD, namely ChE, BACE1, Aβ fibrillation, tau phosphorylation kinases, MAO, PDE5, glutamate, NMDA, $GABA_A$ and 5-hydroxytryptamine (5-HT) receptors, and finally HDAC. After a successive discussion of these targets in individual sections, the last part of the review focuses on multitarget strategies using a β-carboline scaffold deliberately designed for reaching several targets at once, and provides a critical overall analysis of the field together with perspectives for future works.

Acetyl- and butyrylcholinesterase (AChE/BuChE) inhibitors

Acetylcholine, a major neurotransmitter in the CNS, plays a crucial role in the neurological regulation of various functions (*e.g.*, learning, memory, cognition). In AD, its depletion is associated with cognitive deficits, arousing the cholinergic hypothesis in the physiopathology of AD and thus the search for inhibitors of its degrading enzymes, AChE and BuChE. Indeed, some approved drugs (*e.g.*, donepezil and rivastigmin) were put on the market; however, the clinical benefits of these treatments are still low, merely alleviating some of the major symptoms of AD. AChE and BuChE are both present in the brain with different specificities and expression activities. A selective inhibition of AChE is more crucial in the early stage while BuChE inhibition may be critical in the mid to later stages of the pathogenesis. Nevertheless, AChE, whose natural substrate is acetylcholine, remains a primary target; however, BuChE was recently recognized as a new advanced target to treat AD. BuChE is a non-specific cholinesterase able to hydrolyze various types of natural or toxic esters. Both enzymes are serine hydrolases with a catalytic active site (CAS) located at the bottom of a 20 Å gorge, less restrictive in the case of BuChE, compared to AChE, and a peripheral anionic site (PAS) at the entry of that gorge.

Simple β-carbolines and reduced analogues. If the β-carboline scaffold by itself clearly appeared as unable to efficiently bind both AChE and BuChE (IC_{50} >40 µM for **9a**)[10,11] the insertion of simple substituents at various positions only led to moderately active analogues at the micromolar range against both enzymes.[10–22] Indeed, while the introduction of polar groups at position 1 was slightly beneficial in some cases, especially compared with methyl analogues (IC_{50} = 4.0 µM for **10** *vs.* >10 µM for **1**, Figure 2), the 9-substituted β-carbolines looked more promising. In particular, the 9-propargyl moiety produced the best results, regardless of other positions status: despite 1-methyl, 7-methoxy substitutions, harmine-

related compound **11** shared with its naked analogue the same AChE inhibition potency (IC_{50} = 2.0 and 1.9 µM, respectively). However, the introduction of extended or polar substituents at position 9 of compound **11** gave lower activities in all cases. If isoxazoline derivatives were associated with a ten-fold drop of inhibition potency (IC_{50} = 11 µM for the most active analogue **12**),[12] a large series of triazoles and hydrazides was found completely inactive against AChE (IC_{50} >100 µM).[13] Natural β-carbolines bearing a 9-methoxy group were also marginally active.[23] Globally, the functionalization of positions 1 and 7 only provided a limited impact (*e.g.*, IC_{50} >10 µM for **1**, **9a** and **9b**). Attempts to explore substitutions at positions 3, 4 and 6 failed, as the resulting derivatives were found even less potent than their parent compounds. Partial or total reduction of the pyridine ring afforded comparable results. The dihydro-β-carboline **2** especially showed similar inhibition values than its fully oxidized counterpart **1**,[14,15] while 1-hydroxydihydro-β-carboline was mostly inactive.[24] Regarding tetrahydro-β-carbolines, no activity improvement was recorded as well (*e.g.*, IC_{50} >10 µM for **1** and **3**, as well as for **9a** and its reduced counterpart),[14,21] except for enantiopure compound **13** (IC_{50} = 2.5 µM) and for the only 8-substituted analogue, **14**, that reached an IC_{50} of 2.0 µM,[25] making position 8 of β-carbolines a potentially valuable subject for further studies. Examining basic interactions between simple β-carbolines and the active site of AChE provided elements of interest. For example, the planar structure of harmane (**9b**) was found in docking experiments to mainly interact with aromatic residues of the CAS of AChE, especially Trp84 and Phe330.[18] A hydrogen bond would also occur between the indole NH and His440, and overall the interaction pattern reported appeared as quite similar to tacrine (a well-known planar inhibitor) interactions. Globally, the piecemeal BuChE inhibition results gave similar trends than for AChE, disregarding a few exceptions. Several 1-substituted compounds, inactive against AChE, were though tested on BuChE, and if compound **15**, for example, revealed a promising activity (IC_{50} = 1.3 µM), submicromolar 1-naphthyl analogue

16 constituted a real breakthrough in the quest of efficient BuChE inhibitors (IC_{50} = 0.22 µM).[26] Docking studies showed that **16** seemed to bind in a similar fashion than donepezil, a well-known cholinesterase inhibitor. In particular, the position of **16** allowed the formation of a key hydrogen bond between the indole NH and the OH group of Ser198, as well as π–π stacking interactions with Trp231 and His438.

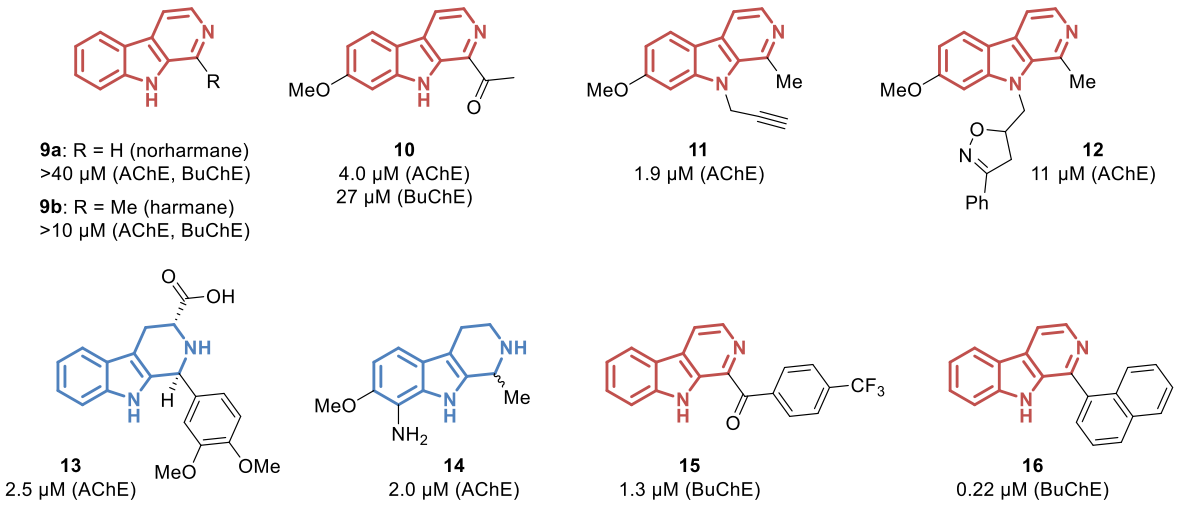

Figure 2. Selected structures and IC_{50} of simple substituted β-carbolines as AChE and/or BuChE inhibitors.

β-Carboliniums and R^2 substituent refinement: towards nanomolar range derivatives. Differences are classically observed in terms of anti-cholinesterase activity between neutral compounds and corresponding ammonium salts. It was often suggested that they could be related to a choline mimic effect, and then several authors focused on developing β-carboliniums for improving β-carboline scaffold affinity. At first glance, the substitution of the pyridine ring at position 2 by a methyl group appeared to yield mixed results for the corresponding pyridiniums. Indeed, if some improvements of activity were recorded, sometimes ten-fold (*e.g.*, IC_{50} >40 µM for **9a** *vs.* around 5 µM for **17**), in other cases the IC_{50} values remained very similar.[10,27] However, when replacing the methyl group by bulkier substituents, more potent compounds were identified, with submicromolar potency. For

example, 2-propylated counterpart of **17** reached an IC_{50} value of 0.85 µM, *vs.* 4.1–6.7 µM for **17** itself.[28] If the ester derivative **18** eventually showed the best activity among simple substituents at position 2 (IC_{50} = 0.25 µM),[29] the phenyl analogues were also very potent (IC_{50} = 0.42–0.76 µM, 0.54 µM for **19** and 0.42 µM for **20**),[30] especially considering the possibilities of further fine-tuned modifications of the phenyl ring. Indeed, Zhou *et al.* generated very recently a systematic catalogue of compounds with various phenyl substitutions in order to determine the most favorable substituent at position 2 of the β-carbolinium scaffold.[30] Among the groups (fluoro, chloro, bromo, iodo, methyl, hydroxyl, methoxy, cyano, etc.) and positions (*ortho*, *meta*, *para*, etc.) evaluated, a few molecules led to inhibition values under 0.30 µM. Compounds **21a** and **21b** (IC_{50} = 0.29 µM and 0.24 µM respectively) especially shed light on the potential beneficial role of a *para* substitution, probably through a steric favorable effect, a feature confirmed by several other comparisons (*e.g.*, IC_{50} = 0.56 µM for **21c** *vs.* >9 µM for *ortho* and *meta* analogues, 0.43 µM for **21d** *vs.* >10 µM for *ortho* and *meta* analogues) and by molecular docking of **21a**, **21e** and their respective *meta* isomers, that showed inappropriate sterical clash with residue Asn87 in the case of *meta* substituents. A disubstituted analogue, **22**, displayed the best value, almost reaching the two-digits nanomolar range (IC_{50} = 0.11 µM). It is worth noting that the aforementioned molecules exhibited a remarkable selectivity between AChE and BuChE, unlike the other compounds described so far. Inhibition values against BuChE were systematically around 100 times higher than against AChE (*e.g.*, IC_{50} = 32–60 µM for **21a**–**e** against BuChE), with a 390-fold difference as the maximum, in the case of a 4'-bromo-2'-fluoro derivative (IC_{50} = 0.30 µM against AChE *vs.* 116 µM against BuChE).[30] Finally, the partial reduction of the pyridine moiety exerted a global detrimental effect on anti-AChE activity (*e.g.*, IC_{50} = 1.5–6.8 µM for **23a**–**c** *vs.* 0.24–0.43 µM for **21a**, **21b** and **21d**). A 100-fold drop was even measured when reducing compound **22** into the 3,4-dihydro counterpart

24 (IC_{50} = 0.11 µM and >10 µM respectively). This phenomenon could be explained by the predicted binding modes of compounds **21a**, **21e** and **23a** in the AChE active sites. In docking experiments, the aromatic core of the β-carbolines was found to be embedded in a group of aromatic residues, such as Trp86, Tyr337, Trp439 and Tyr449. Thus, when partially reducing the pyridine ring, a crucial π–π interaction between this group and the indole ring of Trp86 could be lost, jeopardizing the global affinity of the compounds.[30]

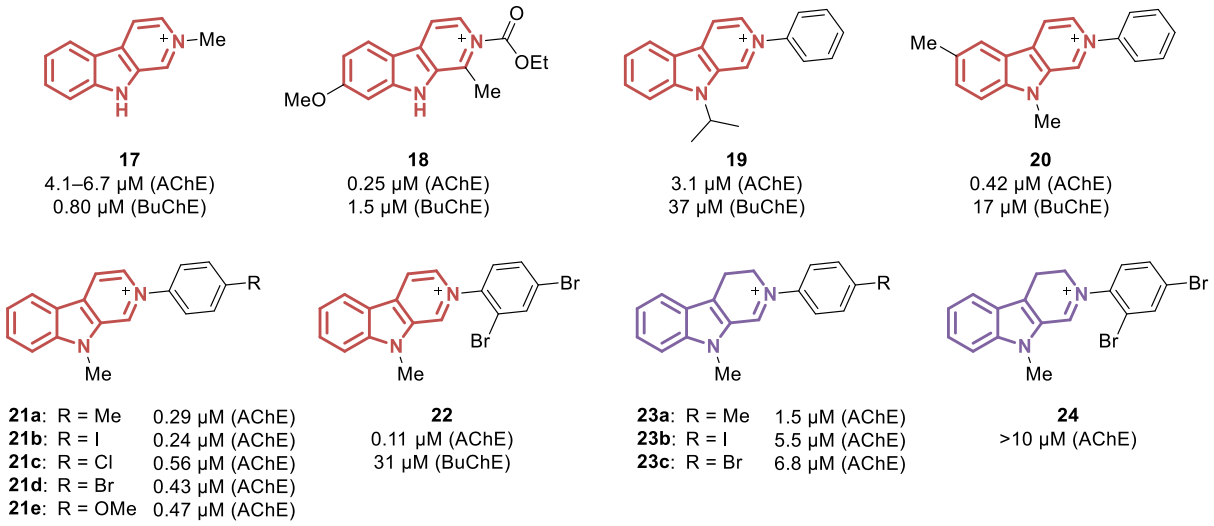

Figure 3. Selected structures and IC_{50} of β-carboliniums as AChE and/or BuChE inhibitors.

Extended β-carbolines and indoquinolizidines: from active natural products to lead molecules. Numerous extensions of the β-carboline scaffold were provided by nature, and especially molecules with an additional fused six-membered ring, namely indoloquinolizidines. Phytochemistry works around these compounds sometimes gave the opportunity to retrieve sporadic data about their AChE and/or BuChE inhibition potency. Overall, most of these compounds were found active only at concentrations >10 µM, but a couple of structural elements were able to decrease the IC_{50} values. Once again, the introduction of a positive charge at the nitrogen atom of the quinolizidine part of these

molecules gave interesting results: the quinolizidinium salt **25** was 30 times more potent against AChE than the neutral counterpart (IC_{50} = 4.1 µM and 121 µM respectively, Figure 4).[31] Surprisingly, limited modifications of **25** also led to more active derivatives: the reduction of ethylenyl group or the introduction of a hydroxyl group yielded analogues with IC_{50} values of 5.2 µM and 10 µM, respectively.[31] Globally, the glycosylated analogue **26** displayed the best potential in this series but eventually remained in the micromolar range (IC_{50} = 1.9 µM).[32] The other disparate compounds did not succeed to improve anti-AChE and anti-BuChE activity, including complex imbricated polycyclic and/or positively charged derivatives.[19,29,33–36] The presence of a fifth fused six-membered ring, common in natural products, appeared as beneficial for anti-AChE and anti-BuChE activities, as witnessed by the good AChE and BuChE inhibition properties of reserpine **4** (IC_{50} = 1.7 µM and 2.8 µM, respectively, Figure 1).[37] Even little substituted analogues reached decent micromolar-range inhibition of BuChE (but not AChE), such as compound **27** (IC_{50} = 1.0 µM).[17] Especially, in docking experiments **27** was found to fit deep in the bottom gorge of BuChE, establishing hydrogen bonds with residues Ser198 and His438, and an anchoring π–π stacking with Trp84 at the choline binding site.[17] Contrariwise, when considering cationic derivatives low micromolar or submicromolar activities against AChE were recorded (*e.g.*, IC_{50} = 0.78 µM and 1.5 µM for **28** and **29**, respectively).[10,38] Compound **29** was predicted to bind in the hydrophobic pocket of the PAS, formed by Phe330, Phe331, Tyr334, Tyr121, with a main π–π interaction between the terminal aromatic ring of **30** and Trp279, mostly matching donepezil interaction pattern.[39] The presence of an additional nitrogen atom at position 14, which was associated with the natural evodiamine subclass of β-carbolines, gave rise to an increased potency in terms of BuChE inhibition, while improving the BuChE *vs.* AChE selectivity of these agents. Indeed, compounds **30** and **31** concomitantly achieved a submicromolar range potency (IC_{50} = 0.5 µM and 0.88 µM respectively against BuChE) and a

4–7-fold better IC_{50} against BuChE *vs.* AChE (IC_{50} = 3.4 µM and 3.0 µM respectively against AChE).[40,41] Extended substitution at position 3 was thus investigated using a carbamate linker and either 5-oxo or 5-deoxo versions of the evodiamine scaffold. Among the twelve analogues reported, all compounds were barely inactive against AChE, especially the 5-oxo derivatives, but some derivatives emerged as good inhibitors of BuChE (IC_{50} = 1.0–4.0 µM). More strikingly, compound **32** revealed a very high potential against BuChE, showing an IC_{50} of 77 nM, the best value found among β-carboline derivatives to date, together with an exquisite BuChE *vs.* AChE selectivity index of more than 130.[41] Finally, the impact of position 3 substitution was further scrutinized using a partially or completely oxidized evodiamine scaffold, without the 14-methyl group (*i.e.*, rutaecarpine scaffold). All the compounds tested, bearing an amido bridge linked to various secondary amines, reached submicromolar potency.[42] Especially, compounds **33** and **34** were associated with IC_{50} of 29 nM and 10 nM against AChE, while being very selective (IC_{50} = 0.84 µM and 5.4 µM against BuChE, respectively), a property rationalized by molecular docking.

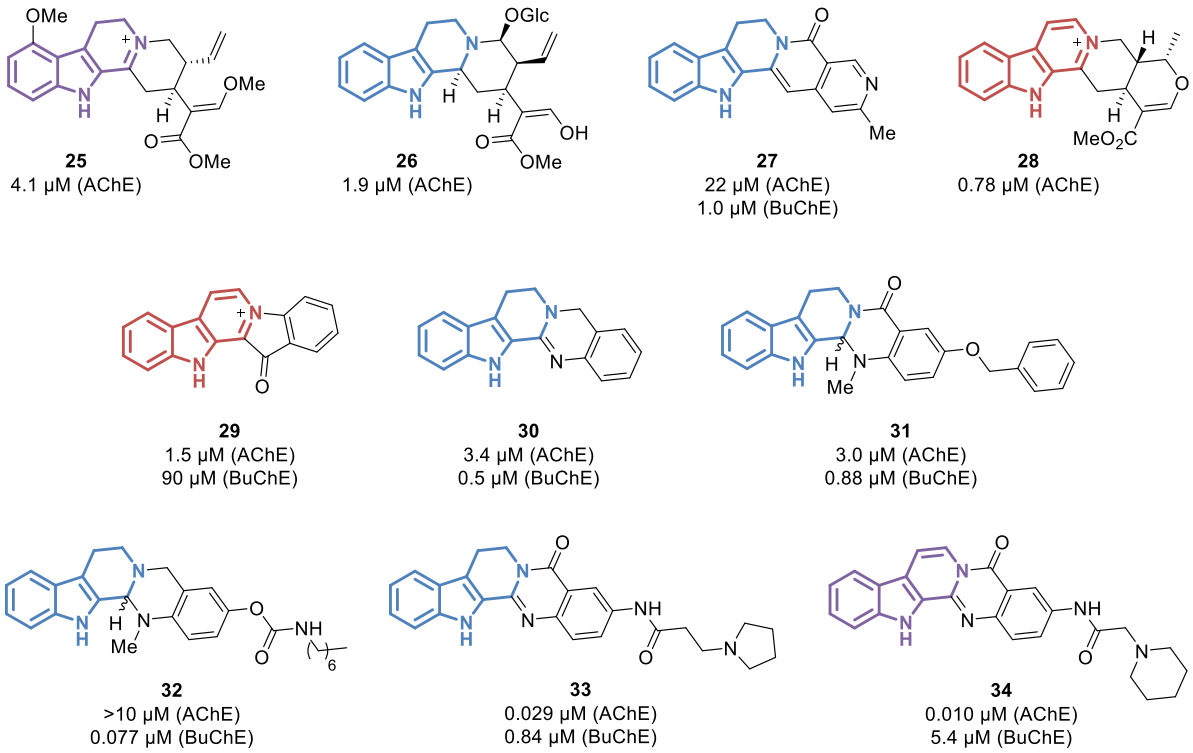

Figure 4. Selected structures and IC_{50} of natural or bioinspired extended β-carbolines as AChE and/or BuChE inhibitors.

Aβ peptide production and fibrillation inhibitors

One of the main hallmarks of AD is the accumulation of neurotoxic aggregates of Aβ peptides that could be self-induced or promoted by AChE and finally deposit in the form of amyloid plaques, with various consequences such as the unbalance of intracellular Ca^{2+} levels leading to apoptosis or neuronal inflammatory response. The Aβ peptides result from the sequential cleavage of APP by β-site APP cleaving enzyme 1 (BACE1), the initial key enzyme in the amyloidogenic metabolic pathway, and γ-secretase. BACE1 is thus considered as a very interesting target for the development of new drugs for AD treatment. Many forms of Aβ have been previously described such as monomers, soluble oligomers and fibrils with different levels of toxicity. During the aggregation process, Aβ fibrils entrap electrochemically active metal ions, mainly Cu and Zn ions, that can generate reactive oxygen species (ROS). Metal-

ion chelators are therefore another research focus within the context of the Aβ cascade hypothesis to reduce the aggregation of Aβ fibrils and thus the generation of ROS. Accordingly, Aβ aggregation and BACE1 inhibitors, metal chelation and radical scavenging are all attractive approaches that can be independently or simultaneously targeted to disrupt the formation of amyloid peptides and/or plaques.

Structual elements for BACE1 inhibition. Regarding β-carbolines, after virtual screening studies of the Thai medicinal database, the natural product ochrolifuanine E **35** was identified as a BACE1 inhibitor with good predicted pharmacokinetic properties, including blood-brain barrier (BBB) crossing level, but a quite high toxicity.[43] In line with docking studies, (*S*)-3-(azidomethyl)-2,3,4,9-tetrahydro-1*H*-pyrido[3,4-*b*]indole was chemically modulated and, among the twenty-two synthesized compounds, **36** showed the most potent inhibitory activity on BACE1 (IC_{50} = 1.5 µM, Figure 5). The binding mode of **36** highlighted hydrogen bonding interactions between the two polar hydrogen of the β-carboline core and residues Asp32 and Asp228 of BACE1. The introduction of more polar, bulkier or halogenated substituents generally led to less active compounds.

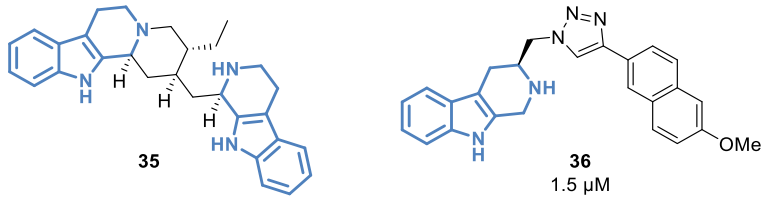

Figure 5. Selected structures and IC_{50} of β-carbolines as BACE1 inhibitors.

Inhibition of Aβ fibrillation and/or oligomerization. Among others, compounds **16** (Figure 2) and **37**, which are BuChE inhibitors, were evaluated at 100 µM for their ability to prevent the formation of Aβ fibrils and soluble Aβ oligomers, described as the more neurotoxic form of Aβ peptides (39% and 58% respectively for **16**, 34% and 82% for **37**).[26] Unlike previous

studies suggesting that a compound is either a fibril or an oligomer inhibitor, compound **16** is able to inhibit both forms. Some other natural β-carbolines, mainly vinpocetine and reserpine **4** (Figure 1), have been reported in piecemeal studies to have neuroprotective effects linked to Aβ aggregation and/or toxicity.[37,44,45] After identification of the marine fascaplysin **29** (Figure 4) as an Aβ fibrillization inhibitor, the synthetic 9-methyl derivative **38**, originally designed as an AChE inhibitor, was recognized as a more potent analogue able to directly interact with Aβ through ionic interactions with the negatively charged residues of Aβ. Finally, 9-methylfascaplysin not only inhibited the formation of Aβ fibrillization but also prevented the formation of Aβ oligomers *in vitro*.[46] Natural β-carbolines isolated from *Picrasma quassioides* were also evaluated for their inhibitory effect on $A\beta_{42}$ aggregation, and the most active compound **39b**, a racemic bis-β-carboline, showed an IC_{50} value of 10 μM, whereas the *N*-unsubstituted analogue **39a** and other isolated monomeric β-carbolines were inactive or marginally active.[23,47]

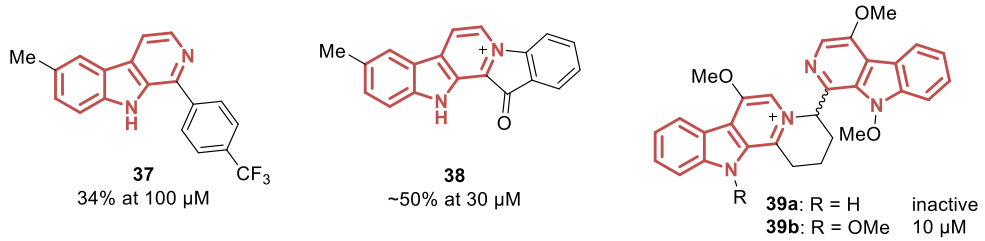

Figure 6. Selected structures, IC_{50} and aggregation inhibition percentages of β-carbolines as Aβ aggregation inhibitors.

Tau phosphorylation kinases inhibitors (GSK-3β, DYRK1A, CDK5, CK1/2, CLK1)

Tau is a hydrophilic microtubule-associated protein that plays an important role in the assembly and stability of microtubules and, therefore, in the normal brain function. In AD, tau is abnormally hyperphosphorylated, resulting in conformational changes and ultimately in the formation of neurofibrillary tangles (NFTs), highly disruptive and toxic intracellular aggregates that deposit in the brain, leading to neuronal dysfunction and death. To prevent the formation of NFTs, considered as the second main marker of Alzheimer's disease, kinase inhibitors were identified or designed. Thus, several studies were dedicated to the inhibition of tau phosphorylation kinases, which mostly belong to the CMGC kinase group, namely GSK-3β, DYRK1A, CDK5, casein kinases 1 and 2 (CK1/2) and dual specificity protein kinase (CLK1), among other minor contributions.[48] Especially, harmine **1** was found as one of the most active inhibitors of DYRK1A (IC_{50} = 22–130 nM, Figure 1), while analogues norharmane **9a** and harmane **9b** were mostly inactive (IC_{50} >1.8 µM, Figure 2).[49–57] However, upon fixing a hydroxy or methoxy group at position 7, some room at position 9 seems to be available for receiving substituents of various sizes, as witnessed by the good potencies of compounds **40** and **41a**–**c** (IC_{50} = 35–59 nM), **41d** being the most promising member of the series (IC_{50} = 25 nM, Figure 7).[49,57–61] Only the presence of a 9-carboxylic acid moiety compromised significantly the activity (IC_{50} = 1.1 µM). Further variations at position 7 revealed a general drop of activity upon methoxy replacement, except for the methyl ester **42a** (IC_{50} = 27 nM, *vs.* 2.0–9.8 µM for **42b–d**). Position 1 was finally modulated by the introduction of substituents of various sizes, with only little impact on the anti-DYRK1A effect (IC_{50} = 56–110 nM for **43a–c**). Contrariwise, the partial reduction of harmine has proved to be unsuccessful (**2**, IC_{50} = 4.6–9.0 µM).[49,50] Some of these elements were rationalized by the publication of three crystal structures of β-carboline–DYRK1A complexes with compounds **1**, **41d** and **44** (PDB code 3ANR, 6UWY and 4YU2, respectively, Figure 8A–C).[61–63] The harmine **1** flat structure was found encased in the catalytic site between several hydrophobic residues, such as Ala186, Val173, Phe238, Val306, Leu294 and Leu241, establishing hydrogen bond anchors with the main chain of Leu241 and with the side chain amino group of Lys188. As observed previously, free space occurred around position 9 of harmine **1**, and the structures of **41d**–DYRK1A and **44**–DYRK1A complexes confirmed the possibility of introducing bulky groups without causing major steric clashes. The hydrogen bond set up by the 7-methoxy group could explain the inability of naked counterparts **9a** and **9b** to exert any significant effect against the enzyme. Interestingly, harmine **1** was described as partially kinase-selective (

Table 1).[49–57,64,65] Especially, when considering Alzheimer's disease-related kinases, it was found active against DYRK1A and CLK1 (IC_{50} = 22–350 nM and 26–220 nM respectively), but not against CDK5 and CK1/2 (IC_{50} >1.5 µM). Its activity against GSK-3β, on the other hand, was discordant from study to study (IC_{50} = 0.35–10 µM). Another β-carboline-based series of pyrrolo[3',4':5,6]indolizino[8,7-*b*]indole-1,3(2*H*,8*H*)-diones, derived from the natural alkaloid granulatimide, was tested against these same five kinases.[66] Among them, the 7-hydroxy derivative **45** was of particular interest, as it afforded submicromolar values for both CLK1, DYRK1A and GSK-3β (IC_{50} = 0.26 µM, 0.20 µM and 0.42 µM respectively). Other β-carbolines have been developed as dedicated inhibitors of GSK-3β and CDK5, but with poor outputs. However, compound **46** was recently associated with interesting CLK1 inhibition properties (K_i = 0.14 µM) and with exquisite kinase selectivity (IC_{50} >10 µM against a range of ~50 kinases), making it an excellent candidate in the AD context. The crystal structure of a **46**–CLK1 complex (PDB code 6YTG, Figure 8D) revealed a non-canonical binding mode in the active site and the formation of multiple hydrogen bonds between the spiro piperidine moiety, the nitrile group, and residues Lys191, Asp325 and possibly Asn293. In addition, an unusual halogen bond was seen between the 7-chloro group of **46** and residue Glu242. A series of manzamine A (**7**, Figure 1) derivatives have also been provided as potential inhibitors of GSK-3β.[67] Regardless of the modifications made at the indole ring (introduction of hydroxy, ethoxy or arylsulfonyl groups) or at the macrocyclic part (dehydration, insertion of a carbonyl group), the recorded levels of activity remained in all cases marginal (IC_{50} = 5.4–25 µM), the best inhibitor being **47** (IC_{50} = 4.8 µM). Finally, a series of β-carbolines was designed and evaluated against CDK5. The inhibition results remained very modest and did not deliver values below 5 µM (IC_{50} = 5.0 µM for **48**).[68]

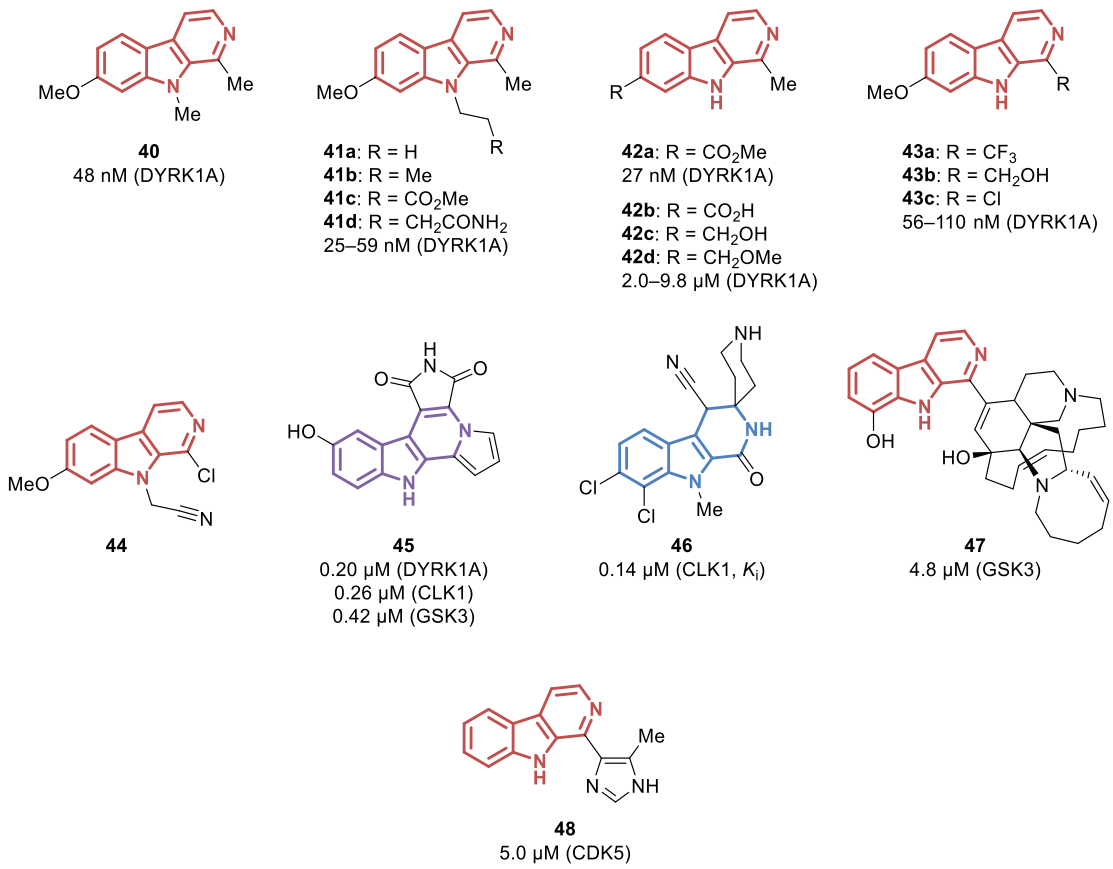

Figure 7. Selected structures of β-carbolines as inhibitors of tau phosphorylation kinases.

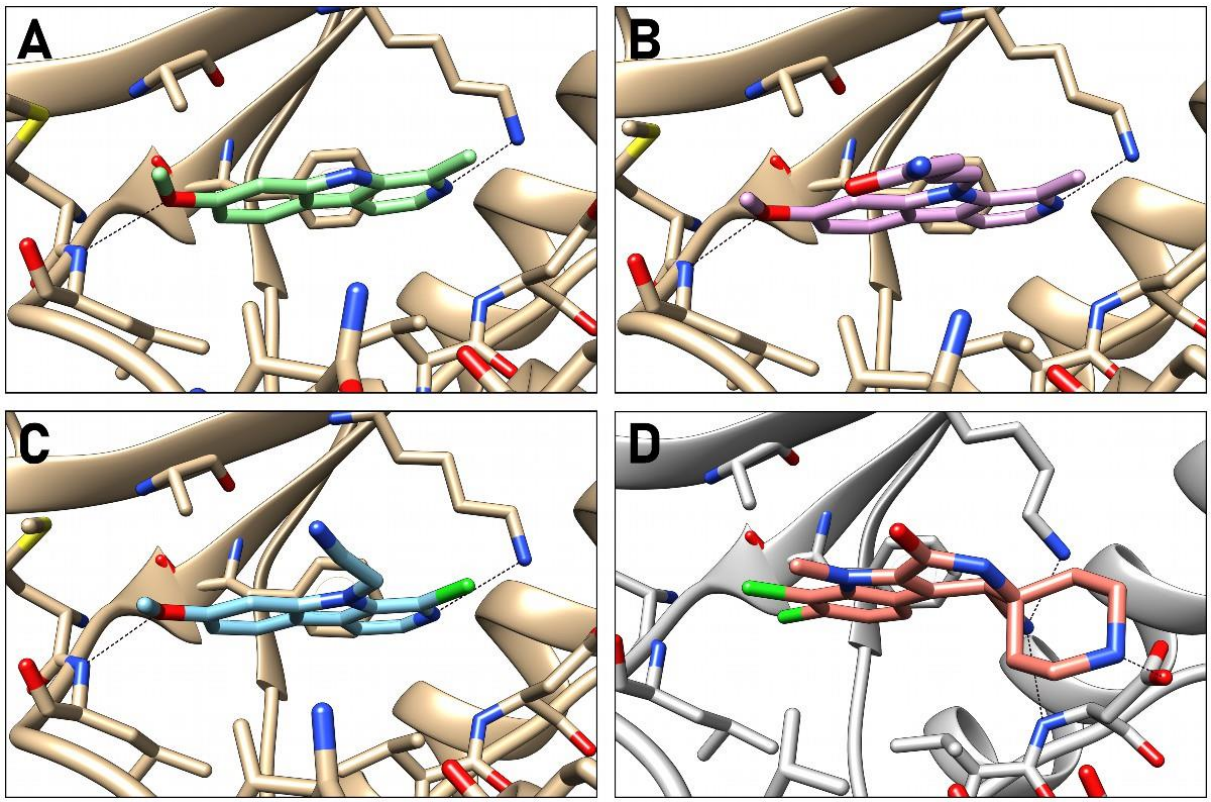

Figure 8. (A) Crystal structure of **1** (in green) bound to DYRK1A (PDB code 3ANR). (B) Crystal structure of **41d** (in mauve) bound to DYRK1A (PDB code 6UWY). (C) Crystal structure of **44** (in blue) bound to DYRK1A (PDB code 4YU2). (D) Crystal structure of **46** (in pink) bound to CLK1 (PDB code 6YTG).

Table 1. IC_{50} Values Obtained for Harmine (1) Against a Panel of Kinases. In Bold, the Main AD-Related Kinases.

Kinase	IC_{50} (µM)	Kinase	IC_{50} (µM)
CDK1	17–18	DYRK2	0.12–3.0
CDK2	33	DYRK3	0.21–0.80
CDK5	8.0–21	DYRK4	9.5–80
CDK7	>10	ERK2	>30
CDK9	0.72	FYN	>250
CK1	1.5–1.8	**GSK-3β**	0.35–10
CK2	>40	LCK	>250
CLK1	0.026–0.22	LYN	>250
CLK2	0.12–0.28	MNB	0.15
CLK3	3.0–10	PIM1	>10
CLK4	0.024–0.050	PIM3	4.3
DYRK1A	0.022–0.35	PKA	>250
DYRK1B	0.028–0.26	PKC	>250

Monoamine oxidases (MAO-A/B) inhibitors

MAO, which are mitochondrial-associated enzymes, selectively catalyze the degradation of various monoamines including oxidation of amine neurotransmitters such as 5-HT, dopamine, norepinephrine or epinephrine. Studies have recently reported high levels of MAO activity in AD patients and promising results were achieved using MAO inhibitors to improve cognitive ability. Indeed, in AD, activated MAO participate to the neurodegenerative processes both through the increase of hydrogen peroxide and thus oxidative stress and *via* indirect production of amyloid β peptide in neurons, *via* the γ-secretase. Selective MAO-B inhibitors are preferred to avoid antidepressant effects and hypersensitive reactions mediated by the inhibition of MAO-A. Selective MAO-A inhibitors are more classically used to treat depression and anxiety by providing emotional stability while MAO-B inhibitors are used in treatment of neurological disease to decrease the production of neurotoxic compounds to enhance the neuronal survival.

Harmane (**9b**, Figure 2) and other β-carbolines are well-known as MAO inhibitors, as they constitute natural key ingredients responsible for the lower MAO activity observed in smokers and coffee consumers, resulting in a neuroprotective effect widely documented.[69,70] Indeed, **9b** was associated in several studies with a submicromolar MAO-A inhibition potential (IC_{50} = 29–340 nM).[33,70–73] The analogous harmine (**1**, Figure 1) was even more potent, showing single-digit nanomolar inhibition values (IC_{50} = 1.0–5.3 nM), and more efficacy, although still moderate, against MAO-B.[60,72–75] As a high-resolution structure of a **1**–MAO-A complex was elucidated by crystallography (PDB code 2Z5X), the structural elements that rule the high inhibition potency are well known (Figure 10A).[76] Harmine is located at the active site, interacting with residues Tyr69, Asn181, Phe208, Val210, Gln215,

Cys323, Ile325, Ile335, Leu337, Phe352, Tyr407, and Tyr444, and with the cofactor flavin adenine dinucleotide (FAD). A reported π–π interaction between Gln215 and the five-membered ring of harmine (3.4 Å), together with a water-bridged hydrogen bond network involving the two nitrogen atoms of the β-carboline structure and Tyr69, Asn181 and Gln215 seems to be an important component of the interaction pattern. An overlay of the complex with a MAO-B structure (PDB 1OJ9)[77] reveals a major steric clash, as Ile335 is replaced by Tyr326 (black arrow in Figure 10B), and Asn181 becomes Cys172 that no longer allows the formation of a water-bridged hydrogen bond. These elements could explain the significant drop in harmine activity when considering MAO-B inhibition. Unsurprisingly, most of the anti-MAO-A modulation efforts were thus achieved based on the harmine structure. Introducing various substituents at position 9 always resulted in a loss of anti-MAO-A activity, and the potency even weakened as the substituent size increased (IC_{50} = 11 nM for **40** *vs.* 0.74 µM and >10 µM for *iso*-propyl and benzyl analogues).[60] If attempts to replace the 7-methoxy group by carbon-based substituents mostly failed (even if **42c** and **42d** still reached decent inhibition values, IC_{50} = 40 nM and 30 nM respectively, Figure 7), the introduction of other 7-alkoxy groups provided derivatives with MAO-A inhibition similar to the parent compound (IC_{50} <5.0 nM for **49a**–**49e**).[78] In addition, compound **49d** was notably able to inhibit MAO-B activity one hundred-times more efficiently than harmine (IC_{50} = 0.22 µM *vs.* 20 µM). At the other side of harmine, the diversification of position 1 was unsuccessful, IC_{50} values against MAO-A systematically rising above 1 µM.[60] All these observations are consistent with the crystal structure of MAO-A, since position 7 clearly appears as the most tolerant to steric hindrance and especially carbon chains, while positions 1 and 9 are already in close contact with adjacent residues. These elements were confirmed by the limited potential of 9-substituted 7-triazolylmethoxy derivatives reported recently.[75] In all cases, as expected, the functionalization of position 9, with phenylpropyl, propyl, butyl or

isobutyl groups, led to derivatives with IC_{50} values against MAO-A of at least 0.43 µM (IC_{50} = 0.43 µM for **50b**), with sometimes interesting action on MAO-B however (*e.g.*, IC_{50} = 0.26 µM for **50a**). The partial reduction of harmine **1**, leading to 3,4-dihydro analogue **2**, afforded retained MAO-A inhibition potency (IC_{50} = 2.5–8.0 nM).[72–74,79] Total reduction of the pyridine ring to give compound **3**, as well as reduction of differently substituted β-carbolines (1-H, 7-OMe, 6-OH, 7-OH) inexorably produced less active molecules, with no specific action on MAO-B as well.[72,73,80–82] Methyl-pyridinium derivatives of harmine and harmaline were also significantly less active on MAO-A (K_i = 69 nM for **51** *vs.* IC_{50} = 1.0–5.3 nM for **1**, and K_i = 140 nM for **52** *vs.* IC_{50} = 2.5–8.0 nM for **2**), as were all the other 2-methyl cationic analogues.[83] Finally, several natural derivatives with more complex structures were tested against MAO-A and MAO-B, but with only limited success.[33,74] If compounds **53** and **54** reached IC_{50} of 0.87 µM and 0.85 µM against MAO-A, the other molecules only yielded values above 1 µM.

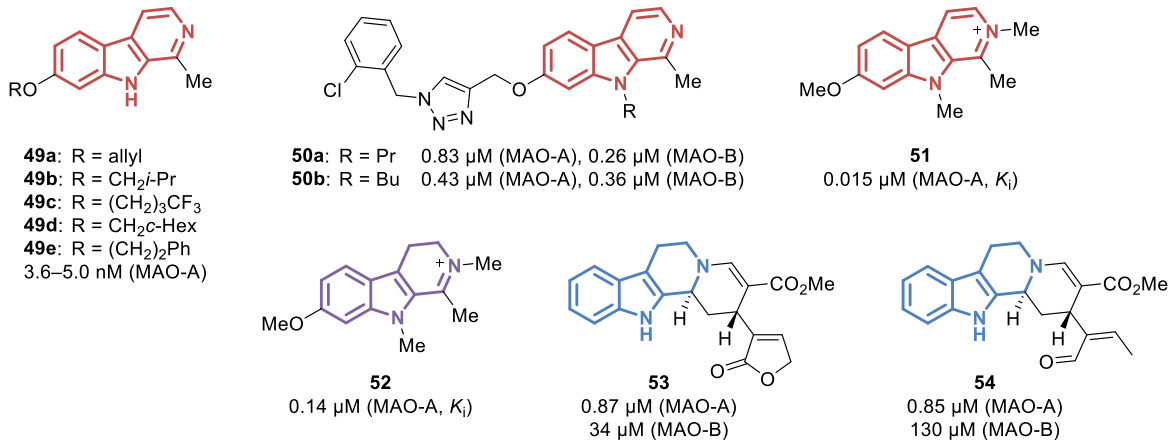

Figure 9. Selected structures and IC_{50} (or K_i where indicated) of β-carbolines as MAO-A/B inhibitors.

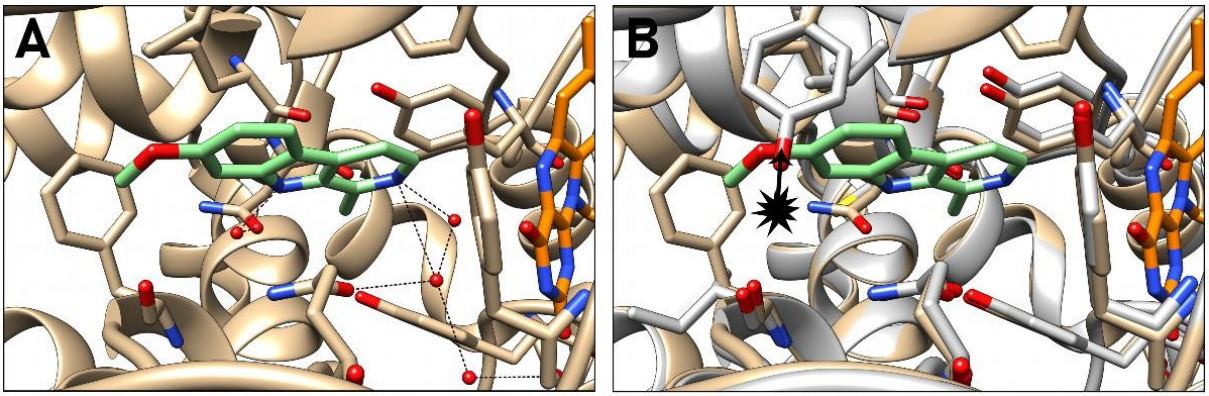

Figure 10. (A) Crystal structure of **1** (in green) bound to MAO-A (PDB code 2Z5X). (B) Overlay of crystal structures of **1** (in green) bound to MAO-A (in gold, PDB code 2Z5X) and of MAO-B (in silver, PDB code 1OJ9). In orange, the FAD cofactor.

Phosphodiesterase type 5 (PDE5) inhibitors

Considering the failing development of effective treatments for AD, focus on other promising strategies highlighted new targets such as PDE. The classification of these enzymes in eleven families, each comprising multiple isoforms and splice variants, mainly relies on their substrate specificity: cyclic adenosine monophosphate (cAMP) and/or cyclic guanosine monophosphate (cGMP). These second messengers, respectively arising from ATP or GTP, are important elements in intraneuronal signal transduction cascades. By elevating cyclic nucleotide levels, PDE inhibitors promote gene transcription *via* the activation of the cAMP response element-binding (CREB), that regulates in turn the expression of genes involved in long-term memory formation.[84,85] Indeed, the natural β-carboline vinpocetine inhibits PDE1 and shows beneficial effects on memory function in rats.[86] To the best of our knowledge vinpocetine is the only β-carboline described to inhibit PDE1, a dual substrate enzyme able to hydrolyze both cAMP and cGMP. There are few studies of β-carboline on PDE targets other than PDE5. Some β-carbolines inhibiting PDE4 were identified[87] but, so far, preclinical studies led on PDE4 inhibitors were hampered by aversive side effects, mainly emesis,

because of the lack of selectivity on the four different gene products (PDE4A–D).[85] On the other hand, several FDA-approved drugs, including the β-carboline tadalafil, inhibit PDE5, a cGMP-specific enzyme, for the treatment of male erectile dysfunction. Incidentally, clinical studies have revealed the potential of these inhibitors to enhance memory and cognitive functions strengthening the relevance of this target.[88]

1-Aryl dihydro-β-carbolines and influence of the R^2 substituent. Several series of simple reduced tricyclic 1-aryl β-carbolines without substitution of the nitrogen at position 2 were evaluated.[89–92] These compounds were mostly inactive or active at the micromolar range. Especially, the substitution of the 1-aryl group showed a limited impact on PDE5 inhibition potency: considering derivatives with 1*R*,3*S* configuration, the replacement of the 4'-bromophenyl group of **55** (IC_{50} = 3.1 µM, Figure 11) with 4'-bromo or 2',4'-dimethoxy analogues provided activities in a similar order of magnitude (IC_{50} = 4.2 µM, and 6.4 µM, respectively). However, the absolute configuration of carbon 1 was more discriminating, as only 1*R*,3*S* and 1*R*,3*R* β-carbolines were found active. The importance of a *R* configuration at carbon 1 was illustrated by the evaluation of the four diastereoisomers of the 1-(2-bromo)aryl analogues, leading to an activity in the case of **55** and its 1*R*,3*R* counterpart (IC_{50} = 3.1 µM and 5.6 µM respectively), whereas no activity was recorded for the two remaining stereoisomers. The same trend was observed for 1-aryl derivatives bearing different phenyl substituents. The thiophenyl analogue was found inactive however.[93] If the substitution of position 2 by a chloroacetyl moiety did generally not improve the potency of the naked analogues (*e.g.*, IC_{50} = 2.7 µM for compound **56**), the introduction of more complex groups at this position produced two main series of more valuable derivatives. In the first series, phenyl-furoyl β-carbolines were evaluated as racemic mixtures, with a 3,4-methylenedioxyphenyl group as the 1-substituent, and all compounds showed anti-PDE5 activity at a submicromolar range.[94] One compound especially yielded a K_i value below 100

nM (K_i = 78 nM for **57a**). A further expansion of substituents of the phenyl-furoyl group provided beneficial effects, when compared with shorter analogues, *e.g.*, **57c** *vs.* **57b** (K_i = 64 nM *vs.* 120 nM), or **58b** *vs.* **58a** (K_i = 51 nM *vs.* 180 nM). The introduction of a piperidyl substituent at the phenyl-furoyl group and the simultaneous replacement of an oxygen atom from the 3,4-methylenedioxy moiety by a carbon provided compound **59**, which showed the best activity of the series (IC_{50} = 8 nM). On the other hand, the reduction of the amido linker was found detrimental. It is worth noting that the evaluation of separated enantiomers of a representative compound confirmed that only the 1*R* configuration enabled PDE5 inhibition, as the 1*R* derivative **60** was found at least 150 times more active than the 1*S* analogue (IC_{50} = 67 nM and >10 µM respectively). Similar results were obtained from the second series, using a pyrimidine ring as a linker between the β-carbolines and the remote phenyl groups, at position 2 (e.g., K_i = 63 nM for compound **61**).[94] Again, the removal of an oxygen atom from the 3,4-methylenedioxyphenyl group at position 1 led to the most active derivative **62**, a dipyridine analogue with a K_i of 4 nM. As the compound was tested as a racemic mixture, it could be supposed that the actual potency of the 1*R* enantiomer is even higher. Among the other modifications tested, the introduction of a carbonyl group at position 4 of the β-carboline scaffold afforded a beneficial result (K_i = 9 nM for **63** *vs.* 63 nM for **61**), while its reduction in the hydroxy counterpart was unfavorable (K_i >100 nM). A replacement of the 3,4-methylenedioxyphenyl group by a 3,4-dimethoxyphenyl substituent also led to a critical drop of anti-PDE5 activity. Interestingly, the alternative use of the rutaecarpine scaffold for anti-PDE5 activity also produces one compound with IC_{50} below 100 nM, compound **64** (IC_{50} = 86 nM), while all other derivatives were found less active.[95]

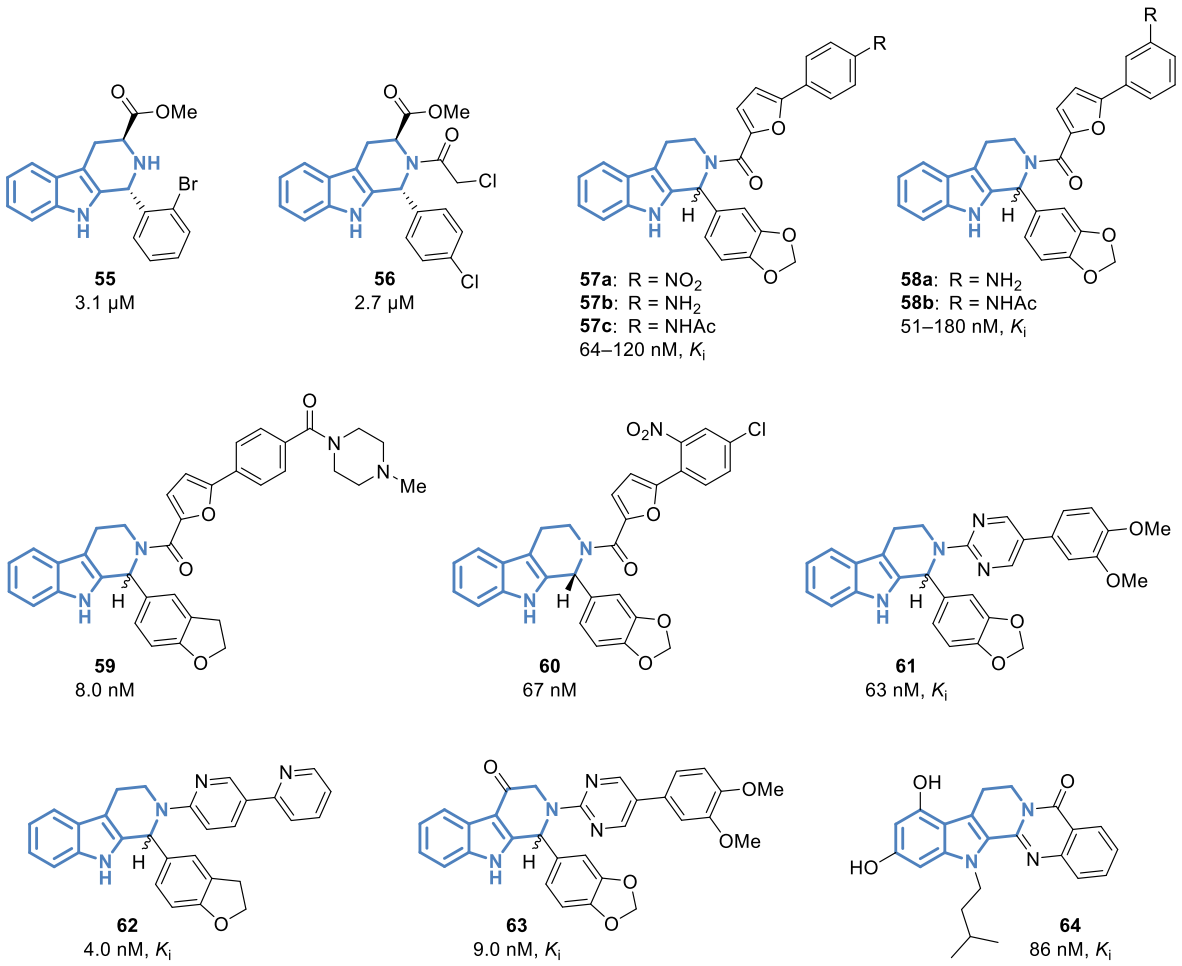

Figure 11. Selected structures and IC_{50} (or K_i where indicated) of 1-aryl dihydro-β-carbolines as PDE5 inhibitors.

β-Carbolines with a fused hydantoin ring. Starting from the β-carboline scaffold itself, GlaxoSmithKline performed a substructure search in their internal database to find more potent PDE5 inhibitors, and a fused β-carboline–hydantoin analogue was identified as promising, with a good recorded selectivity.[96] Thus, they sought to produce numerous derivatives associated with different modulation points. First, from a stereochemistry point of view, a high number of fused β-carboline–hydantoin racemic mixtures did not allow an easy discrimination between *trans* and *cis* forms, showing similar good activities in almost all cases (*e.g.*, IC_{50} = 10 nM for *cis*-**65a** *vs.* 7 nM for *trans*-**65a**, 8 nM for *cis*-**65b** *vs.* 5 nM for

trans-**65b**, 7 nM for *cis*-**65c** *vs.* 3 nM for *trans*-**65c**, Figure 12). Contrariwise, as already observed in the 1-aryl β-carboline series, the *R* configuration (corresponding to the *S* configuration for sulfur-containing compound **68**) of carbon 5, which is the counterpart of carbon 1 in the previous series, appeared as a determinant feature for reaching maximum potency (*e.g.*, IC_{50} = 330 nM for **66** *vs.* no activity for the 5-*S* isomer, 38 nM for **67** *vs.* 640 nM for the 5-*S* isomer, 170 nM for **68** *vs.* no activity for the 5-*R* isomer).[90,92,93] In addition, the *S* configuration at position 11 often promoted anti-PDE5 activity (*e.g.*, IC_{50} = 0.33 µM for **66** *vs.* 1.1 µM for the 11-*R* isomer, 38 nM for **67** *vs.* 290 nM for the 11-*R* isomer), but with some discordant data (*e.g.*, IC_{50} = 0.17 µM for **68** *vs.* 0.47 µM for the 11-*S* isomer). As a result, 5*R*,11*S* analogues often unveiled the most promising profile for building further fine-tuned iterations. Indeed, modulation efforts at various positions while fixing the absolute configurations afforded the best IC_{50} values among tested enantiopure derivatives (IC_{50} = 51 nM for **69a** and 40 nM for **69b**).[89–92,97] Regarding the influence of substituents, if the presence of a 4-methoxyphenyl moiety at position 5 was found beneficial overall (IC_{50} = 5–8 nM for **65b**, *vs.* >20 nM for analogues with chloro or cyano substituents, or with alternative heterocyclic rings), variations of the hydantoin *N*-substituent did not exert a crucial impact. Indeed, ethyl, butyl, and even bulkier benzyl, cyclohexyl and ethylpyridine groups provided single-digit nanomolar activities (IC_{50} <10 nM for **65a**–**c**, among other analogues). Further modulations at these two positions failed to yield derivatives with similar properties. Especially, dimethoxyphenyl, chlorophenyl, bromophenyl and bromothiophenyl groups introduced at position 5 of various β-carboline–hydantoin stereoisomers (with various *N*-substituents, *e.g.*, ethyl, butyl, chlorophenyl) only generated compounds with IC_{50} >38 nM. However, it is worth noting that the best molecules of the series were 5-(bromophenyl) derivatives (**67**, **69a**, **69b**). Replacing the hydantoin ring by an analogous 2-thioxoimidazolidin-4-one was overall detrimental, even if compound **70** eventually reached

the submicromolar range (IC_{50} = 0.56 µM). Interestingly, only one analogue with 3,4-methylenedioxyphenyl substitution at position 5 was tested.[98] Despite the partial reduction of their hydantoin scaffold, compounds **71** and **72** revealed a shared promising IC_{50} of 60 nM. However, the complete reduction of the hydantoin carbonyl groups yielded a completely inactive compound.

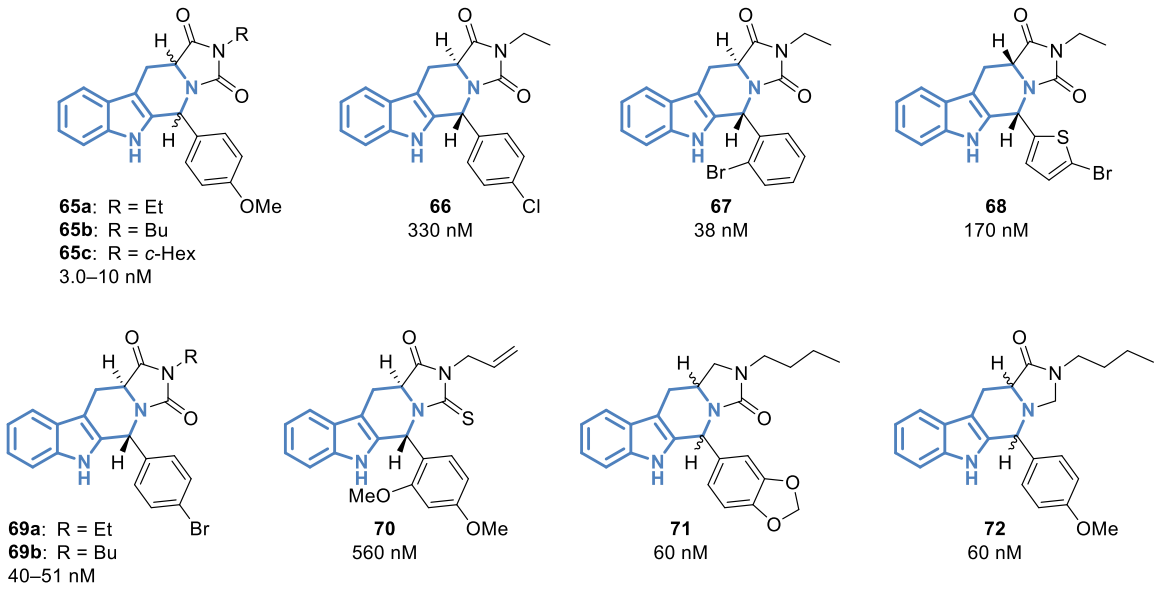

Figure 12. Selected structures and IC_{50} of β-carbolines with a fused hydantoin ring or analogue as PDE5 inhibitors.

β-Carbolines with a fused piperazinedione ring. The expansion of previous β-carboline–hydantoin compounds into piperazinedione analogues gave engaging results. First, the evaluation of pairs of *cis* and *trans* racemic mixtures (*e.g.*, IC_{50} = 5 nM *vs.* 140 nM for *cis*- and *trans*-**73b**, respectively, Figure 13) first revealed a general trend, showcasing the *cis* configuration as the most favorable.[98] Thus, further preliminary studies investigated the substitution of nitrogen 2 of *cis* β-carboline–piperazinedione derivatives and succeeded to identify racemic, one-digit nanomolar inhibitors of PDE5, such as *cis* versions of **73a**–**d**, a result highlighting the considerable steric tolerance at this position (IC_{50} = 5 nM for

cyclohexyl **73c** and 3 nM for benzyl **73d**). All these molecules were associated with the presence of a 3,4-methylenedioxyphenyl group at position 6, which appeared as more advantageous than the 4-methoxyphenyl alternative. Further variations at positions 2 and 6 were performed, including independent analysis of each isolated enantiomer. It seemed that the 6*R*,12a*R* configuration issued the best results overall, followed by the isomer 6*R*,12a*S* (*e.g.*, IC_{50} = 3 nM for **74** *vs.* 1,200 nM for the 12a*S* isomer, 10 nM for **75** *vs.* 9 nM for the 12a*R* isomer).[92,97] By contrast, a *S* configuration at position 6 caused a dramatic loss of activity in each case, with IC_{50} above 1.0 µM. This work led to the discovery of compound **8** which is known as tadalafil (Figure 1), a drug that was marketed as a PDE5 inhibitor in 2003.[98] Tadalafil presented an exquisite PDE5 *vs.* PDE1–4 selectivity, and a far higher selectivity *vs.* PDE6 than sildenafil, the molecule mainly used as medicine for PDE5 inhibition. It also had excellent pharmacokinetic properties together with a high metabolic stability, leading to a good *in vivo* activity. From a structural point of view, the co-crystallization of PDE5 with tadalafil **8** (PDB code 1UDU, Figure 14) allowed to retrieve crucial data about molecular interactions.[99,100] Especially, the pyridine ring is located between Phe820 and Val782, forming a typical P clamp system and an important hydrogen bond with Gln817 side chain. In addition, the flat tetracyclic core of tadalafil is maintained through hydrophobic interactions with Ile768, Ile778, Phe786, Leu804 and Phe820. On the other hand, the 3,4-methylenedioxyphenyl moiety occupies a pocket made of Ala783, Phe786, Phe787, Leu804, Ile813 and Met816. Interestingly, when considering the structure of PDE4 (PDB code 4WCU),[101] the presence of the 3,4-methylenedioxyphenyl group causes a steric clash with M411, potentially explaining the PDE5/PDE4 selectivity observed (IC_{50} = 5 nM for PDE5 *vs.* >10 µM for PDE4, a beneficial ratio given the clinical safety issues raised by PDE4 inhibitors). Finally, the amido *N*-methyl group is located in a very open area, without any close residue. The possibility of introducing more complexity at this position was thus further

evaluated. Overall, among the *R,R* enantiomers tested, only a few showed IC_{50} values similar to those mentioned above.[90,92,97,98] Other studies focused exclusively on 3,4-methylenedioxyphenyl analogues. Interestingly, the tolerance for *N*-substitution was lesser in this context, and small, aliphatic moieties were found more promising for anti-PDE5 activity than aromatic or extended groups (*e.g.*, IC_{50} = 16 nM for **76** *vs.* 5 nM for **8**).[98,102,103] In addition, the introduction of polar groups, such as OH or NH_2, was detrimental, compared to hydrophobic equivalents.[104] Finally, 6-(3,4-methylenedioxyphenyl) compounds bearing (*R*)-pyrrolidine-type substituents at the amido position of the piperazinedione ring were developed as the most potent β-carboline-based PDE5 inhibitors to date. Indeed, these pyrrolidine moieties substituted by various aromatic groups (*e.g.*, pyridine, benzyl, imidazole) were able to bring IC_{50} to very low nanomolar or subnanomolar values (IC_{50} = 0.8–2.0 nM for **77a**, **77b**, **78a** and **78b**).[103,105]

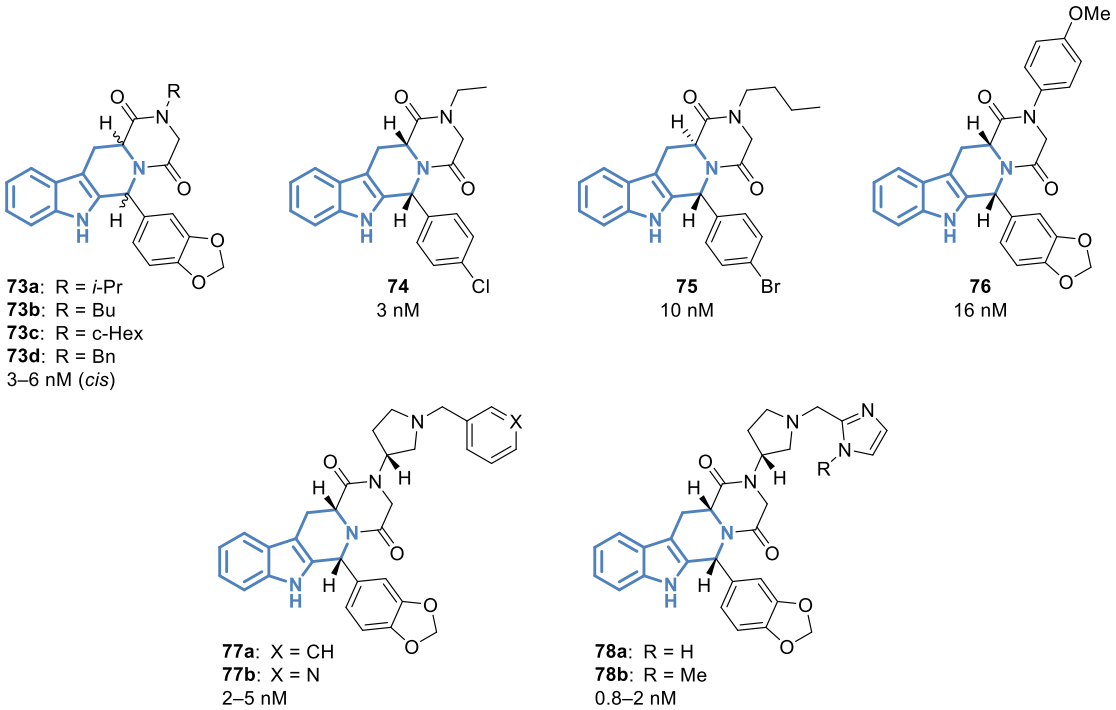

Figure 13. Selected structures and IC_{50} of β-carbolines with a fused piperazinedione ring as PDE5 inhibitors.

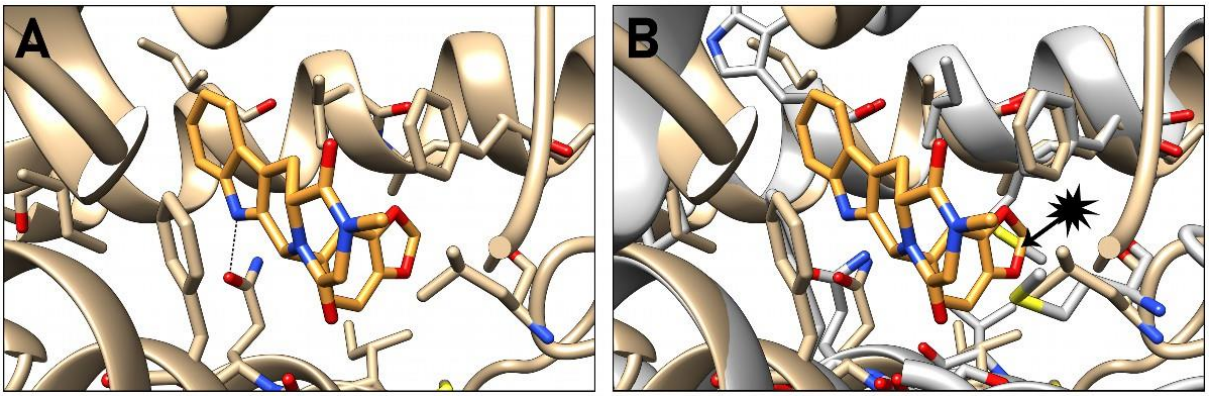

Figure 14. (A) Crystal structure of **8** (in orange) bound to PDE5 (PDB code 1UDU). (B) Overlay of crystal structures of **8** (in orange) bound to PDE5 (in gold, PDB code 1UDU) and of PDE4 (in silver, PDB code 4WCU).

Glutamate receptors binders (NMDA, mGluR)

Glutamate, the primary excitatory neurotransmitter present in the CNS, is implicated in several key brain functions such as learning and memory. Glutamate can bind to two families of receptors: the ionotropic glutamate receptors, mainly NMDA receptors, voltage-dependent channels permeable to Ca^{2+} that mediate excitatory neurotransmission, and the metabotropic receptors (mGluRs) belonging to the G-protein coupled receptors family and known for their neuroprotection properties. In AD, the over-activation of NMDA receptors through excessive binding of glutamate causes a large influx of Ca^{2+} that leads to excitotoxicity, ultimately ending in neuronal degeneration. NMDA antagonists, such as the FDA-approved drug memantine, have demonstrated their neuroprotective role by attenuating incidents of excitotoxicity and thus neuronal death, delivering an efficient symptomatic treatment for AD. The heterooligomeric NMDA receptors comprise at least two types of subunits: NR1 and NR2, the latter occurring in four distinct subtypes (NR2A–D).

Inhibition of NMDA receptors. β-Carbolines were first identified as potent and selective inhibitors of the NMDA receptor NR2B through a SAR study after rigidification of the primarily identified active skeleton.[106] The activity of this series on NR1/2B subtype appeared to be strongly dependent on the presence of a phenolic hydroxyl group, whether at the A- or B-ring (*e.g.*, IC_{50} = 50 nM for **79** *vs.* 3.3 μM for the naked analogue, Figure 15), and its position relative to the basic nitrogen atom of the piperidine ring, the three main active compounds (IC_{50} = 50 nM for **79**, 87 nM for **80**, and 140 nM for **81**) showing similar distances between these two moieties (7.8–8.8 Å). While N^2- or N^9- monosubstituted compounds were generally inactive on NMDA, compound **82** yielded IC_{50} values of 27–28 μM against NR1/2A and NR1/2B, whereas the *R* enantiomer showed no activity.[107] Both enantiomers of the phenyl analogues, with removed methylene links, were also inactive. Indeed, the 'V'-like shape of compound **82** seems to foster interactions with the receptor, as corroborated by docking experiments. The two wings of the 'V' are formed by the tetrahydro-β-carboline core and the benzyl group, which interact in a similar manner than memantine or dizocilpine, *i.e.* with hydrophobic residues Val640, Leu643 and Ala644 (NR2A) or Met641, Val644 and Ala645 (NR1). Another rigidification strategy leading to β-carbolines was initiated after the identification of hit compounds presenting a biological activity on NMDA receptor and displaying both bicyclic lactam and indole moieties.[108] The study focused on nine β-carbolines, varying over their stereochemistry, substitution pattern and lactam-ring size, but the best obtained activity (compound **83**, IC_{50} = 30 μM) remained modest.

Inhibition of mGluR receptors. While the specific involvement of mGluRs in AD pathogenesis is imprecise, their significant role is ascertained by their implication in the modulation of MAPK, directly implicated in the disease process. mGluRs are subdivided into three groups, mGluR1 belonging to group I mGluRs. Since the early 2000s, many reports have shown the neuroprotective effects of the mGluRs modulation, whether by the use of

group II mGluR agonists or by group I mGluR antagonists.[109] Notably, β-carbolines designed from previously identified potent and selective pyrroles were evaluated as mGluR1 antagonists.[110] The SAR study highlighted three main parameters responsible for the improvement of their *in vitro* potency: *(1)* a H-bond acceptor and/or donor on the unsubstituted lactam ring, *(2)* a H-bond acceptor group at R^6 and *(3)* a bulky and lipophilic substituent on the indole ring part and more conveniently at position 6. Structures complying with these criteria exhibited the best activities, and among them **84**, **85** (IC_{50} = 71 nM for both) and **86a** (IC_{50} = 100 nM) were the most promising. For these compounds, *in vivo* pharmacokinetic properties were evaluated on rats, showing oral bioavailability ranging of 9–12% and a maximum exposure in plasma of 37–145 ng/mL. Nevertheless, the most balanced mGluR1 antagonist regarding both *in vitro* activity and pharmacokinetic profile is compound **86b** (IC_{50} = 170 nM), which is in addition associated with a suitable level of brain penetration.

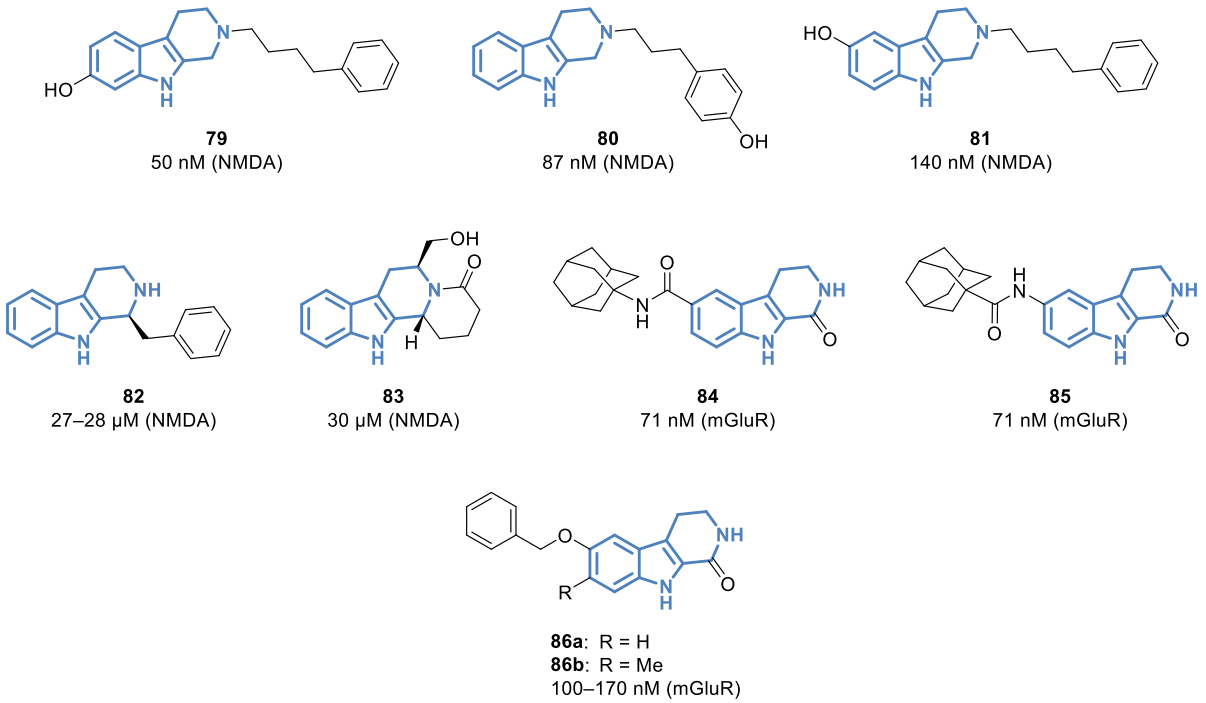

Figure 15. Selected structures and IC_{50} of β-carbolines as glutamate receptors binders.

γ-Aminobutyric acid receptors ($GABA_A$) ligands

While cholinergic and glutamatergic dysfunctions are well known to be disrupted in AD, the increase or decrease GABA levels in AD patient brains have long been discussed. However, despite some initial controversy, the primary inhibitory neurotransmitter GABA, involved in the maintenance of the excitatory/inhibitory balance in the brain, is undoubtedly implicated in AD pathology.[111–113] Indeed, cognitive deficits were related to the dysfunction of presynaptic GABA that acts on $GABA_A$ receptors, widely located in the CNS. The increased GABAergic neurotransmission could be circumvented with an agonism at $GABA_A$ receptors, thus preventing the neuronal death and the formation of β-amyloid fibrils.[114]

Affinity of β-carbolines and influence of the R^3 and R^4 substituents on efficacy. The affinity of β-carbolines for the benzodiazepine binding site of $GABA_A$ receptor was initially discovered in the early 1980's. Even elementary β-carbolines with very low substitution levels achieved to fairly interact with $GABA_A$ receptor in a ubiquitously used [^{3}H]ligand binding inhibition test (usually classical benzodiazepines were employed, such as diazepam, flunitrazepam or flumanezil). This is especially the case with norharmane **9a** and harmane **9b** (IC_{50} = 1.6–8.2 μM and 7.2–25 μM, respectively, Figure 2), while further substitutions and partial or complete saturation of the pyridine ring led to an activity drop (*e.g.*, IC_{50} >100 μM for **1**–**3**, Figure 1).[115–118] In contrast, the introduction of an ester group at position 3 produced compounds with far better affinities, in the nanomolar range. β-CCM **87b**, β-CCE **87c** together with higher homologs **87d** and **87e** thus shared similar IC_{50} values of 1–10 nM, and seemingly constitute the optimal steric hindrance window, as both the carboxylic acid **87a** and the CH_2*t*-Bu **87f** analogues were less active (IC_{50} = 31–33 μM and 0.75 μM, respectively, Figure 16).[115,117,119–125] Interestingly, concomitant substitution of the positions 5 or 6 did not appear to be detrimental in this context, and several derivatives bearing various groups, such

as OH, O*i*-Pr, NHBn or OBn, managed to retain the same level of affinity (*e.g.*, IC_{50} = 4 nM for **88a**, 10 nM for **88b**, *vs.* 1–19 nM for **87b**).[124,126,127] Similarly, when introducing a methoxymethyl substituent at position 3, the affinity values remained in the low nanomolar (*e.g.*, IC_{50} <10 nM for **89a**, **89d**, ZK-93423 **89e** and abecarnil **90**) or subnanomolar ranges (*e.g.*, IC_{50} = 0.9 nM for **89b**, 0.5–1 nM for **89c**, 0.2–2 nM for **91**),[127–130] even if the best values were yielded by 3-methyl analogue **92** (IC_{50} = 0.4–0.7 nM).[131] However the presence of a substituent at position 9 dramatically compromised the affinity for $GABA_A$ receptor (IC_{50} >0.29 µM for 9-methyl counterparts of **87b**, **89d** and **89e**; >5.0 µM for other derivatives).[115,117,127,128] A few other chemical groups led to similar affinity upon further pharmacomodulation at position 3. Among them, the propyl ketone **87g**, nitrile **87h**, isothiocyanate **87i** and propoxy **87j** yielded the best results (IC_{50} <11 nM).[117–120] Reduced versions of β-CCM **87b** and β-CCE **87c** showed far weaker activities (IC_{50} = 6.0 µM).[115] In addition, the early discovery of β-carboline-based agonists and antagonists prompted research groups to establish enlightening structure-efficacy relationships. One striking feature was the shift of the β-carboline 3-esters efficacy along an inverse agonist–agonist continuum, as the carbon chain of the ester became bulkier (Figure 17). Indeed, **87b** and **87c** behave as inverse agonists, **87d** and **87e** as antagonists and higher homologs showed anticonvulsant effects against leptazol-induced seizures, consistent with an agonist action.[132] Several other derivatives with more intrinsic efficacy were identified that fell into one or the other of these categories. Thus, compound **89e** appeared as a full agonist of $GABA_A$ receptor, whereas **91** was identified as a partial agonist, and **87h**, **87j** or **92** were acknowledged to be antagonists. In the other hand, very close analogues were seen as inverse agonists, such as **87g** or less active 3-methoxy and 3-ethoxy derivatives.[120,132133–134] While lacking an apparent rationale, this variability in terms of efficacy should derive from changes in molecular interactions, whose

complete understanding is scrambled by the absence of accurate structural data and by the diversity of $GABA_A$ receptor subtypes.

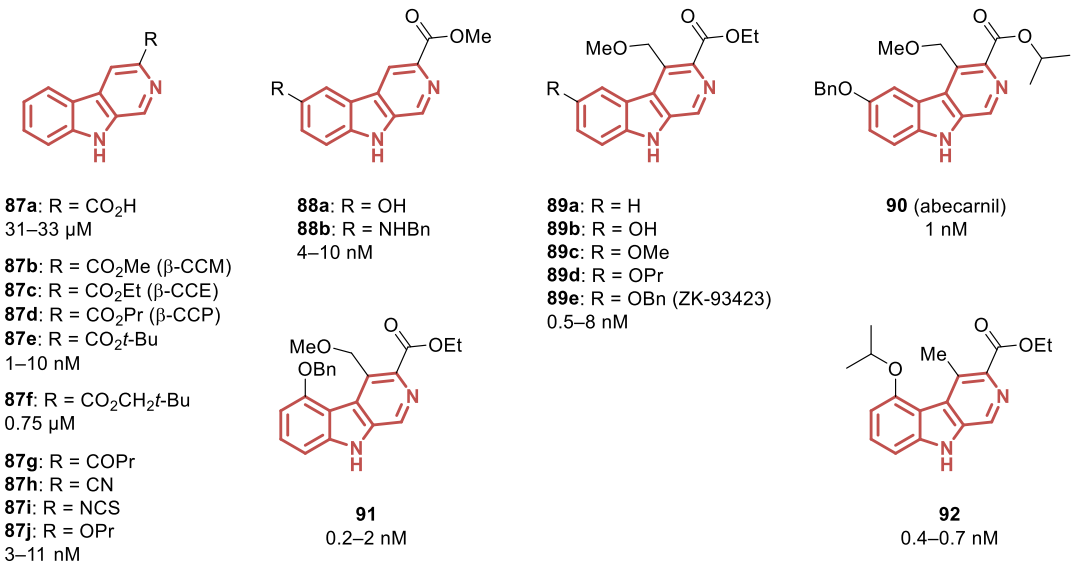

Figure 16. Selected structures and IC_{50} of 3- and 4-substituted β-carbolines as $GABA_A$ ligands.

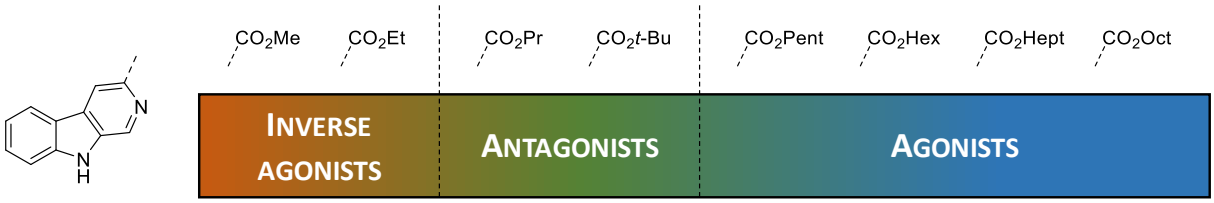

Figure 17. $GABA_A$ efficacy continuum of β-carbolines 3-esters as a function of the ester chain length.

Receptor subtypes selectivity and additional combinations of substituents. The $GABA_A$ receptor complex displays high molecular diversity and is made from a combination of various subunits. At least fifteen different subunits have been identified and could explain the diversity of pharmacological effects observed in presence of ligands.[128] In an initial pharmacophoric model, two hydrogen bond donating sites were suggested, termed H_1 and H_2. Especially, H_2 was thought to correspond to the position 4 of β-carbolines, where the presence of an oxygen atom appeared as beneficial. In addition, the occupation of a lipophilic area at

this site seemed to contribute to an agonist activity, as testified by 4-methoxymethyl derivatives **89e** and **91**. The evaluation of β-carbolines against specific receptor subtypes was a step further towards rationalization at the molecular level. The affinities of some of the best β-carbolines discovered previously for $GABA_A$ receptor subtypes $\alpha_1\beta_3\gamma_2$, $\alpha_2\beta_3\gamma_2$, $\alpha_3\beta_3\gamma_2$, $\alpha_4\beta_3\gamma_2$, $\alpha_5\beta_3\gamma_2$ and $\alpha_6\beta_3\gamma_2$ (shortened respectively as α_1, α_2, α_3, α_4, α_5 and α_6 subtypes) were thus assessed. First, all β-carbolines were found far less active against the subtypes α_4 and α_6 (K_i >1.0 µM in almost all cases), while the remaining four subtypes afforded very low nanomolar K_i values (

Table 2). Interestingly, if globally compounds devoid of 4-substitution showed some selectivity for α_1 (*e.g.*, **87b**, **87e**, **87g**, **87j**, **88b**), 4-methoxymethyl analogues did not discriminate between α_1, α_2, α_3, and α_5 subtypes (*e.g.*, **89a**, **89d**, **89e**, **90**).[128,135–139] The residue His105, which is present in subunits α_1, α_2, α_3, and α_5, and replaced by an arginine in α_4 and α_6, was proposed to play a central role in this selectivity. Indeed, the affinity values of compounds **87b**, **87c** and **90** for subtype α_5 dropped significantly upon mutation of His105 into Arg105 (K_i = 4.4 µM, 1.9 µM and 6.2 µM respectively, *vs.* 44–68 nM, 27–110 nM and 5–8 nM respectively for the wild type).[137] Further works were undertaken for exploring the selectivity profile of β-carbolines, especially by combining a favorable 3-substituent with diverse groups at positions 6 and 7. Hence, the production of 6,7-dimethoxy analogues afforded surprising pan-subtype inhibitors **93a** and **93b**, which are quite unique in their ability to bind efficiently to α_6 (K_i = 130 nM and 75 nM respectively, Figure 18).[128,135] Introducing other substituents at these positions, such as nitro, isothiocyanate, or ethynyl, provided additional compounds of interest (*e.g.*, **94**, **95**, **96**), but with a more classical selectivity profile, except for **96**. The

derivatization at position 6 using aryl or heteroaryl moieties, including phenyl, naphthyl, furyl and thiophenyl mostly failed to significantly improve both affinity and selectivity, while a phenyl ester group at position 3 was associated with enhanced α_1 selectivity (*e.g.*, for **97**, IC_{50} = 34 nM against α_1 *vs.* >1.0 µM against $\alpha_{2\text{-}6}$).[135,138] Finally, derivative **98** was the only reported example of an active N^2-substituted β-carboline, revealing especially a good affinity for α_1 and α_2 subtypes (K_i = 7 nM and 12 nM respectively).[140]

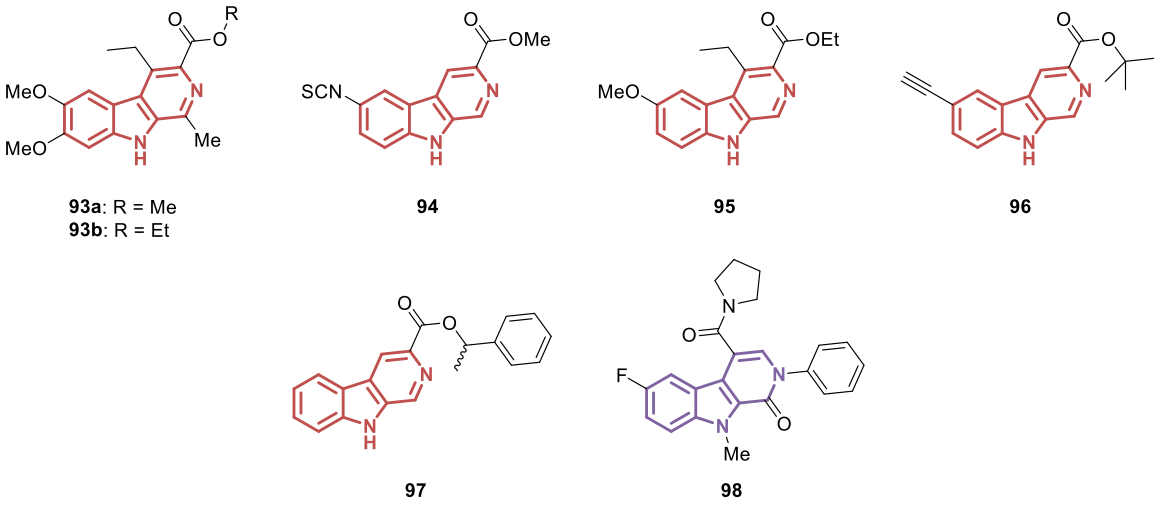

Figure 18. Selected structures of second-generation β-carbolines as $GABA_A$ ligands.

Table 2. K_i Values Obtained for β-Carbolines Against a Panel of $GABA_A$ Subtypes.

Cd	K_i α_1 (nM)	K_i α_2 (nM)	K_i α_3 (nM)	K_i α_4 (nM)	K_i α_5 (nM)	K_i α_6 (nM)
87b	2	7	72	1000–1300	44–68	4400
87c	1	5	6	1000	27–110	2700–3100
87e	0.7	15	19	1000–3000	110	>5000
87g	2	16	21	—	1000	>3000
87j	5	52	69	1000	590	>1000
88b	5	30	49	—	480	>10000
89a	0.6	3	5	—	10	1200
89b	2	5	11	—	19	3000
89c	0.1	1	2	—	4	480

89d	0.5	1	2	—	2	1300
89e	4	4	6	—	5	>1000
90	1–12	2–15	4–8	1200–2000	5–8	6400–10000
93a	6	8	4	—	1	130
93b	6	19	4	—	3	75
96	1	110	100	2000	210	2000
97	34	1000	1000	1000	1000	3000
99a	1	1	1	—	40	>1000
99b	4	12	24	—	210	>10000
99c	3	12	11	—	230	>10000
101	2	12	16	—	200	>10000
102	3	24	31	—	240	>10000

Pyridodiindoles and other fused ring systems. Beyond the introduction of simple substituents in the β-carboline scaffold, derivatives including additional fused rings were developed. Especially, pyridodiindoles were conceived as a very rigid and planar platform made of five fused aromatic rings, based on a β-carboline core. Interestingly, the naked pyridodiindole **99a** was found as the most active representative of this new class of $GABA_A$ ligand (IC_{50} = 4 nM), while appending various substituents consistently led to weaker activity records (Figure 19).[118,119,141] However, if the introduction of 2'- and 3'-substituents was really prejudicial, similar substitutions at positions 4' and 5' afforded compounds with some retained affinity, as illustrated by the chloro analogues (IC_{50} = 10 nM and 80 nM for **99b** and the 5'-chloro analogue of **99a**, respectively, *vs.* 0.72 μM and 2.2 μM for 2'- and 3'-chloro analogues of **99a**, respectively). In particular, at position 4' there seems to be some room for a substituent, regardless of its chemical nature (halogens of various sizes, methoxy, hydroxy, with IC_{50} <0.019 μM for **99b** and **99c**) but with limitations in terms of steric hindrance (IC_{50} >4.0 μM for the benzyl analogue **99d**). As previously observed with simple β-carbolines, the substitution of the N^9 with a methyl group led to a substantially decreased activity, while functionalization of the position 6 gave valuable compounds. Especially, by adding nitro or bromo groups, IC_{50} values were obtained that remained similar to the naked parent **99a** (IC_{50}

= 4 nM for **100a** and 6 nM for **100b**). Finally, when exploring the impact of substituting the indole NH position and position 1 of the β-carboline, detrimental effects were seen in each case. A closer look to the subtype-related potency distribution showed selectivity profiles very similar to those observed with simpler β-carbolines (

Table 2).[135] However, the affinity for subtype α_5 was significantly lower in all cases (*e.g.*, K_i = 40 nM against α_5 *vs.* 1 nM against α_{1-3} for **99a**; K_i = 230 nM against α_5 *vs.* <12 nM against α_{1-3} for **99d**). The insertion of an extra intracyclic nitrogen atom at the indole part of **99a** induced a loss of activity, irrespectively of its position.[135] If compounds **101** and **102** managed to keep a similar activity range against α_1, their action against the other subtypes dropped significantly. Other nitrogen positions afforded even less potent compounds against all subtypes. Conversely, the conversion of the β-carboline core into the carbazole counterpart by replacing the nitrogen atom at position 2 by a CH moiety strongly weakened the activity (IC_{50} = 1.9–2.0 µM *vs.* 4 nM for **99a**), highlighting the crucial importance of the carboline skeleton.[118,119] Finally, other classes of heterocyclic-fused β-carbolines were developed, *i.e.*, oxazolo[4,5-*g*]-β-carbolines and pyrazino[2,3-*g*]-β-carbolines.[129] These molecules, incorporating a classical 4-methoxymethyl group, were found highly potent, hitting the subnanomolar range (IC_{50} = 0.8–0.9 nM for **103**–**106**) regardless of the structural features embedded (isopropyl ester group or isoxazole ring at position 3, oxazolo or pyrazino groups at positions 5 and 6).

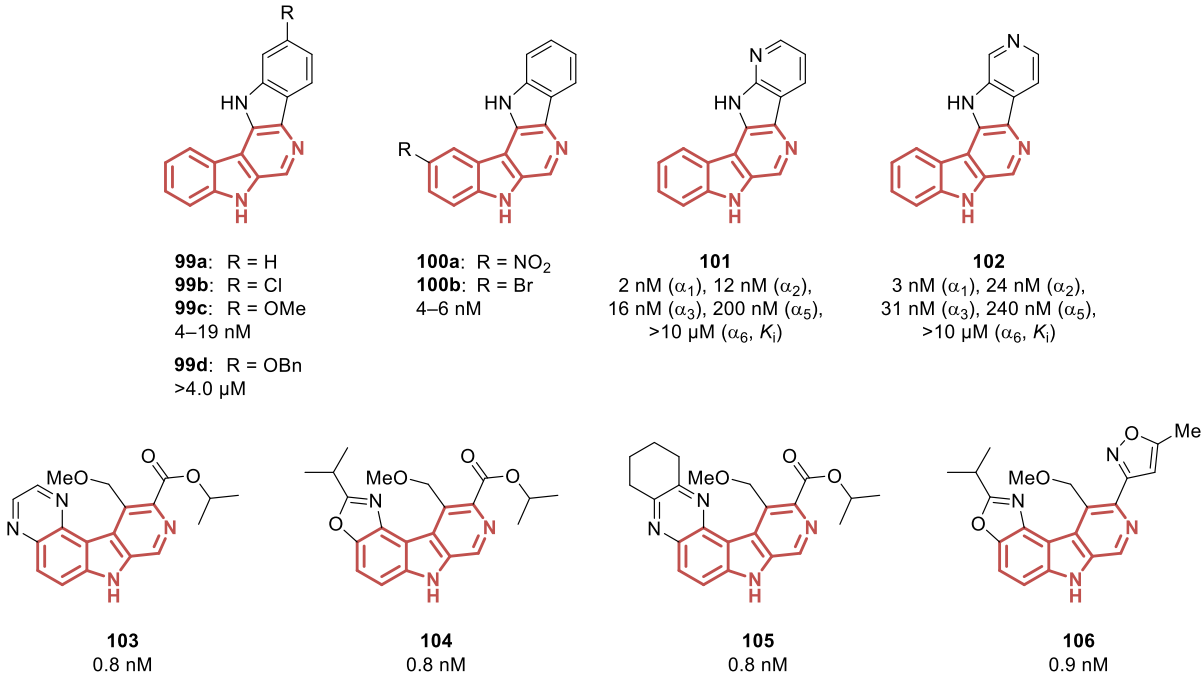

Figure 19. Selected structures and IC_{50} (or K_i where indicated) of fused β-carboline-based aromatic derivatives as $GABA_A$ ligands.

5-Hydroxytryptamine (5-HT) receptors binders

The implications of the serotonergic system, and therefore its neurotransmitter 5-HT, in Alzheimer's disease are diverse and complex, especially due to multiple interactions with other neurotransmitters such as acetylcholine, glutamate or GABA. Serotonin is a monoamine neurotransmitter acting on fourteen pre- and postsynaptic subtypes of receptors divided in seven families (5-HT_1 to 5-HT_7) and mainly located in brain areas involved in particular in learning and memory. Among them, subtypes 1, 3, 4, 6 and 7 are of particular interest in the AD context. 5-HT_4 and 5-HT_7 receptor agonists as well as 5-HT_1, 5-HT_3 and 5-HT_6 antagonists have shown pro-cognitive effects in animal studies or clinical trials.[114,142,143]

Tetrahydro-β-carbolines and R^1/R^9 substituents exploration. If tetrahydro-β-carbolines of classical structures, such as **3** (Figure 1), showed only weak activities against 5-HT receptors,

improvements were observed upon methoxy or bromo position shifts (*e.g.*, K_i <0.18 µM for **107a** and **107b** against 5-HT_{2A} and 5-HT_{2C} *vs.* >10 µM for **3**).[144–147] Especially, 8-bromo-tetrahydro-β-carboline provided the only inhibition constants below 100 nM, against 5-HT_{2A} and 5-HT_{2C}, while the 6- and 7-methoxy derivatives, mostly inactive against subtypes 1A, 2A and 2C, showed interesting levels of activity against 5-HT_{2B} (K_i >1.0 µM *vs.* 0.16 µM and 0.39 µM, respectively). The 1-methyl-8-methoxy tetrahydro-β-carboline reached a K_i value of 0.45 µM against 5-HT_{1A}, while all other tested molecules remained at the micromolar range. Hence, some selectivity was clearly observed upon substituent modifications, allowing the tetrahydro-β-carbolines to preferentially inhibit either subtypes 1A, 2A, 2B or 2C, depending of the position and nature of the chemical groups introduced. In addition, the introduction of benzyl groups at position 1 led to 5-HT_{2B} inhibitors with far better affinities, sometimes in the low subnanomolar range. Especially, 3',4'-dimethoxy derivatives **108a**–**108d**, **109**, **110a**–**b** and **111a**–**b** were found to inhibit 5-HT_{2B} with K_B values below 0.3 nM, while concomitantly targeting the 2A and 2C subtypes, with a weaker potency however.[148] The best value was recovered from **112**, which exhibited a K_B of 80 pM, and a good selectivity for 5-HT_{2B} *vs.* 5-HT_{2A} and 5-HT_{2C} (~100-fold). Interestingly, the substitution pattern of the β-carboline core affected only marginally the 5-HT_{2B} inhibition activities observed, considering either the position (*e.g.*, K_B = 80–500 pM for the various methyl derivatives **108a**, **109**, **110a** and **112**) or the nature (*e.g.*, K_B = 100–700 pM for 6-substituted compounds **108a**–**d**) of the substituents. Contrariwise, the length of the methylene linker appeared as a crucial feature, as both the lower and the higher homologues led to significantly reduced action. Shifting the 3',4'-dimethoxybenzyl group to position 2 was also unsuccessful. However, the introduction of naphthyl moieties in place of the 3',4'-dimethoxyphenyl part of the molecule afforded results in a similar range of affinity (K_B = 400 pM for **113**). The natural indoloquinolizidine yohimbine (**5**, Figure 1), which was found as a potent ligand of 5-HT receptors (K_i = 25–160

nM against 1A, 1B and 1D subtypes, >1.0 µM against 2A and 2C), confirmed the steric tolerance and activity potential of bulky groups at positions 1 and 2 of the scaffold.[149] Finally, the substitution of both nitrogen atoms of the tetrahydro-β-carboline scaffold resulted to nanomolar inhibition values, with a modest 1A over 2A selectivity. Methoxyphenyl groups linked by various alkylpiperazyl chains at position 9, together with ketones introduced at position 2, led to K_i values of 20–59 nM against 5-HT_{1A} (a more relevant subtype in the AD context) and 44–340 nM against 5-HT_{2A}, with a very little influence of the structure variations (*e.g.*, K_i = 20 nM and 44 nM for **114** against 1A and 2A subtypes, respectively).[150]

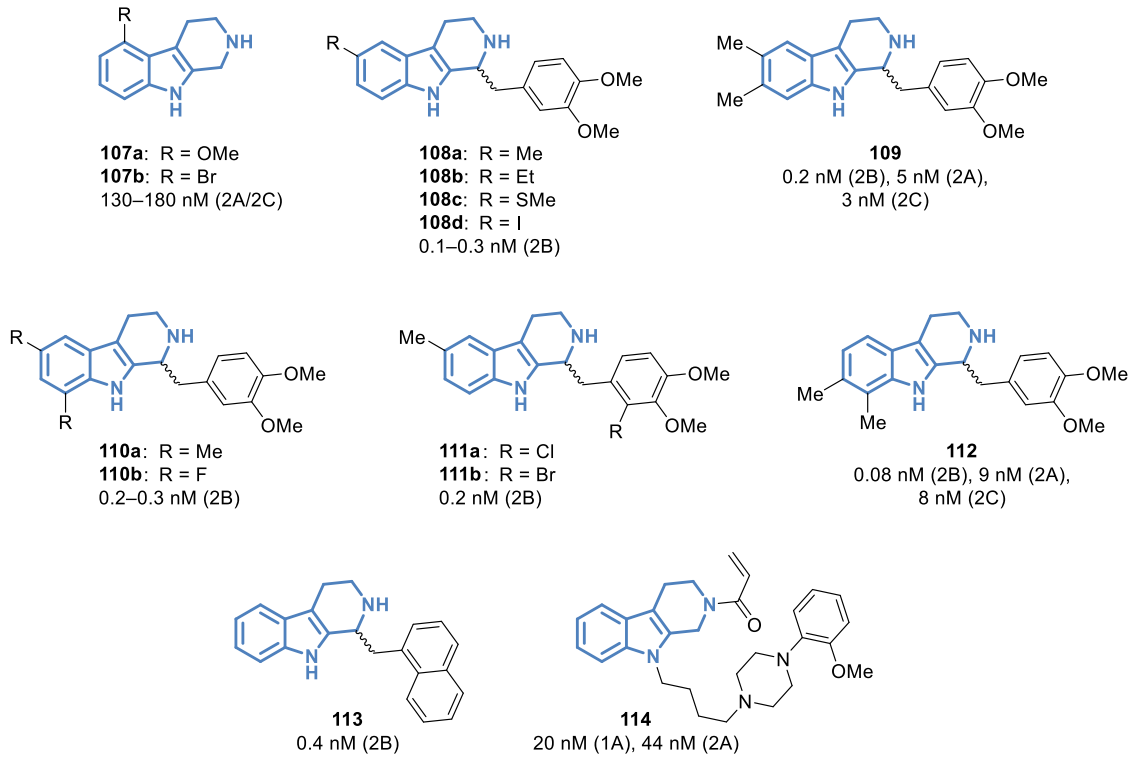

Figure 20. Selected structures and K_i of tetrahydro-β-carbolines as ligands of various subtypes of 5-HT receptors.

Dihydro- and fully aromatic derivatives. On the other hand, when considering the 3,4-dihydro counterparts of the reduced β-carbolines, various effects were observed. The insertion of the double bond led either to a significant improvement of the potency (*e.g.*, K_i = 0.92 µM *vs.* >10 µM against 5-HT_{2C} for **115a** and its tetrahydro analogue, respectively, Figure 21), to a

mere conservation of the efficiency or to an activity drop (*e.g.*, K_i = 0.13 µM *vs.* 0.47 µM against 5-HT_{2A} for **107a** and its oxidized version, respectively).[144–146] However, compounds **116a** and **116b** were the only to reach inhibition values below 100 nM (K_i = 69 nM and 75 nM against 5-HT_{2C}, respectively). A more systematic exploration of 5-HT receptor subtypes provided additional data for representative dihydro-β-carbolines **2** (Figure 1), **115a**, and **115b** (Table 3).[146,147] Similar selectivity profiles were seen for both compounds, targeting preferentially subtypes 2B and 7, and to a lesser extent 1A, 2A, 2C and 6. Compound **115b** showed in addition a good potency against 5-HT_{5A} (K_i = 0.85 µM). Further oxidation of the β-carboline pyridine ring afforded completely unsaturated analogues. Once again, the insertion of an additional double bond yielded mixed results: if some derivatives were definitely more active against 5-HT_{2A} (*e.g.*, K_i = 0.15–0.40 µM for **1** and **9b**, *vs.* 0.99–7.8 µM for **2** and **115b**), some others were less potent than their dihydro parent (*e.g.*, K_i = 4.2–5.6 µM for **115a** *vs.* >10 µM for the fully aromatic analogue).[144,145,151] There were less variations when considering the 1A and 2C subtypes however. Unlike the tetrahydro-β-carboline series, the activity of fully aromatic analogues against 5-HT_{2B} was hardly the best among 5-HT subtypes, often exceeded by the anti-5-HT_{2A} potency (*e.g.*, 1.4 µM *vs.* 0.69 µM for **117** and 1.5 µM *vs.* 0.56 µM for **118**). The introduction of heteroaromatic groups at position 1 partially restored a selectivity profile reminiscent of the tetrahydro-β-carbolines, with moderate activities however.[151] Among the evaluated scaffolds, the indole afforded the best results, with for example compounds **119a** (K_i = 0.25–0.90 µM against 5-HT_{2A-C}), **119b** (K_i = 0.17–0.20 µM against 5-HT_{2B-C}) and **120** (K_i = 0.10–0.81 µM against 5-HT_{2A-C}). However, these molecules were not tested against more AD-relevant 5-HT receptor subtypes.

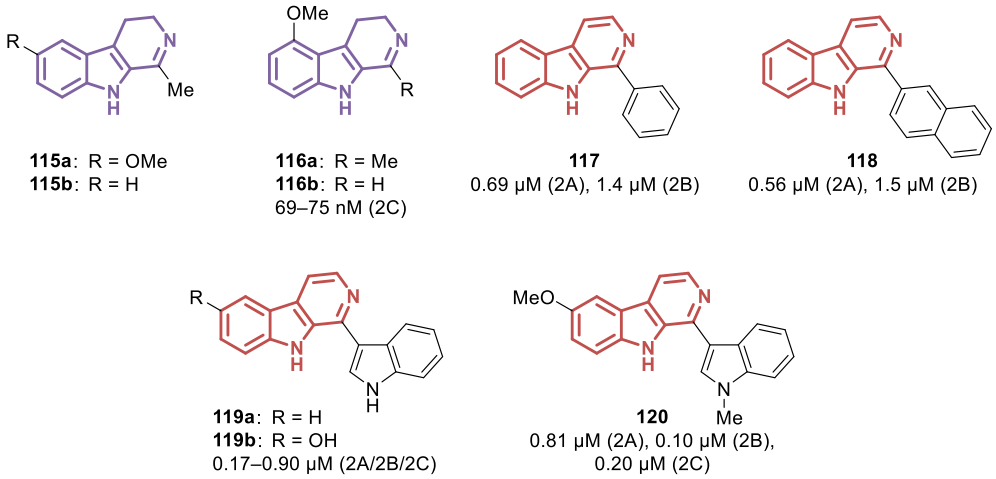

Figure 21. Selected structures and K_i of dihydro- and fully aromatic β-carbolines as ligands of 5-HT receptors.

Table 3. K_i Values Obtained for β-Carbolines Against a Panel of 5-HT Receptor Subtypes.

Cd	1A K_i (μM)	1B K_i (μM)	1D K_i (μM)	2A K_i (μM)	2C K_i (μM)	3 K_i (μM)	5A K_i (μM)	6 K_i (μM)	7 K_i (μM)
2	>10	>10	>10	5.0–7.8	9.4	>10	>10	1.5	5.5
115a	>10	>10	>10	4.2–5.6	0.92	>10	>10	1.9	3.0
115b	1.7–3.4	>10	>10	0.99–1.2	1.9	>10	0.85	1.5	0.28

Histone deacetylase (HDAC) inhibitors

Epigenetic regulation of gene expression *via* histone modification is a recent field explored in the understanding of AD. HDAC and histone acetyltransferases plays an important role in the acetylation balance of histone for which abnormalities were observed in the pathology of AD. If the targeting of HDAC was clearly associated with neuroprotective properties in AD models, their action and the precise role of each isozyme is still unknown. Nevertheless, it is now largely accepted that HDAC inhibitors may impact proteins involved in AD, such as Aβ, GSK-3β or tau. To date, several approaches aim at developing pan-HDAC inhibitors, but with expected collateral effects, as some isozymes play important and diverse neurologic functions. On the other hand, class I HDACs and HDAC6 (class IIb) have notably been proposed as targets of interest for AD treatments.[152,153] As a consequence, literature around β-carboline

HDAC inhibitors is still piecemeal. However, the presence of a zinc-chelating hydroxamic acid unit, reminiscently of the structure of SAHA (suberanilohydroxamic acid, or vorinostat, a drug marketed as antineoplastic agent through HDAC inhibition), is a feature shared by all reported β-carboline-based inhibitors. First, introducing the hydroxamic acid function at position 3 of the β-carboline scaffold provided a range of inhibitors.[154] Exploring the chain length of amido-linked derivatives showed that longer arms were favorable, especially when three methylene carbons or more are present (IC_{50} = 1.4–1.8 µM for **121c**–**e** *vs.* >3.2 µM for **121a** and **121b**, Figure 22). Thus, several analogous linear derivatives were tested, with amido or urea links, and led to submicromolar potency (*e.g.*, IC_{50} = 270 nM for **122**).[155] Considering individual HDAC isozymes, these molecules were found more active against HDAC1 and HDAC6 than against HDAC8, but with a small gap (*e.g.*, IC_{50} = 26 nM against HDAC1 and 34 nM against HDAC6 *vs.* 160 nM against HDAC8, for **122**). Again, compounds bearing shorter carbon chains showed less potential. The introduction of an aromatic link between the hydroxamic acid group and the β-carboline scaffold provided analogues with improved action on HDAC1 (*e.g.*, IC_{50} = 9.3 nM for **123a** *vs.* 26 nM for **122**). The modulation of position 1 produced even better activities, reaching the single-digit nanomolar and subnanomolar ranges against HDAC1, HDAC3 and HDAC6, while exerting low action on HDAC8 (*e.g.*, for **123b**, IC_{50} = 4.7 nM against HDAC1, 0.4 nM against HDAC3 and 0.9 nM against HDAC6 *vs.* 880 nM against HDAC8, a 200–2000-fold difference). The insertion of a *N*-substituted amido linker provided various results against nuclear HeLa HDACs, the presence of a 1-(4-methoxy)phenyl group being more favorable than the 1-methyl and unsubstituted counterparts (*e.g.*, IC_{50} = 960 nM for **124a** and 340 nM for **124b**).[156] The *N*-substituent was further explored and the presence of terminal amino groups yielded the best inhibition values (IC_{50} = 92 nM for **124d** and 120 nM for **124e**).[157] It is worth noting that the evaluation of compound **124c** against a series of HDAC isozymes confirmed the potency of these compounds against

HDAC1 and HDAC6 (IC_{50} = 4.1 nM and 2.6 nM respectively) and their inactivity against HDAC8 (IC_{50} >1.0 µM), but this time also against HDAC2 and HDAC4 (IC_{50} >1.0 µM). Alternatively, β-carbolines bearing the hydroxamic acid moiety at position 9 were investigated. A similar trend was observed regarding the potency of aromatic *vs.* aliphatic links (*e.g.*, IC_{50} = 1.4 nM for **125a** against HDAC6 *vs.* 550 nM for the analogue bearing a $(CH_2)_5$ linker), but the most striking feature was the vastly improved HDAC6 *vs.* HDAC1 selectivity (*e.g.*, for **125b**, IC_{50} = 2.5 nM against HDAC6 *vs.* 9700 nM against HDAC1; for **125c**, IC_{50} = 0.9 nM against HDAC6 *vs.* 4300 nM against HDAC1, an almost 5000-fold gap), which was inexistent with 3-substituted analogues.[158,159] Tetracyclic derivatives shared a similar profile, with sometimes anti-HDAC6 inhibition values at the subnanomolar range (*e.g.*, IC_{50} = 0.9 nM for **126** and K_i = 0.7 nM for **127**), and overall conserved potency no matter the scaffold structure.[160,161] This series was explored further and revealed fairly selective inhibition of HDAC6 among HDAC1, HDAC2, HDAC4, HDAC8 and HDAC10. Finally, indoloquinolizidine-based compounds showed a broader inhibition spectrum of HDACs, as **128** for example exhibited similar values for HDAC1, HDAC3 and HDAC6 (IC_{50} = 24 nM, 71 nM and 13 nM respectively).[162] Compound **130** was the only representative of a 2-substituted β-carboline–hydroxamic acid hybrid, with an interesting potency against HeLa HDACs (IC_{50} = 44 nM).[163]

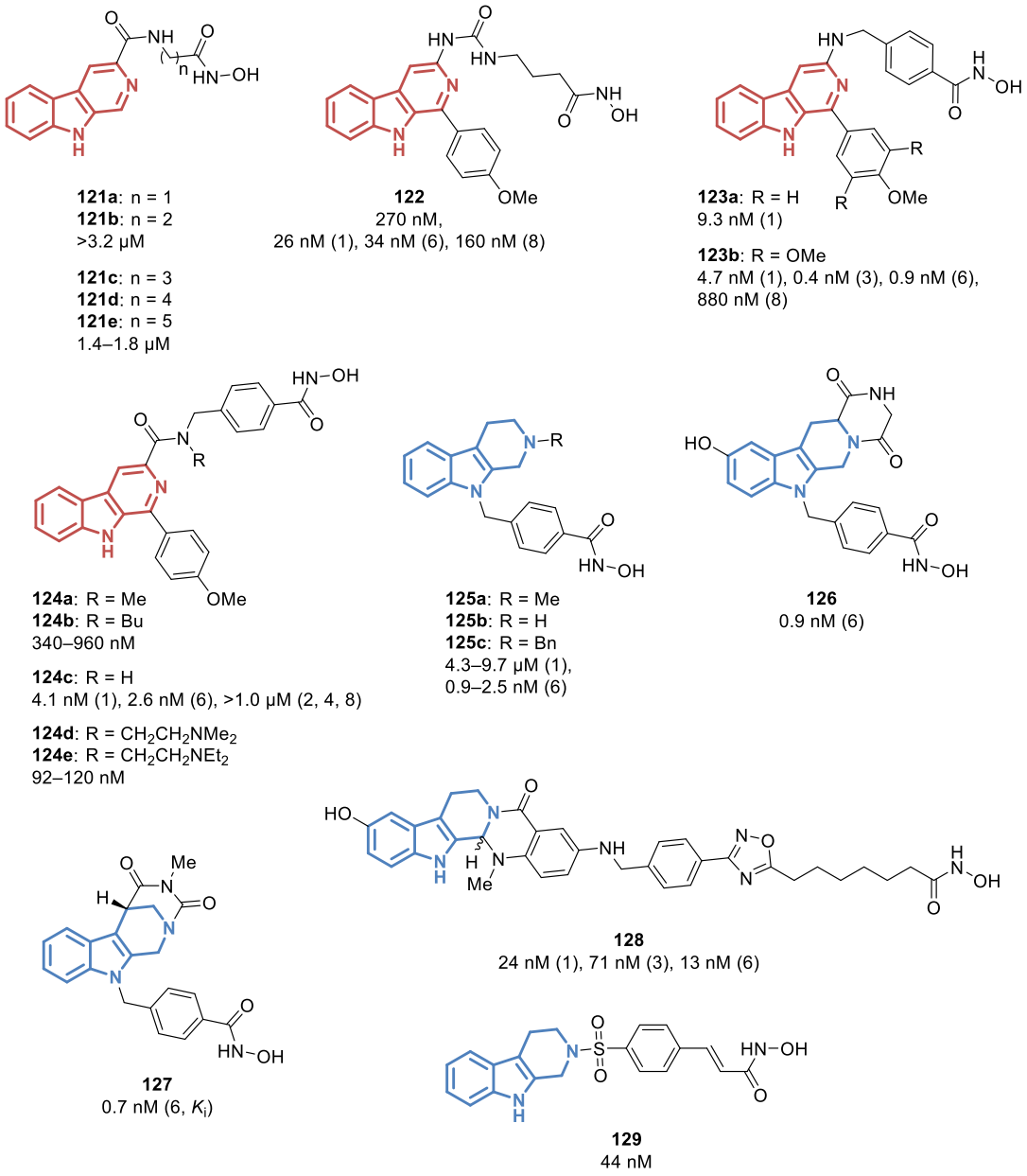

Figure 22. Selected structures and IC_{50} (or K_i where indicated) of β-carbolines as inhibitors of HDAC.

β-Carboline-based multitarget strategies

As previously mentioned, due to the insufficient knowledge of the etiology of AD and its multifactorial nature, a change in the therapeutic paradigm appeared to be essential: the unsuccessful 'one drug-one target' strategy is now increasingly overtaken by the design of MTDL. Indeed, positive results (additive or synergistic, *i.e.*, even better than those obtained

for each ligand separately) can be expected by simultaneously interacting on different targets known to be intricated in the complex network of several pathological AD-related events. The MTDL strategy is an alternative to the most classical multiple target approach that relies on the combination of at least two known drugs and can suffer many drawbacks. The attractive MTDL strategy can involve the hybridization of several pharmacophoric moieties, active on different targets, or the design of a molecule able to interact with multiple targets;[7–9] several natural products with these properties have notably been described and could benefit from further investigations in the frame of innovative anti-AD drug development. In this part, we will only focus on the first approach in which a deliberated chemical design is required. The second one, driven by multiple biological tests on isolated or synthesized molecules to specify their bioactive scope, has already been reviewed independently in the previous target-by-target parts. While the identity of the targets addressed in the MTDL strategies unsurprisingly matches those described above, the target pairs selection for undertaking a *de novo* design can represent a critical step of the process. In order to interfere at the initial phase of the disease, to slow down its evolution, or to optimally reverse AD progression, acting on the synaptic or neuronal loss would be helpful. In particular, the cholinergic neurons loss in AD patients is massive (almost 80%)[7] and lots of MTDL appropriately embed a scaffold targeting the cholinergic system. Furthermore, the preferred strategies were set up to interfere with both a symptomatic target (mainly receptors) and a disease-modifying target (such as Aβ, tau or neuroprotection), or at least with two different hypotheses of AD, as already mentioned.[164] Based on these elements, four main MTDL strategies involving β-carbolines have been reported so far.

Targeting AChE/BuChE and Aβ aggregation. Among MTDL, AChE/BuChE inhibitors represent the largest group, and it is naturally the case for β-carboline-including MTDL. Indeed, besides their catalytic activities, AChE and BuChE possess aggregation-promoting

properties (Aβ fibrils and NFTs) involving their PAS. Therefore, in addition to their symptomatic effect, AChE/BuChE inhibitors targeting the PAS or dual-site inhibitors (acting on both CAS and PAS) could simultaneously decrease the rate of formation of Aβ fibrils and thus prevent the progression of AD. To evaluate this effect, Aβ anti-aggregation properties have classically been evaluated through two procedures in order to discriminate between self-induced Aβ and/or AChE-induced Aβ aggregation inhibition. Moreover, several multifunctional AChE/BuChE inhibitors with Aβ anti-aggregation properties feature additional activities (*e.g.*, antioxidant, neuroprotective, metal chelation). Such a set of properties has often been tested for newly synthesized MTDL.[165] Rutaecarpine, a natural product used in Chinese traditional medicine for diverse pharmacological activities, including neuroprotection, was used as a template in two independent research developments. First, a SAR analysis performed on a series of 3-aminoalkanamido-substituted 7,8-dehydrorutaecarpine, inspired from previously reported compounds such as **33** or **34** (Figure 4), showed some requirements to enhance the multitarget character of the series. Pyridinium substituents especially promoted a dual inhibitory potency against AChE (*e.g.*, IC_{50} = 0.8 nM and 0.6 nM for **130a** and **130b**, Figure 23) and Aβ aggregation (*e.g.*, 91–93% of inhibition of AChE-induced $A\beta_{1-42}$ aggregation at 25 μM for **130a** and **130b**); in return the positive charge seemed to compromise antioxidative activity.[166] However, compound **130b** was associated with additional metal-chelating properties, of great interest in the frame of AD. Interestingly, the potency of these compounds was found to be variable against BuChE. Hence, if some analogues were able to interact efficiently with both enzymes, some others were very selective agents with an AChE *vs.* BuChE index up to ~3000 (*e.g.*, **130a**–**b**). These compounds seem to interact with the PAS of AChE, including hydrophobic contacts with Phe331, Phe330, Tyr334, Tyr121 or Phe290, but with a linker long enough for catching additional cation–π interactions with Trp84 and Tyr130 at the CAS of the enzyme, resulting

in a global higher affinity. Second, rutaecarpine was also derivatized with sulfonamido-linked groups. Compound **131** was especially obtained as a selective inhibitor of BuChE (IC_{50} = 3.6 μM), able to interact with both the CAS and PAS of BuChE (mainly through hydrogen bonding with Thr120 and contacts with Trp82, Gly115, Gly116, Gly121, Pro285, Ser287 or Tyr332), but unable to efficiently bind AChE (IC_{50} >100 μM), yielding a molecule with a similar scaffold than **130a**–**b** but with reverse selectivity.[167] Besides its moderate self-induced Aβ aggregation inhibition properties (59% at 100 μM), **131** revealed suitable physicochemical properties and antioxidant activity, along with a selective chelation of biometal ion Cu^{2+}. Unsurprisingly, hybrids of tacrine (a fragment known to bind to the CAS of AChE) and β-carboline (an aromatic moiety potentially able to interact with the PAS) behave as mixed-type ChE inhibitors (*e.g.*, IC_{50} = 32 nM and 41 nM against AChE and BuChE for **132**, IC_{50} = 22 nM and 40 nM for **133**), as suggested by molecular modelling, with good inhibition of Aβ aggregation (*e.g.*, 41% and 66% of inhibition of self-induced $Aβ_{1–42}$ aggregation at 20 μM for **132** and **133**).[168] In addition to its ability to cross the BBB, compound **133** also displayed good biometal-chelating abilities, a promising inhibition of Cu^{2+}-induced Aβ aggregation, and moderate antioxidant properties. A similar biological profile was obtained from two distinct series of bivalent β-carbolines incorporating a hydrophilic spacer, designed for solubility purposes. In the first series, containing fully aromatic β-carboline dimers linked by nitrogen 9, compound **134** showed modest activity against AChE/BuChE with a slight selectivity for BuChE (IC_{50} = 16 μM and 1.8 μM) and good Aβ aggregation inhibition properties (72% at 25 μM).[169] In the second series, which gathers tetrahydro-β-carboline dimers connected through nitrogen 2, compound **135** exhibited very similar potency (IC_{50} = 18 μM and 1.7 μM against AChE and BuChE, and 83% of inhibition of Aβ aggregation at 25 μM), and exerted extra neuroprotective effect in several *in vitro* studies. But overall, the lack of stereocontrol and the subsequent probable coexistence of several stereoisomers of **135** and derivatives in mixture

prevented any further analysis. In addition, cytotoxicity experiments demonstrated that compounds **134** and **135** are neurotoxic at 10 μM. To address the latter issue, β-carboline-cinnamic acid hybrids were designed based on the previously reported anti-AD properties of cinnamic acid derivatives. Compound **136** inhibited BuChE selectively (IC_{50} = 21 μM *vs.* 1.3 μM against AChE and BuChE respectively), consistent with its predicted binding modes at BuChE active site, and with its significant inhibition of Aβ aggregation (72% at 20 μM).[170] Indeed, **136** could interlock in β-sheet, as observed in docking calculations. In addition, its profile includes neuroprotective effects and low neurotoxicity, and *in vivo* evaluations in AD model mice showed beneficial effects on several behavioral parameters such as restoration of learning and memory functions, without acute toxicity.

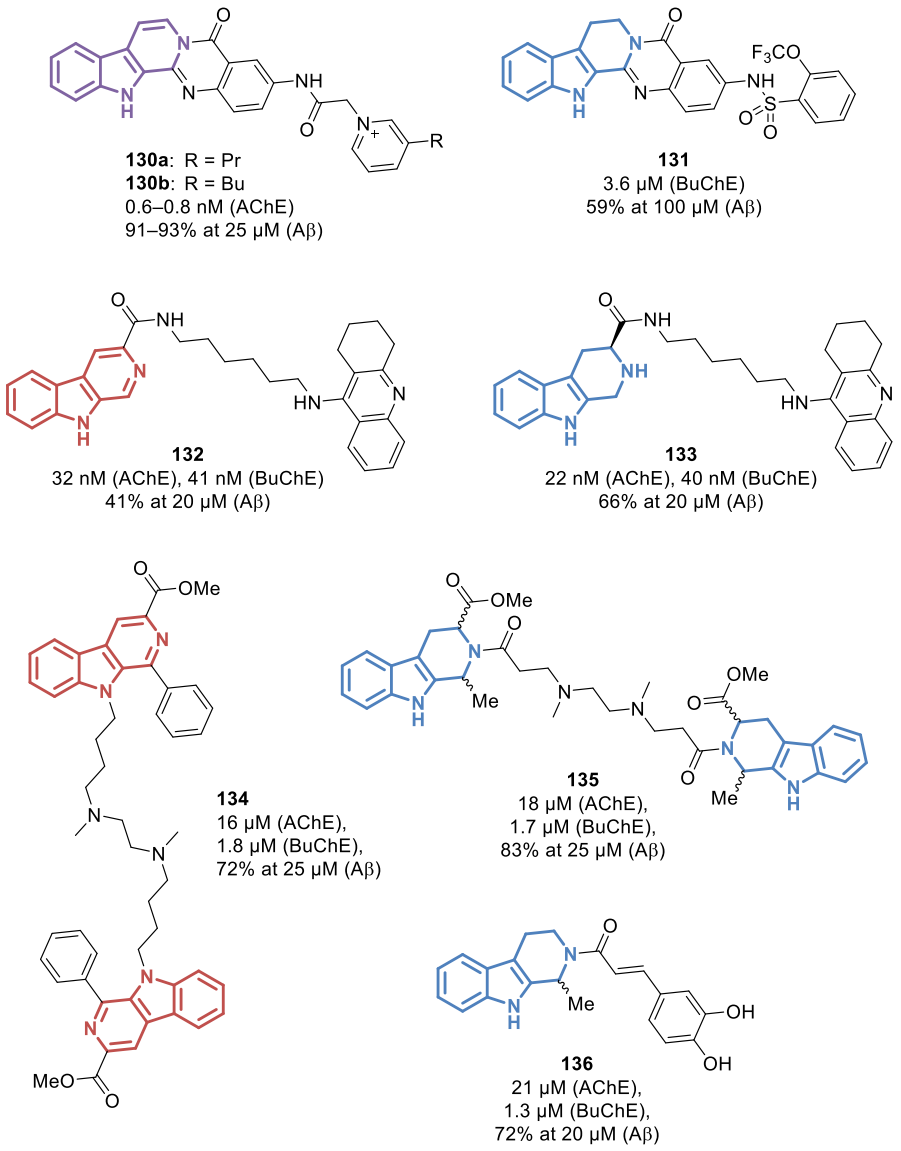

Figure 23. Selected structures, IC_{50} and aggregation inhibition percentages of β-carbolines as multitarget agents, inhibitors of AChE/BuChE and Aβ aggregation.

Targeting BACE1 and Aβ aggregation. The simultaneous targeting of BACE1 and Aβ aggregation allows to disrupt both the production of Aβ and associated pathological events. Thus, starting from previous results obtained against individual targets, and following a multifunctional approach, researchers developed additional compounds designed to not only target BACE1 but also provide anti-Aβ aggregation, metal complexation and radical scavenging properties.[171] Compound **137** (IC_{50} >50 μM against BACE1, IC_{50} = 30 μM against

Aβ aggregation, IC_{50} = 43 μM for antioxidant activity, and 43% of metal chelating capability at 100 μM) is representative of this multifunctional strategy: while retaining the tryptoline core with the two requisite NH groups for BACE1 interaction, it displays an additional phenolic structure playing a role in free radical scavenging but also improving Aβ binding with an evaluated optimal distance of 13–14 Å between the two aromatic moieties. In order to improve the poor inhibitory activity of this series against BACE1, the phenolic part was finally substituted by another more hydrophobic tryptoline moiety; however, the length between the terminal aromatic rings was maintained for the anti-Aβ-aggregation activity (IC_{50} = 17 μM against BACE1, and 80% of Aβ aggregation inhibition at 100 μM for **138**).[172]

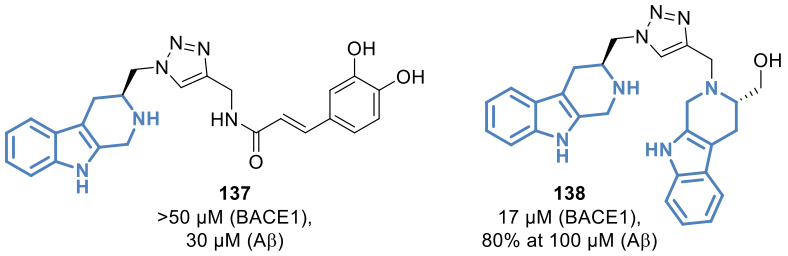

Figure 24. Selected structures, IC_{50} and aggregation inhibition percentages of β-carbolines as multitarget agents, inhibitors of BACE1 and Aβ aggregation.

Targeting AChE and PDE5. While AChE and PDE5 are both involved in memory and cognition processes, the inhibition of these targets implies different and dissociable mechanisms.[173] The design of innovative AChE/PDE5 dual inhibitors potentially producing a synergistic effect on AD thus appears as a relevant MTDL strategy. An initial focus on the repurposing and redeveloping of an existing marketed drug, tadalafil (**8**, Figure 1), a selective PDE5 inhibitor, was a potential starting point for designing dual inhibitors (IC_{50} = 26 μM for **8**). Reminiscently of previous SAR results on anti-PDE5 tadalafil analogues (which denoted some tolerance at this position, Figure 13), the introduction of a donepezil-inspired

benzylpiperidine fragment at position N^2 resulted in an improvement of AChE inhibitory activity while maintaining a decent anti-PDE5 selective action. After the identification of the main important structural elements regarding each target independently (stereochemistry, nature of the substituent, alkyl chain length and bulkiness), the most active compounds (IC_{50} = 36 nM and 32 nM against AChE, and IC_{50} = 0.15 and 1.5 µM against PDE5 for **139** and **140** respectively, Figure 25) were evaluated *in vivo* in an AD mouse model; the citrate salt of compound **140** was finally pointed as the most potent AChE/PDE5 dual-target anti-AD lead compound. Unsurprisingly, the predicted binding mode of **140** on PDE5 was very reminiscent of the tadalafil interaction pattern previously reported (Figure 14), including the hydrogen bond with Gln817 and close contacts with Phe820, Val782 and Leu804. Regarding the AChE–**140** interaction pattern, docking simulations showed possible binding at both the CAS and PAS, the benzylpiperidine fragment being anchored at the bottom of the AChE gorge and interacting with Trp86 and Trp337. The same moiety in donepezil showed similar contacts.[174] However the poor water solubility of this compound restricted possible further development, mainly for oral bioavailability issues. Additional modifications achieved at various positions of the scaffold provided for example compounds **141** (IC_{50} = 15 nM against AChE and 3.2 µM against PDE5) and **142** (IC_{50} = 31 nM against AChE and 0.20 µM against PDE5) which fulfilled the expectations in terms of potency, selectivity and physicochemical properties (water solubility of 420 and 1400 µg/mL for citrate salts of **141** and **142**). Especially, an *in vivo* evaluation underlined the capacity of **141** to cross the BBB and to target both the cholinergic system and the cGMP signaling pathway. In a passageway water maze test performed on mice, **141** led to a reduced escape latency and improved the memory and cognitive functions in a similar way than the reference donepezil at 10 mg/kg. In addition, **141** exhibited an enhancement of central CREB protein phosphorylation, thereby potentially

contributing to an amelioration of scopolamine-induced cognitive impairment in mice, and revealing a promising profile as an anti-AD, multitarget drug candidate.[175]

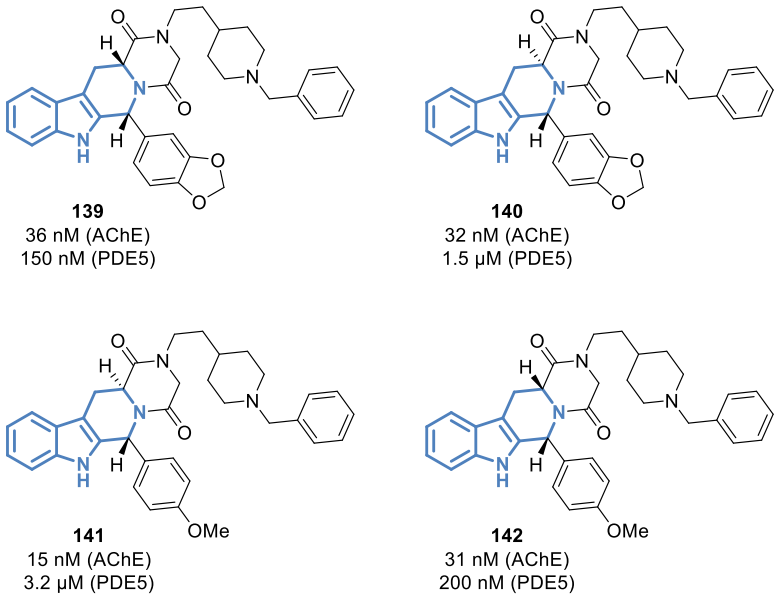

Figure 25. Selected structures and IC_{50} of β-carbolines as multitarget agents, inhibitors of AChE and PDE5.

Targeting AChE/BuChE and NMDA. The combination of donepezil, an AChE inhibitor, and memantine, the only marketed NMDA antagonist, is now a commonly used treatment for moderate to severe AD that has demonstrated beneficial effects. The development of new hybrids, that could alleviate AD symptoms, is thus one of the most promising MTDL strategies. Inspired by the bis-tacrine template that is far more potent on AChE than the monomeric analogue, homobivalent β-carbolines were designed with various length spacer. As for the tacrines, the optimal distance between the two pharmacophoric moieties is usually fixed at 7−9 carbons with loss of activity for shorter linkages and solubility issues for longer ones.[28,176] By anchoring the linker either at N^2 or N^9 positions of the β-carboline scaffold, two series were developed and reported. The homodimers linked at the N^2 position always kept some anti-ChE activities, often below 200 nM, while the potency against NMDA receptors varied. Especially, compound **143** reached decent ChE inhibition (IC_{50} = 86 nM and 22 nM

against AChE and BuChE, respectively, Figure 26) and promising values against NMDA receptors (IC_{50} = 2.6 µM and 1.8 µM against NR1/2A and NR1/2B, respectively), despite a longer 12-carbons linker, whereas tetrahydro-β-carboline analogues were globally less active. The other series produced molecules with much more variability in their AChE/BuChE and NMDA inhibition potencies: if the best AChE inhibitor **144** (IC_{50} = 0.5 nM) was also the most active against NMDA (IC_{50} = 1.4 µM and 2.9 µM, respectively), closely related analogues were found to be completely inactive against AChE (IC_{50} >10 µM) and NMDA (percentage of excitotoxicity at 25 µM around 100%). The activity of some compounds on MAO-A/B was also evaluated but yielded weak values. For reducing the molecular weight of the homobivalent β-carbolines in order to improve bioavailability while retaining both activities against AChE and NMDA, new β-carboline scaffolds were synthesized, but the results were underwhelming.[11] The best MTDL identified showed only weak activities compared to the homobivalent β-carbolines (IC_{50} = 0.6 µM against AChE and BuChE, 35 µM and 5 µM against NR1/2A and NR1/2B, respectively, for compound **145**). Nevertheless, the SAR studies corroborated the higher potency of quaternary derivatives for NMDA activity and demonstrated that the incorporation of a propargyl moiety, known for its neuroprotective properties in selegiline and rasagiline, has no beneficial effect herein.

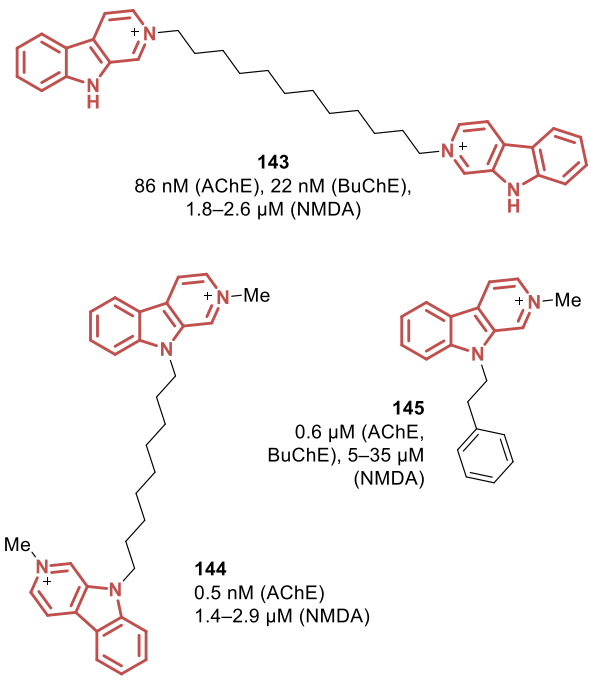

Figure 26. Selected structures and IC_{50} of β-carbolines as multitarget agents, inhibitors of AChE/BuChE and NMDA.

Targeting PDE5 and HDACs. Reminiscently of the respective works on PDE5 and HDAC inhibition, the development of dual inhibitors targeting both enzymes gathered the tadalafil scaffold and a linked zinc-chelating group. Especially, several mixtures of enantiomers bearing a hydroxamic acid head were examined.[177] While these compounds partially lost the initial anti-PDE5 potency of tadalafil **8**, and did not reach HDAC inhibition values similar to those obtained in HDAC-dedicated studies, in some cases submicromolar IC_{50} values were yielded. Especially, compound **146** associated an IC_{50} of 0.31 μM against PDE5 (a significant drop of activity compared to **8**, possibly due to the mixture of diastereoisomers tested) with values below 80 nM for HDAC1 and HDAC6 (Figure 27). While PDE5 inhibition was improved by implementing more flexible and/or shorter linkages between the tadalafil scaffold and the hydroxamic acid head, such modifications dramatically compromised anti-HDAC potency, regardless of the subtype (IC_{50} = 0.12 μM and 0.14 μM against PDE5 for **147** and **148**, *vs.* 2.5 μM to >20 μM for HDACs subtypes 1, 2 and 6). Similarly, the development

of *ortho*-aminoanilide analogues only afforded marginally active molecules (IC_{50} >2.0 µM against all tested targets).[178] However, a further focus on the activities of all isolated stereoisomers would shed light on the real potential of these structures. Besides, a series of isolated stereoisomers of slightly different structure was reported very recently.[179] Interestingly, some compounds managed to efficiently bind to HDACs while incorporating short linkers, an observation that contradicts previously described results. Even a four-carbon derivative, compound **149a**, was able to inhibit both PDE5 (IC_{50} = 12 nM) and HDAC (IC_{50} = 131 nM) with decent activity levels; shorter one-, two- and three-carbons analogues failed to efficiently bind HDAC, although their anti-PDE5 activities were exquisite (IC_{50} = 2.0–20 nM for four molecules). Compound **149b** was even more promising (IC_{50} = 7.0 nM and 61 nM against PDE5 and HDAC, respectively), but anti-PDE5 activity started to drop as the anti-HDAC effect increased with the introduction of a sixth carbon (*e.g.*, IC_{50} = 126 nM and 9.1 nM against PDE5 and HDAC, respectively, for compound **150**). The last molecule also showed some HDAC subtype selectivity, as if HDAC6 and HDAC8 were targeted with IC_{50} values of 90–200 nM, HDAC1 was associated with far weaker activity (IC_{50} = 1.65 µM). These results highlight the need for a balanced linker size and flexibility, as favorable elements for anti-PDE5 and anti-HDAC activities seem to be opposite.

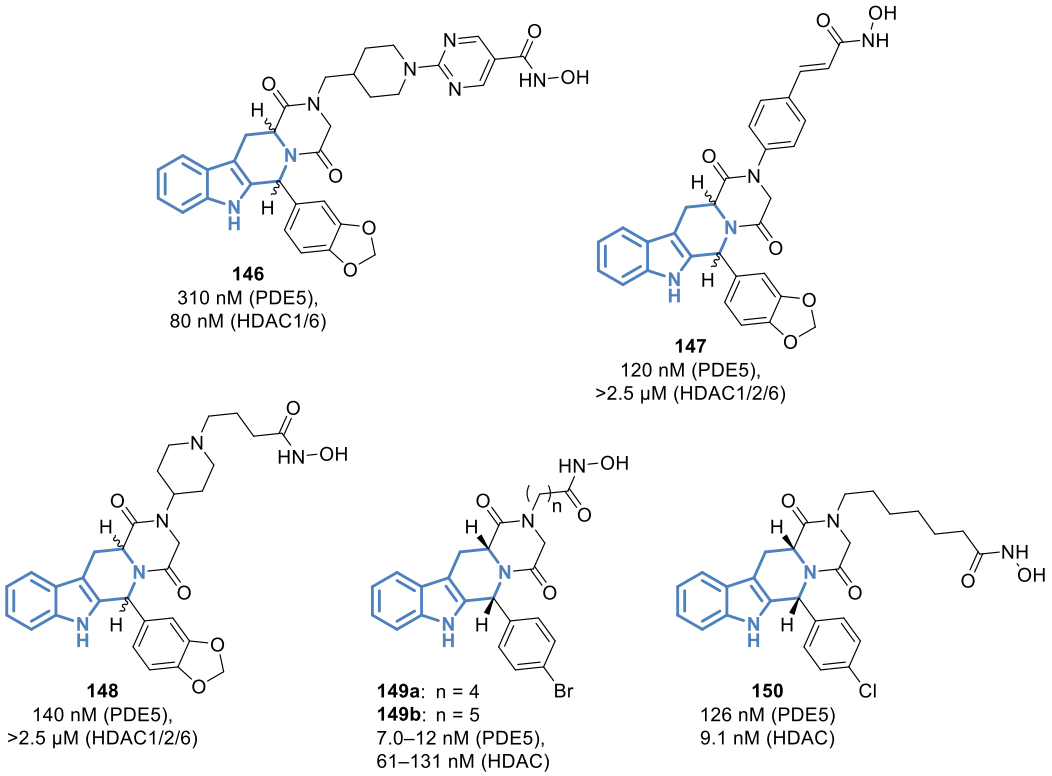

Figure 27. Selected structures and IC_{50} of β-carbolines as multitarget agents, inhibitors of PDE5 and HDAC.

Conclusion and prospects

To date, only symptomatic treatments are available for countering the progression of AD, and the development of new compounds presents higher failure rates, compared to other diseases. Yet, the initial "one-target-one-compound" paradigm has produced a great number of molecules for addressing individual targets involved in the etiology ofthe disease. But AD is intrinsically multifactorial, and the complex interplay of the pathogenesis has dismissed most of the studies performed with blinkers. The emergence of widely chosen multitargeting compounds, able to concurrently tackle several pathogenetic pathways, is a promising tool to take them off. Apart from classical drug combination and co-formulation, two main polypharmacological approaches have been of increasing importance in the past few years: the association of two or more ligands through an adequate linker; and the hybridization

between several active skeletons, often fused or merged to provide compact molecules with optimal size. Both strategies rely on successful stories and FDA-approved drugs in various contexts. In the particular case of AD, some specific limitations appear however. First, the lack of appropriate animal models for AD is critical and makes it difficult to retrieve preclinical data. Second, the necessity of the BBB crossing is a sizeable issue, hampering a full delivery of the biological activity for a wide range of compounds. However, the β-carboline scaffold has several assets. As a natural product family, it is attractive for CNS-targeting medicinal development: ~84% of approved drugs for CNS diseases are natural or bioinspired products. Furthermore, since natural derivatives from coffee or tobacco, such as harmane or norharmane, are known to readily exert neurological actions, the BBB crossing could not be an intractable concern for β-carbolines. In addition, the scaffold presents a high structural analogy with native brain molecules, such as neurotransmitters 5-HT or melatonin, indicating a probable capacity to easily transit throughout the brain and to interact with several biomolecules and receptors of interest. Indeed, numerous studies have demonstrated the potential of β-carbolines to target AD-related biomolecules, feeding an impressive and ever-growing SAR meta-analysis. Through this Perspective, we have first tried to draw up the main lines target by target, summarized in Figure 28. The scheme clearly shows that the β-carboline scaffold has been extensively exploited by medicinal chemists for the design of inhibitors of AD-related targets. Both rings have provided positive modifications, in almost every possible substitution positions. Additional fused rings have been added at several points, leading to highly modified analogues, often with very good activity records. While the SAR is overall very complex and hard to condense, several elements deserve to be highlighted. First, convergent favorable components are observed. The position 7 of the scaffold, when receiving an alkyl ether substituent, is able to foster the activity against DYRK1A, MAO, and $GABA_A$ to a lesser extent. Similar effects could be seen at position 2,

where the substitution of the intracyclic nitrogen promotes NMDA, AChE and PDE5 inhibition simultaneously, or at position 1, where the presence of close aryl groups (0–1-carbon linker) is a crucial feature for PDE5 inhibition and 5-HT receptor binding. Second, sometimes the structural features required for the activity are not linked to a particular position, providing a flexibility that is precious for MTDL design. This is the case for HDAC targeting, needing the presence of a zinc-chelating head, such as an hydroxamic acid moiety, which can be placed at various positions without compromising the activity. The binding to NMDA receptors is also conditional on the global 'V-like' shape of the compound, achievable through different molecular layouts starting from the initial rather linear skeleton. Finally, in some cases it appears to be possible to reach several targets by arranging independently several parts of the scaffold. As seen for example when examining the aforementioned crystal structures, at least a part of the molecule always points towards an open area, giving some latitude for modifying this position without triggering an activity loss. As such, it would be very engaging to see if the combination of a 5,6-fused heterocycle, for $GABA_A$ binding, with a β-carboline core extended at the opposite side with a hydantoin or a piperidine ring, for PDE5 inhibition (and for incidentally consolidating $GABA_A$ binding with the amido group thereby introduced at position 3) would deliver a retained activity against both targets — to take just one example. Overall, the meta-analysis performed herein could help researchers in the field to design new β-carbolines able to simultaneously or synergistically tackle multiple AD targets, while keeping a good ability to cross the BBB, for ultimately affording drug candidates of higher potential. By combining the targeting of disease-modifying pathways and symptomatic processes, the next-generation anti-AD agents represent a great promise for the future of AD treatments. The β-carboline platform would be a robust flagship for such an adventure.

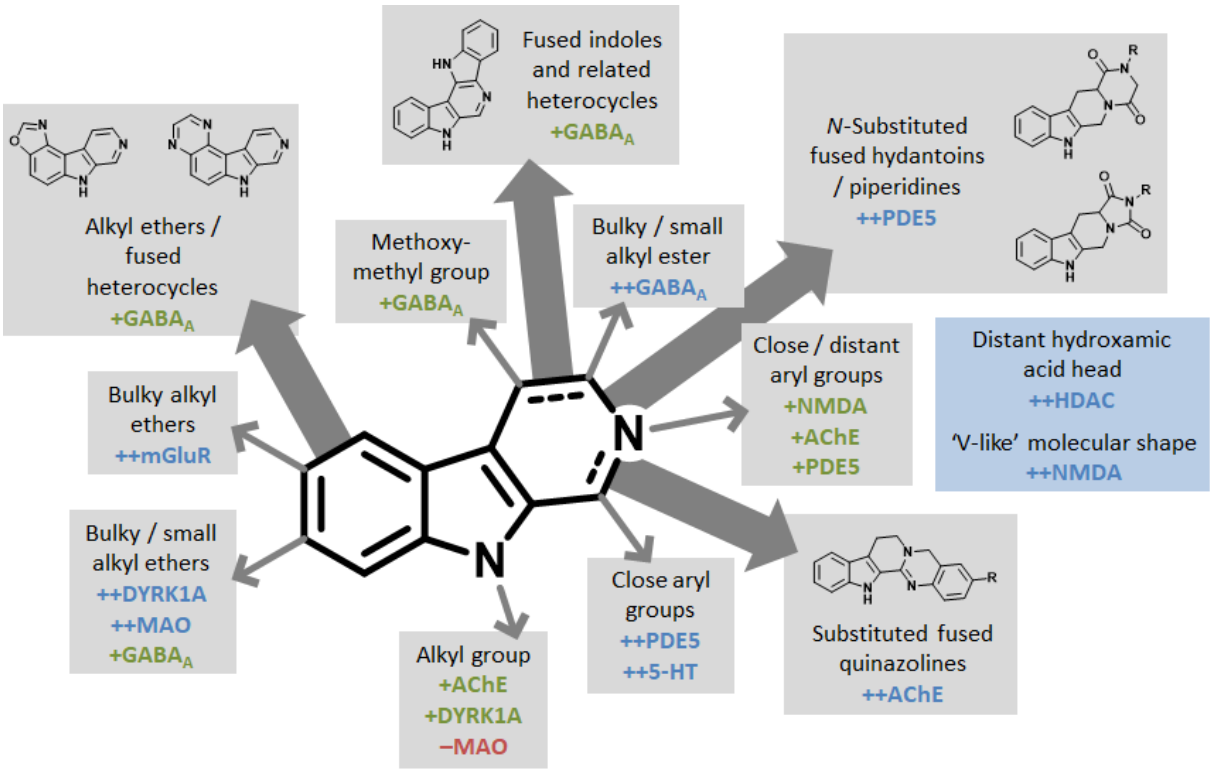

Figure 28. Overview of crucial (++), favorable (+) and unfavorable (–) elements of SAR regarding the effect of β-carbolines on the previously mentioned AD-related targets.

Author information

Corresponding Authors

Marine Peuchmaur – *Département de Pharmacochimie Moléculaire (DPM), UMR 5063, Univ. Grenoble Alpes, 38041 Grenoble, France*; orcid.org/0000-0002-8926-1922; Marine.Peuchmaur@univ-grenoble-alpes.fr

Romain Haudecoeur – *Département de Pharmacochimie Moléculaire (DPM), UMR 5063, Univ. Grenoble Alpes, 38041 Grenoble, France*; orcid.org/0000-0002-6271-4717; Romain.Haudecoeur@univ-grenoble-alpes.fr

Authors

Aurélien Beato – *Département de Pharmacochimie Moléculaire (DPM), UMR 5063, Univ. Grenoble Alpes, 38041 Grenoble, France*

Anthonin Gori – *Département de Pharmacochimie Moléculaire (DPM), UMR 5063, Univ. Grenoble Alpes, 38041 Grenoble, France and CHANEL Parfums Beauté, F-93500 Pantin, France*; orcid.org/0000-0001-6494-6768

Benjamin Boucherle – *Département de Pharmacochimie Moléculaire (DPM), UMR 5063, Univ. Grenoble Alpes, 38041 Grenoble, France*; orcid.org/0000-0002-1174-4449

Author Contributions

A.B. and A.G. contributed equally to this work.

Notes

The authors declare no competing financial interest.

Biographies

Aurélien Beato is a chemical engineer graduated from Sigma Clermont (France) in 2019 and is currently doing his second year Ph.D. thesis in Organic Chemistry at the Department of Medicinal Chemistry of University Grenoble Alpes (France) under the supervision of Dr. Marine Peuchmaur and Dr. Benjamin Boucherle. He is working on the diversity-oriented chemical modification of natural extracts of plants.

Anthonin Gori obtained his Ph.D. in Organic Chemistry and Phytochemistry from University Grenoble Alpes (France) in 2020 under the supervision of Dr. Marine Peuchmaur and Dr. Benjamin Boucherle (CIFRE grant, CHANEL Parfums Beauté). He was hired as

project leader at Clarins (France). His researches are essentially focused on natural products and bioactive compounds from plants.

Benjamin Boucherle is a Pharm.D. graduated from the University of Grenoble (2005). He obtained his Ph.D. in Medicinal Chemistry in 2008 under the supervision of Prof. J.-L. Décout, working on CFTR modulators. After a postdoctoral position (2009–2011) focused on protein–protein interaction inhibitors in the Chemistry School of Clermont-Ferrand (France), he moved back to Grenoble for a medicinal chemistry project targeting cystic fibrosis (2012–2015). He is currently lecturer in medicinal chemistry and pharmacognosy at the Faculty of Pharmacy at University Grenoble Alpes. His researches are dedicated to the development of bioactive substances from chemical synthesis or natural products isolation.

Marine Peuchmaur is a chemical engineer graduated from Ecole Nationale Supérieure de Chimie de Montpellier (France). She obtained in 2007 her Ph.D. in Chemical Biology from University Grenoble Alpes (France), under the supervision of Dr. Yung-Sing Wong. After two postdoctoral internships at the University of Montpellier (IBMM, France, 2007–2008) and at Trinity College (Dublin, Ireland, 2008–2009), she was hired in 2009 as a lecturer in organic chemistry at the Faculty of Pharmacy (University Grenoble Alpes). Her research work in the Department of Medicinal Chemistry focuses on both phytochemistry and organic synthesis for medicinal chemistry topics (design and synthesis of bioactive molecules or tools for biochemists). She received in 2015 the Accreditation to Supervise Research (HDR).

Romain Haudecoeur obtained his Ph.D. in Chemical Biology from University Grenoble Alpes (France) in 2011, under the supervision of Prof. Ahcène Boumendjel. He joined the group of Dr. David Monchaud at the University of Burgundy (Dijon, France) as a

postdoctoral associate in the same year. He was then appointed as Researcher in 2012 in the Department of Medicinal Chemistry of University Grenoble Alpes and received in 2020 the Accreditation to Supervise Research (HDR). His research work essentially focuses on the rational targeting of biological macromolecules, with the aim of developing new bioinspired, bioactive and smart compounds for modulating the function of proteins such as tyrosinases, viral polymerases and membrane ABC transporters.

Acknowledgements

The authors are grateful to ANR ("Agence Nationale de la Recherche") for financial support through Labex ARCANE and CBH-EUR-GS (Grant ANR-17-EURE-0003). The authors thank the French MESR ("Ministère de l'Enseignement supérieur, de la Recherche et de l'Innovation") for the fellowship grant of A.B. and the company Chanel Parfums Beauté and the ANRT ("Association Nationale Recherche Technologie") for the CIFRE ("Conventions Industrielles de Formation par la Recherche") grant of A.G. (Grant 2017/0042).

Abbreviations used

5-HT, 5-hydroxytryptamine; Aβ, amyloid-β; AChE, acetylcholinesterase; AD, Alzheimer's disease; APP, amyloid precursor protein; ATP, adenosine triphosphate; BACE1, β-site APP cleaving enzyme 1; BBB, blood-brain barrier; BuChE, butyrylcholinesterase; cAMP, cyclic adenosine monophosphate; CAS, catalytic active site; CDK5, cyclin-dependent kinase 5; cGMP, cyclic guanosine monophosphate; ChE, cholinesterase; CK1/2, casein kinase 1/2; CLK1, dual specificity protein kinase; CNS, central nervous system; CREB, cAMP response element-binding; DYRK1A, dual specificity tyrosine-phosphorylation-regulated kinase 1A;

FAD, flavin adenine dinucleotide; FDA, Food and Drug Administration; GABA, γ-aminobutyric acid; GSK-3β, glycogen synthase kinase 3; GTP, guanosine triphosphate; HDAC, histone deacetylase; NFTs, neurofibrillary tangles; mGluR, glutamate metabotropic receptor; NMDA, *N*-methyl-D-aspartate; NR, NMDA receptor subunits; MAO, monoamine oxidase; MAPK, mitogen-activated protein kinase; MTDL, multitarget-directed ligand; PAS, peripheral anionic site; PDB, Protein Data Bank; PDE, phosphodiesterase; ROS, reactive oxygen species; SAR, structure-activity relationship.

References

(1) Cao, R.; Peng, W.; Wang, Z.; Xu, A. β-Carboline alkaloids: biochemical and pharmacological functions. *Curr. Med. Chem.* **2007**, *14*, 479–500.

(2) Dai, J.; Dan, W.; Schneider, U.; Wang, J. β-Carboline alkaloids monomers and dimers: occurrence, structural diversity, and biological activities. *Eur. J. Med. Chem.* **2018**, *157*, 622–656.

(3) Nikam T. D.; Nitnaware K. M.; Ahire M. L. Alkaloids Derived from Tryptophan: Harmine and Related Alkaloids. In Natural Products; Ramawat, K. G., Mérillon J.-M., Eds.; Springer: Berlin, Heidelberg, 2013; pp 553–574.

(4) Abeysinghe, A. A. D. T.; Deshapriya R. D. U. S.; Udawatte, C. Alzheimer's disease; a review of the pathophysiological basis and therapeutic intervention. *Life Sci.* **2020**, *256*, 117996.

(5) Mohamed T.; Rao P. P. N.; Alzheimer's disease: emerging trends in small molecule therapies. *Curr. Med. Chem.* **2011**, *18*, 4299–4320.

(6) Xie, J.; Liang, R.; Wang, Y.; Cao, X.; Niu, B. Progress in target drug molecules for Alzheimer's disease. *Curr. Top. Med. Chem.* **2020**, **20**, 4–36.

(7) León, R.; Garcia A. G.; Marco-Contelles, J. Recent advances in the multitarget-directed ligands approach for the treatment of Alzheimer's disease. *Med. Res. Rev.* **2013**, *33*, 139–189.

(8) Guzior, N.; Więckowska, A.; Panek, D.; Malawska, B. Recent development of multifunctional agents as potential drug candidates for the treatment of Alzheimer's disease. *Curr. Med. Chem.* **2015**, *22*, 373–404.

(9) Maramai, S.; Benchekroun, M.; Gabr, M. T.; Yahiaoui, S. Multitarget therapeutic strategies for Alzheimer's disease: review on emerging target combinations. *BioMed Res. Int.* **2020**, 5120230.

(10) Ghosal, S.; Bhattachary S. K.; Mehta, R. Naturally occurring and synthetic β-carbolines as cholinesterase inhibitors. *J. Pharm. Sci.* **1972**, *61*, 808–810.

(11) Otto, R.; Penzis, R.; Gaube, F.; Winckler, T.; Appenroth, D.; Fleck, C.; Tränkle, C.; Lehmann, J.; Enzensperger, C. Beta and gamma carboline derivatives as potential anti-Alzheimer agents: a comparison. *Eur. J. Med. Chem.* **2014**, *87*, 63–70.

(12) Filali, I.; Bouajila, J.; Znati, M.; Bousejra-El Garah, F.; Ben Jannet, H. Synthesis of new isoxazoline derivatives from harmine and evaluation of their anti-Alzheimer, anti-cancer and anti-inflammatory activities. *J. Enz. Inhib. Med. Chem.* **2015**, *30*, 371–376.

(13) Filali, I.; Belkacem, M.A.; Ben Nejma, A.; Souchard, J.-P.; Ben Jannet, H.; Bouajila, J. Synthesis, cytotoxic, anti-lipoxygenase and anti-acetylcholinesterase capacities of novel derivatives from harmine. *J. Enz. Inhib. Med. Chem.* **2016**, *31*, 23–33.

(14) Khorana, N.; Changwichit, K.; Ingkaninan, K.; Utsintong, M. Prospective acetylcholinesterase inhibitory activity of indole and its analogs. *Bioorg. Med. Chem. Lett.* **2012**, *22*, 2885–2888.

(15) Zhao, T.; Ding, K.; Zhang, L.; Cheng, X.; Wang, C.; Wang, Z. Acetylcholinesterase and butyrylcholinesterase inhibitory activities of β-carboline and quinoline alkaloids derivatives from the plants of genus *Peganum*. *J. Chem.* **2013**, 717232.

(16) Liu, W.; Yang, Y.; Cheng, X.; Gong, C.; Li, S.; He, D.; Yang, L.; Wang, Z.; Wang, C. Rapid and sensitive detection of the inhibitive activities of acetyl- and butyryl-cholinesterases inhibitors by UPLC–ESI-MS/MS. *J. Pharm. Biomed. Anal.* **2014**, *94*, 215–220.

(17) Liew, S. Y.; Khaw, K. Y.; Murugaiyah, V.; Looi, C. Y.; Wong, Y. L.; Mustafa, M. R.; Litaudon, M.; Awang, K. Natural indole butyrylcholinesterase inhibitors from *Nauclea officinalis*. *Phytomedicine* **2015**, *22*, 45–48.

(18) Torres, J. M.; Lira, A. F.; Silva, D. R.; Guzzo, L. M.; Sant'Anna, C. M. R.; Kümmerle, A. E.; Rumjanek, V. M. Structural insights into cholinesterases inhibition by harmane β-carbolinium derivatives: a kinetics – molecular modeling approach. *Phytochemistry* **2012**, *81*, 24–30.

(19) Fadaeinasab, M.; Basiri, A.; Kia, Y.; Karimian, H.; Ali, H. M.; Murugaiyah, V. New indole alkaloids from the bark of *Rauvolfia reflexa* and their cholinesterase inhibitory activity. *Cell. Physiol. Biochem.* **2015**, *37*, 1997–2011.

(20) Schott, Y.; Decker, M.; Rommelspacher, H.; Lehmann, J. 6-Hydroxy- and 6-methoxy-β-carbolines as acetyl- and butyrylcholinesterase inhibitors. *Bioorg. Med. Chem. Lett.* **2006**, *16*, 5840–5843.

(21) Yang, Y.; Cheng, X.; Liu, W.; Chou, G.; Wang, Z.; Wang, C. Potent AChE and BChE inhibitors isolated from seeds of *Peganum harmala* Linn by a bioassay-guided fractionation. *J. Ethnopharmacol.* **2015**, *168*, 279–286.

(22) Arshad, A. S. M.; Chear, N. J. Y.; Ezzat, M. O.; Hanapi, N. A.; Meesala, R.; Arshad, S.; Mansor, S. M.; Mordi, M. N. Synthesis, characterization and crystal structure of new tetrahydro-β-carboline as acetylcholinesterase inhibitor. *J. Mol. Struct.* **2020**, *1200*, 127070.

(23) Zhang, J.; Zhao, S.-S.; Xie, J.; Yang, J.; Chen, G.-D.; Hu, D.; Zhang, W.-G.; Wang, C.-X.; Yao, X.-S.; Gao, H. *N*-methoxy-*β*-carboline alkaloids with inhibitory activities against Aβ_{42} aggregation and acetylcholinesterase from the stems of *Picrasma quassioides*. *Bioorg. Chem.* **2020**, *101*, 104043.

(24) Fadaeinasab, M.; Hadi, A. H. A.; Kia, Y.; Basiri, A.; Murugaiyah, V. Cholinesterase enzymes inhibitors from the leaves of *Rauvolfia reflexa* and their molecular docking study. *Molecules* **2013**, *18*, 3779–3788.

(25) Abuhamdah, S.; Habash, M.; Taha, M. O. Elaborate ligand-based modeling coupled with QSAR analysis and in silico screening reveal new potent acetylcholinesterase inhibitors. *J. Comput. Aided Mol. Des.* **2013**, *27*, 1075–1092.

(26) Horton, W.; Sood, A.; Peerannawar, S.; Kugyela, N.; Kulkarni, A.; Tulsan, R.; Tran, C. D.; Soule, J.; LeVine III, H.; Török, B.; Török, M. Synthesis and application of β-carbolines as novel multi-functional anti-Alzheimer's disease agents. *Bioorg. Med. Chem. Lett.* **2017**, *27*, 232–236.

(27) Tadokoro, Y.; Nishikawa, T.; Ichimori, T.; Matsunaga, S.; Fujita, M. J.; Sakai, R. *N*-Methyl-*β*-carbolinium salts and an *N*-methylated 8-oxoisoguanine as acetylcholinesterase inhibitors from a solitary ascidian, *Cnemidocarpa irene*. *ACS Omega* **2017**, *2*, 1074–1080.

(28) Rook, Y.; Schmidtke, K.-U.; Gaube, F.; Schepmann, D.; Wünsch, B.; Heilmann, J.; Lehmann, J.; Winckler, T. Bivalent *β*-carbolines as potential multitarget anti-Alzheimer agents. *J. Med. Chem.* **2010**, *53*, 3611–3617.

(29) Yang, Y.; Cheng, X.; Liu, W.; Han, Z.; Chou, G.; Wang, Y.; Sun, D.; Wang, Z.; Wang, C. Peganumine B–I and two enantiomers: new alkaloids from the seeds of *Peganum harmala* Linn. and their potential cytotoxicity and cholinesterase inhibitory activities. *RSC Adv.* **2016**, *6*, 15976–15987.

(30) Zhou, B.; Zhang, B.; Li, X.; Liu, X.; Li, H.; Li, D.; Cui, Z.; Geng, H.; Zhou, L. New 2-aryl-9-methyl-*β*-carbolinium salts as potential acetylcholinesterase inhibitor agents: synthesis, bioactivity and structure–activity relationship. *Sci. Rep.* **2018**, *8*, 1559.

(31) Cao, X.-F.; Wang, J.-S.; Wang, X.-B.; Luo, J.; Wang, H.-Y.; Kong, L.-Y. Monoterpene indole alkaloids from the stem bark of *Mitragyna diversifolia* and their acetylcholine esterase inhibitory effects. *Phytochemistry* **2013**, *96*, 389–396.

(32) Cardoso, C. L.; Castro-Gamboa, I.; Siqueira Silva, D. H.; Furlan, M.; de A. Epifanio, R.; da Cunha Pinto, A.; Moraes de Rezende, C.; Alencar Lima, J.; da Silva Bolzani, V. Indole glucoalkaloids from *Chimarrhis turbinata* and their evaluation as antioxidant agents and acetylcholinesterase inhibitors. *J. Nat. Prod.* **2004**, *67*, 1882–1885.

(33) Passos, C. S.; Simões-Pires, C. A.; Nurisso, A.; Soldi, T. C.; Kato, L.; de Oliveira, C. M. A.; de Faria, E. O.; Marcourt, L.; Gottfried, C.; Carrupt, P.-A.; Henriques, A.T. Indole alkaloids of *Psychotria* as multifunctional cholinesterases and monoamine oxidases inhibitors. *Phytochemistry* **2013**, *86*, 8–20.

(34) Mroue, M.A.; Euler, K.L.; Ghuman, M.A.; Alam, M. Indole alkaloids of *Haplophyton crooksii*. *J. Nat. Prod.* **1996**, *59*, 890–893.

(35) Jiang, W.-W.; Su, J.; Wu, X.-D.; He, J.; Peng, L.-Y.; Cheng, X.; Zhao, Q.-S. Geissoschizine methyl ether *N*-oxide, a new alkaloid with antiacetylcholinesterase activity from *Uncaria rhynchophylla*. *Nat. Prod. Res.* **2015**, *29*, 842–847.

(36) Geissler, T.; Brandt, W.; Porzel, A.; Schlenzig, D.; Kehlen, A.; Wessjohann, L.; Arnold, N. Acetylcholinesterase inhibitors from the toadstool *Cortinarius infractus*. *Bioorg. Med. Chem.* **2010**, *18*, 2173–2177.

(37) Kashyap, P.; Kalaiselvan, V.; Kumar, R.; Kumar, S. Ajmalicine and reserpine: indole alkaloids as multi-target directed ligands towards factors implicated in Alzheimer's disease. *Molecules* **2020**, *25*, 1609.

(38) Perreira, D. M.; Ferreres, F.; Oliveira, J. M. A.; Gaspar, L.; Faria, J.; Valentão, P.; Sottomayor, M.; Andrade, P. B. Pharmacological effects of *Catharanthus roseus* root alkaloids in acetylcholinesterase inhibition and cholinergic neurotransmission. *Phytomedicine* **2010**, *17*, 646–652.

(39) Bharate, S. B.; Manda, S.; Joshi, P.; Singh, B.; Vishwakarma, R. A. Total synthesis and anti-cholinesterase activity of marine-derived bis-indole alkaloid fascaplysin. *Med. Chem. Commun.* **2012**, *3*, 1098–1103.

(40) Decker, M. Novel inhibitors of acetyl- and butyrylcholinesterase derived from the alkaloids dehydroevodiamine and rutaecarpine. *Eur. J. Med. Chem.* **2005**, *40*, 305–313.

(41) Huang, G.; Kling, B.; Darras, F. H.; Heilmann, J.; Decker, M. Identification of a neuroprotective and selective butyrylcholinesterase inhibitor derived from the natural alkaloid evodiamine. *Eur. J. Med. Chem.* **2014**, *81*, 15–21.

(42) Wang, B.; Mai, Y.-C.; Li, Y.; Hou, J.-Q.; Huang, S.-L.; Ou, T.-M.; Tan, J.-H.; An, L.-K.; Li, D.; Gu, L.-Q.; Huang, Z.-S. Synthesis and evaluation of novel rutaecarpine derivatives and

related alkaloids derivatives as selective acetylcholinesterase inhibitors. *Eur. J. Med. Chem.* **2010**, *45*, 1415–1423.

(43) Jiaranaikulwanitch, J.; Boonyarat, C.; Fokin, V. V.; Vajragupta, O. Triazolyl tryptoline derivatives as β-secretase inhibitors. *Bioorg. Med. Chem. Lett.* **2010**, *20*, 6572–6576.

(44) Pereira, C.; Agostinho, P.; Oliveira, C. R. Vinpocetine attenuates the metabolic dysfunction induced by amyloid β-peptides in PC12 cells. *Free Rad. Res.* **2000**, *33*, 497–506.

(45) Zhang, Y.; Wang, J.; Wang, C.; Li, Z.; Liu, X.; Zhang, J.; Lu, J.; Wand, D. Pharmacological basis for the use of evodiamine in Alzheimer's disease: antioxidation and antiapoptosis. *Int. J. Mol. Sci.* **2018**, *19*, 1527–1540.

(46) Sun, Q.; Liu, F.; Sang, J.; Lin, M.; Ma, J.; Xiao, X.; Yan, S.; Naman, C. B.; Wang, N.; He, S.; Yan, X.; Cui, W.; Liang, H. 9-methylfascaplysin is a more potent Aβ aggregation inhibitor than the marine-derived alkaloid, fascaplysin, and produces nanomolar neuroprotective effects in SH-SY5Y cells. *Mar. Drugs* **2019**, *17*, 121–135.

(47) Guo, E.; Hu, Y.; Du, T.; Zhu, H.; Chen, L.; Qu, W.; Zhang, J.; Xie, N.; Liu, W.; Feng, F.; Xu, J. Effects of *Picrasma quassioides* and its active constituents on Alzheimer's disease *in vitro* and *in vivo*. *Bioorg. Chem.* **2019**, *92*, 103258–103266.

(48) Martin, L.; Latypova, X.; Wilson, C. M.; Magnaudeix, A.; Perrin, M.-L.; Yardin, C.; Terro, F. Tau protein kinases: involvement in Alzheimer's disease. *Ageing Res. Rev.* **2013**, *12*, 289–309.

(49) Frost, D.; Meechoovet, B.; Wang, T.; Gately, S.; Giorgetti, M.; Shcherbakova, I.; Dunckley, T. β-Carboline compounds, including harmine, inhibit DYRK1A and tau phosphorylation at multiple Alzheimer's disease-related sites. *PLoS One* **2011**, *6*, e19264.

(50) Adayev, T.; Wegiel, J.; Hwang, Y.-W. Harmine is an ATP-competitive inhibitor for dual-specificity tyrosine phosphorylation-regulated kinase 1A (Dyrk1A). *Arch. Biochem. Biophys.* **2011**, *507*, 212–218.

(51) Bain, J.; Plater, L.; Elliott, M.; Shpiro, N.; Hastie, C. J.; McLauchlan, H.; Klevernic, I.; Arthur, J. S. C.; Alessi, D. R.; Cohen, P. The selectivity of protein kinase inhibitors: a further update. *Biochem. J.* **2007**, *408*, 297–315.

(52) Cozza, G.; Sarno, S.; Ruzzene, M.; Girardi, C.; Orzeszko, A.; Kazimierczuk, Z.; Zagotto, G.; Bonaiuto, E.; Di Paolo, M. L.; Pinna, L. A. Exploiting the repertoire of CK2 inhibitors to target DYRK and PIM kinases. *Biochim. Biophys. Acta* **2013**, *1834*, 1402–1409.

(53) Göckler, N.; Jofre, G.; Papadopoulos, C.; Soppa, U.; Tejedor, F. J.; Becker, W. Harmine specifically inhibits protein kinase DYRK1A and interferes with neurite formation. *FEBS J.* **2009**, *276*, 6324–6337.

(54) Grabher, P.; Durieu, E.; Kouloura, E.; Halabalaki, M.; Skaltsounis, L.A.; Meijer, L.; Hamburger, M.; Potterat, O. Library-based discovery of DYRK1A/CLKA inhibitors from natural product extracts. *Planta Med.* **2012**, *78*, 951–956.

(55) Mariano, M.; Hartmann, R. W.; Engel, M. Systematic diversification of benzylidene heterocycles yields novel inhibitor scaffolds selective for Dyrk1A, Clk1 and CK2. *Eur. J. Med. Chem.* **2016**, *112*, 209–216.

(56) Tahtouh, T.; Elkins, J. M.; Filippakopoulos, P.; Soundararajan, M.; Burgy, G.; Durieu, E.; Cochet, C.; Schmid, R. S.; Lo, D. C.; Delhommel, F.; Oberholzer, A. E.; Pearl, L. H.; Carreaux, F.; Bazureau, J.-P.; Knapp, S.; Meijer, L. Selectivity, cocrystal structures, and neuroprotective properties of leucettines, a family of protein kinase inhibitors derived from the marine sponge alkaloid leucettamine B. *J. Med. Chem.* **2012**, *55*, 9312–9330.

(57) Loidreau, Y.; Dubouilh-Benard, C.; Nourrisson, M.-R.; Loaëc, N.; Meijer, L.; Besson, T.; Marchand, P. Exploring kinase inhibition properties of 9*H*-pyrimido[5,4-*b*]- and [4,5-*b*]indol-4-amine derivatives. *Pharmaceuticals* **2020**, *13*, 89.

(58) Drung, B.; Scholz, C.; Barbosa, V. A.; Nazari, A.; Sarragiotto, M. H.; Schmidt, B. Computational & experimental evaluation of the structure/activity relationship of β-carbolines as DYRK1A inhibitors. *Bioorg. Med. Chem. Lett.* **2014**, *24*, 4854–4860.

(59) Rüben, K.; Wurzlbauer, A.; Walte, A.; Sippi, W.; Bracher, F.; Becker, W. Selectivity profiling and biological activity of novel β-carbolines as potent and selective DYRK1 kinase inhibitors. *PLoS One* **2015**, *10*, e0132453.

(60) Balint, B.; Weber, C.; Cruzalegui, F.; Burbridge, M.; Kotschy, A. Structure-based design and synthesis of harmine derivatives with different selectivity profiles in kinase versus monoamine oxidase inhibition. *ChemMedChem* **2017**, *12*, 932–939.

(61) Kumar, K.; Wang, P.; Wilson, J.; Zlatanic, V.; Berrouet, C.; Khamrui, S.; Secor, C.; Swartz, E. A.; Lazarus, M.; Sanchez, R.; Stewart, A. F.; Garcia-Ocana, A.; DeVita, R. J. Synthesis and biological validation of a harmine-based, central nervous system (CNS)-avoidant, selective, human *β*-cell regenerative dual-specificity tyrosine phosphorylation-regulated kinase A (DYRK1A) inhibitor. *J. Med. Chem.* **2020**, *63*, 2986–3003.

(62) Ogawa, Y.; Nonaka, Y.; Goto, T.; Ohnishi, E.; Hiramatsu, T.; Kii, I.; Yoshida, M.; Ikura, T.; Onogi, H.; Shibuya, H.; Hosoya, T.; Ito, N.; Hagiwara, M. Development of a novel selective inhibitor of the Down syndrome-related kinase Dyrk1A. *Nat. Commun.* **2010**, *1*, 86.

(63) Chaikuad, A.; Wurzlbauer, A.; Nowak, R.; von Delft, F.; Arrowsmith, C. H.; Edwards, A. M.; Bountra, C.; Bracher, F.; Knapp, S. Crystal structure of DYRK1A with harmine-derivatized AnnH-75 inhibitor. PDB entry 4YU2 (DOI: 10.2210/pdb4YU2/pdb).

(64) Song, Y.; Kesuma, D.; Wang, J.; Deng, Y.; Duan, J.; Wang, J. H.; Qi, R. Z. Specific inhibition of cyclin-dependent kinases and cell proliferation by harmine. *Biochem. Biophys. Res. Commun.* **2004**, *317*, 128–132.

(65) Dasappa, J. K.; Nagendra, H. G. Preferential selectivity of inhibitors with human tau protein kinase Gsk3*β* elucidates their potential roles for off-target Alzheimer's therapy. *Int. J. Alz. Dis.* **2013**, 809386.

(66) Deslandes, S.; Lamoral-Theys, D.; Frongia, C.; Chassaing, S.; Bruyère, C.; Lozach, O.; Meijer, L.; Ducommun, B.; Kiss, R.; Delfourne, E. Synthesis and biological evaluation of analogs of the marine alkaloids granulatimide and isogranulatimide. *Eur. J. Med. Chem.* **2012**, *54*, 626–636.

(67) Hamann, M.; Alonso, D.; Martin-Aparicio, E.; Fuertes, A.; Pérez-Puerto, M. J.; Castro, A.; Morales, S.; Navarro, M. L.; del Monte-Millan, M.; Medina, M.; Pennaka, H.; Balaiah, A.; Peng, J.; Cook, J.; Wahyuono, S.; Martinez, A. Glycogen synthase kinase-3 (GSK-3) inhibitory activity and structure–activity relationship (SAR) studies of the manzamine alkaloids. Potential for Alzheimer's disease. *J. Nat. Prod.* **2007**, *70*, 1397–1405.

(68) Song, Y.; Wang, J.; Teng, S. F.; Kesuma, D.; Deng, Y.; Duan, J.; Wang, J. H.; Qi, R. Z.; Sim, M. M. β-Carbolines as specific inhibitors of cyclin-dependent kinases. *Bioorg. Med. Chem. Lett.* **2002**, *12*, 1129–1132.

(69) Herraiz, T.; Chaparro, C. Human monoamine oxidase is inhibited by tobacco smoke: β-carboline alkaloids act as potent and reversible inhibitors. *Biochem. Biophys. Res. Commun.* **2005**, *326*, 378–386.

(70) Herraiz, T.; Chaparro, C. Human monoamine oxidase enzyme inhibition by coffee and β-carbolines norharman and harman isolated from coffee. *Life Sci.* **2006**, *78*, 795–802.

(71) Rommelspacher, H.; May, T.; Salewski, B. Harman (1-methyl-β-carboline) is a natural inhibitor of monoamine oxidase type A in rats. *Eur. J. Pharmacol.* **1994**, *252*, 51–59.

(72) Santillo, M.F.; Liu, Y.; Ferguson, M.; Vohra, S.N.; Wiesenfeld, P. L. Inhibition of monoamine oxidase (MAO) by β-carbolines and their interactions in live neuronal (PC12) and liver (HuH-7 and MH1C1) cells. *Toxicol. Vitro* **2014**, *28*, 403–410.

(73) Fernandez de Arriba, A.; Lizcano, J. M.; Balsa, M. D.; Unzeta, M. Inhibition of monoamine oxidase from bovine retina by β-carbolines. *J. Pharm. Pharmacol.* **1994**, *46*, 809–813.

(74) Samoylenko, V.; Rahman, M. M.; Tekwani, B. L.; Tripathi, L. M.; Wang, Y.-H.; Khan, S. I.; Khan, I. A.; Miller, L. S.; Joshi, V. C.; Muhammad, I. *Banisteriopsis caapi*, a unique combination of MAO inhibitory and antioxidative constituents for the activities relevant to neurodegenerative disorders and Parkinson's disease. *J. Ethnopharmacol.* **2010**, *127*, 357–367.

(75) Haider, S.; Alhusban, M.; Chaurasiya, N. D.; Tekwani, B. L.; Chittiboyina, A. G.; Khan, I. A. Isoform selectivity of harmine-conjugated 1,2,3-triazoles against human monoamine oxidase. *Future Med. Chem.* **2018**, *10*, 1435–1448.

(76) Son, S.-Y.; Ma, J.; Kondou, Y.; Yoshimura, M.; Yamashita, E.; Tsukihara, T. Structure of human monoamine oxidase A at 2.2-Å resolution: the control of opening the entry for substrates/inhibitors. *Proc. Natl. Acad. Sci. USA* **2008**, *105*, 5739–5744.

(77) Binda, C.; Li, M.; Hubalek, F.; Restelli, N.; Edmondson, D. E.; Mattevi, A. Insights into the mode of inhibition of human mitochondrial monoamine oxidase B from high-resolution crystal structures. *Proc. Natl. Acad. Sci. USA* **2003**, *100*, 9750–9755.

(78) Reniers, J.; Robert, S.; Frederick, R.; Masereel, B.; Vincent, S.; Wouters, J. Synthesis and evaluation of β-carboline derivatives as potential monoamine oxidase inhibitors. *Bioorg. Med. Chem.* **2011**, *19*, 134–144.

(79) Glover, V.; Liebowitz, J.; Armando, I.; Sandler, M. *β*-Carbolines as selective monoamine oxidase inhibitors: *in vivo* implications. *J. Neural Transmission* **1982**, *54*, 209–218.

(80) Miralles, A.; Esteban, S.; Sastre-Coll, A.; Moranta, D.; Asensio, V. J.; Garcia-Sevilla, J.A. High-affinity binding of β-carbolines to imidazoline I_{2B} receptors and MAO-A in rat tissues: norharman blocks the effect of morphine withdrawal on DOPA/noradrenaline synthesis in the brain. *Eur. J. Pharmacol.* **2005**, *518*, 234–242.

(81) Herraiz, T.; Chaparro, C. Analysis of monoamine oxidase enzymatic activity by reversed-phase high performance liquid chromatography and inhibition by β-carboline alkaloids occurring in foods and plants. *J. Chromatogr. A* **2006**, *1120*, 237–243.

(82) Meller, E.; Friedman, E.; Schweitzer, J. W.; Friedhoff, A. J. Tetrahydro-*β*-carbolines: specific inhibitors of type A monoamine oxidase in rat brain. *J. Neurochem.* **1977**, *28*, 995–1000.

(83) Kim, H.; Sablin, S. O.; Ramsay, R. R. Inhibition of monoamine oxidase A by *β*-carboline derivatives. *Arch. Biochem. Biophys.* **1997**, *337*, 137–142.

(84) Heckman, P. R. A.; Wouters, C.; Prickaerts, J. Phosphodiesterase inhibitors as a target for cognition enhancement in aging and Alzheimer's disease: a translational overview. *Curr. Pharm. Des.* **2015**, *21*, 317–331.

(85) García-Osta, A.; Cuadrado-Tejedor, M.; García-Barroso, C.; Oyarzábal, J.; Franco, R. Phosphodiesterase as therapeutic targets for Alzheimer's disease. *ACS Chem. Neurosci.* **2012**, *3*, 832–844.

(86) Shang, Y.; Wang, L.; Li, Y.; Gu, P.-f. Vinpocetine improves scopolamine induced learning and memory dysfunction in C57 BL/6J mice. *Biol. Pharm. Bull.* **2016**, *39*, 1412–1418.

(87) Abdelwaly, A.; Salama, I.; Gomaa, M.; Helal, M. A. Discovery of tetrahydro-β-carboline derivatives as a new class of phosphodiesterase 4 inhibitors. *Med. Chem. Res.* **2017**, *26*, 3173–3187.

(88) García-Barroso, C.; Ricobaraza, A.; Pascual-Lucasa, M.; Unceta, N.; Rico, A. J.; Goicolea, M.; Sallés, J.; Lanciego, J.; Oyarzábal, J.; Franco, R.; Cuadrado-Tejedor, M.; García-Osta, A. Tadalafil crosses the blood brain barrier and reverses cognitive dysfunction in a mouse model of AD. *Neuropharmacology*. **2012**, *64*, 114–123.

(89) Abadi, A. H.; Abouel-Ella, D. A.; Ahmed, N. S.; Gary, B. D.; Thaiparambil, J. T.; Tinsley, H. N.; Keeton, A. B.; Piazza, G. A. Synthesis of novel tadalafil analogues and their evaluation as phosphodiesterase inhibitors and anticancer agents. *Arzneimittelforschung* **2009**, *59*, 415–421.

(90) Abadi, A. H.; Gary, B. D.; Tinsley, H. N.; Piazza, G. A.; Abdel-Halim, M. Synthesis, molecular modeling and biological evaluation of novel tadalafil analogues as phosphodiesterase 5 and colon tumor cell growth inhibitors, new stereochemical perspective. *Eur. J. Med. Chem.* **2010**, *45*, 1278–1286.

(91) Abadi, A. H.; Lehmann, J.; Piazza, G. A.; Abdel-Halim, M.; Ali, M.S.M. Synthesis, molecular modeling, and biological evaluation of novel tetrahydro-β-carboline hydantoin and tetrahydro-β-carboline thiohydantoin derivatives as phosphodiesterase 5 inhibitors. *Int. J. Med. Chem.* **2011**, 562421.

(92) Ahmed, N. S.; Gary, B. D.; Tinsley, H. N.; Piazza, G. A.; Laufer, S.; Abadi, A. H. Design, synthesis and structure–activity relationship of functionalized tetrahydro-β-carboline derivatives as novel PDE5 inhibitors. *Arch. Pharm. Chem. Life Sci.* **2011**, *11*, 149–157.

(93) El-Gamil, D. S.; Ahmed, N. S.; Gary, B. D.; Piazza, G. A.; Engel, M.; Hartmann, R. W.; Abadi, A. H. Design of novel β-carboline derivatives with pendant 5-bromothienyl and their evaluation as phosphodiesterase-5 inhibitors. *Arch. Pharm. Chem. Life Sci.* **2013**, *346*, 23–33.

(94) Sui, Z.; Guan, J.; Macielag, M. J.; Jiang, W.; Qiu, Y.; Kraft, P.; Bhattacharjee, S.; John, T.M.; Craig, E.; Haynes-Johnson, D.; Clancy, J. Synthesis and biological activities of novel β-carbolines as PDE5 inhibitors. *Bioorg. Med. Chem. Lett.* **2003**, *13*, 761–765.

(95) Huang, X.-F.; Dong, Y.-H.; Wang, J.-H.; Ke, H.-M.; Song, G.-Q.; Xu, D.-F. Novel PDE5 inhibitors derived from rutaecarpine for the treatment of Alzheimer's disease. *Bioorg. Med. Chem. Lett.* **2020**, *30*, 127097.

(96) Daugan A.; Grondin, P.; Ruault, C.; Le Monnier de Gouville, A.-C.; Coste, H.; Kirilovsky, J.; Hyafil, F.; Labaudinière, R. The discovery of tadalafil: a novel and highly selective PDE5 inhibitor. 1: 5,6,11,11a-tetrahydro-1*H*-imidazo[1',5':1,6]pyrido[3,4-*b*]indole-1,3(2*H*)-dione analogues. *J. Med. Chem.* **2003**, *46*, 4525–4532.

(97) Ahmed, N. S.; Ali, A. H.; El-Nashar, S. M.; Gary, B. D.; Fajardo, A. M.; Tinsley, H. N.; Piazza, G. A.; Negri, M.; Abadi, A. H. Exploring the PDE5 H-pocket by ensemble docking and structure-based design and synthesis of novel β-carboline derivatives. *Eur. J. Med. Chem.* **2012**, *57*, 329–343.

(98) Daugan A.; Grondin, P.; Ruault, C.; Le Monnier de Gouville, A.-C.; Coste, H.; Linget, J.-M.; Kirilovsky, J.; Hyafil, F.; Labaudinière, R. The discovery of tadalafil: a novel and

highly selective PDE5 inhibitor. 2: 2,3,6,7,12,12a-hexahydropyrazino[1',2':1,6]pyrido[3,4-*b*]indole-1,4-dione analogues. *J. Med. Chem.* **2003**, *46*, 4533–4542.

(99) Sung, B.-J.; Hwang, K. Y.; Jeon, Y. H.; Lee, J. I.; Heo, Y.-S.; Kim, J. H.; Moon, J.; Yoon, J. M.; Hyun, Y.-L.; Kim, E.; Eum, S. J.; Park, S.-Y.; Lee, J.-O.; Lee, T. G.; Ro, S.; Cho, J. M. Structure of the catalytic domain of human phosphodiesterase 5 with bound drug molecules. *Nature* **2003**, *425*, 98–102.

(100) Card, G. L.; England, B. P.; Suzuki, Y.; Fong, D.; Powell, B.; Lee, B.; Luu, C.; Tabrizizad, M.; Gillette, S.; Ibrahim, P. N.; Artis, D. R.; Bollag, G.; Milburn, M. V.; Kim, S.-H.; Schlessinger, J.; Zhang, K.Y.J. Structural basis for the activity of drugs that inhibits phosphodiesterases. *Structure* **2004**, *12*, 2233–2247.

(101) Felding, J.; Sorensen, M. D.; Poulsen, T. D.; Larsen, J.; Andersson, C.; Refer, P.; Engell, K.; Ladefoged, L. G.; Thormann, T.; Vinggaard, A. M.; Hegardt, P.; Sohoel, A.; Nielsen, S. F. Discovery and early clinical development of 2-{6-[2-(3,5-Dichloro-4-pyridyl)acetyl]-2,3-dimethoxyphenoxy}-*N*-propylacetamide (LEO 29102), a soft-drug inhibitor of phosphodiesterase 4 for topical treatment of atopic dermatitis. *J. Med. Chem.* **2014**, *57*, 5893–5903.

(102) Beghyn, T.; Hounsou, C.; Deprez, B. P. PDE5 inhibitors: an original access to novel potent arylated analogues of tadalafil. *Bioorg. Med. Chem. Lett.* **2007**, *17*, 789–792.

(103) Maw, G. N.; Allerton, C. M. N.; Gbekor, E.; Million, W. A. Design, synthesis and biological activity of β-carboline-based type-5 phosphodiesterase inhibitors. *Bioorg. Med. Chem. Lett.* **2003**, *13*, 1425–1428.

(104) Elhady, A. K.; Sigler, S. C.; Noureldin, N.; Canzoneri, J. C.; Ahmed, N. S.; Piazza, G. A.; Abadi, A. H. Structure-based design of novel tetrahydro-beta-carboline derivatives with a

hydrophilic side chain as potential phosphodiesterase inhibitors. *Sci. Pharm.* **2016**, *84*, 428–446.

(105) Beghyn, T. B.; Charton, J.; Leroux, F.; Henninot, A.; Reboule, I.; Cos, P.; Maes, L.; Deprez, B. Drug-to-genome-to-drug, step 2: reversing selectivity in a series of antiplasmodial compounds. *J. Med. Chem.* **2012**, *55*, 1274–1286.

(106) Tamiz, A. P.; Whittemore, E. R.; Woodward, R. M.; Upasani, R. B.; Keana, J. F. W. Structure-activity relationship for a series of 2-substituted 1,2,3,4-tetrahydro-9*H*-pyrido[3,4-*b*]indoles : potent subtype-selective inhibitors of *N*-methyl-D-aspartate (NMDA) receptors. *Bioorg. Med. Chem. Lett.* **1999**, *9*, 1619–1624.

(107) Espinoza-Moraga, M.; Caballero, J.; Gaube, F.; Winckler, T.; Santos, L. S. 1-Benzyl-1,2,3,4-tetrahydro-*β*-carboline as channel blocker of *N*-methyl-D-aspartate receptors. *Chem. Biol. Drug Des.* **2012**, *79*, 594–599.

(108) Pereira N. A. L.; Sureda F. X.; Pérez M.; Amat M.; Santos M. M. M. Enantiopure indolo[2,3-*a*]quinolizidines: synthesis and evaluation as NMDA receptor antagonists. *Molecules* **2016**, *21*, 1027–1038.

(109) Lee, H.-g.; Zhu, X.; O'Neill, M. J.; Webber, K.; Casadesus, G.; Marlatt, M.; Raina K. R.; Perry, G.; Smith, M. A. The role of metabotropic glutamate receptors in Alzheimer's disease. *Acta Neurobiol. Exp.* **2004**, *64*, 89–98.

(110) Di Fabio, R.; Micheli, F.; Alvaro, G.; Cavanni, P.; Donati, D.; Gagliardi, T.; Fontana, G.; Giovannini, R.; Maffeis, M.; Mingardi, A.; Tranquillini, M. E.; Vitulli, G. From pyrroles to 1-oxo-2,3,4,9-tetrahydro-1*H*-β-carbolines: a new class of orally bioavailable mGluR1 antagonists. *Bioorg. Med. Chem. Lett.* **2007**, *17*, 2254–2259.

(111) Govindpani, K.; Calvo-Flores Guzmán, B.; Vinnakota, C.; Waldvogel, H. J.; Faull, R. L.; Kwakowsky, A. Towards a better understanding of GABAergic remodeling in Alzheimer's disease. *Mol. Sci.* **2017**, *18*, 1813−1853.

(112) Calvo-Flores Guzmán, B.; Vinnakota, C.; Govindpani, K.; Waldvogel, H. J.; Faull, R. L. M.; Kwakowsky, A. The GABAergic system as a therapeutic target for Alzheimer's disease. *J. Neurochem.* **2018**, *146*, 649−669.

(113) Roy, U.; Stute, L.; Höfling, C.; Hartlage-Rübsamen, M.; Matysik, J.; Roβner, S.; Alia, A. Sex- and age-specific modulation of brain GABA levels in a mouse model of Alzheimer's disease. *Neurobiol. Aging* **2018**, *62*, 168−179.

(114) Kaur, S.; DasGupta, G.; Singh, S. Altered neurochemistry in Alzheimer's disease: targeting neurotransmitter receptor mechanisms and therapeutic strategy. *Neurophysiology* **2019**, *51*, 293−309.

(115) Robertson, H. A.; Baker, G. B.; Coutts, R. T.; Benderly, A.; Locock, R. A.; Martin, I. L. Interactions of β-carbolines with the benzodiazepine receptor: structure-activity relationships. *Eur. J. Pharm.* **1981**, *76*, 281–284.

(116) Rommelspacher, H.; Nanz, C.; Borbe, H. O.; Fehske, K. J.; Müller, W. E.; Wollert, U. 1-Methyl-*β*-carboline (harmane), a potent endogenous inhibitor of benzodiazepine receptor binding. *Naunyn-Schmiedeberg's Arch. Pharmacol.* **1980**, *314*, 97–100.

(117) Lawson, J. A.; Uyeno, E. T.; Nienow, J.; Loew, G. H.; Toll, L. Structure-activity studies of β-carboline analogs. *Life Sci.* **1984**, *34*, 2007–2013.

(118) Allen, M. S.; Hagen, T. J.; Trudell, M. L.; Codding, P. W.; Skolnick, P.; Cook, J. M. Synthesis of novel 3-substituted *β*-carbolines as benzodiazepine receptor ligands: probing the benzodiazepine receptor pharmacophore. *J. Med. Chem.* **1988**, *31*, 1854–1861.

(119) Allen, M. S.; Tan, Y.-C.; Trudell, M. L.; Narayanan, K.; Schindler, L. R.; Martin, M. J.; Schultz, C.; Hagen, T. J.; Koehler, K. F.; Codding, P. W.; Skolnick, P.; Cook, J. M. Synthetic and computer-assisted analyses of the pharmacophore for the benzodiazepine receptor inverse agonist site. *J. Med. Chem.* **1990**, *33*, 2343–2357.

(120) Allen, M. S.; LaLoggia, A. J.; Dorn, L. J.; Martin, M .J.; Costantino, G.; Hagen, T. J.; Koehler, K. F.; Skolnick, P.; Cook, J. M. Predictive binding of β-carboline inverse agonists and antagonists via the CoMFA/GOLPE approach. *J. Med. Chem.* **1992**, *35*, 4001–4010.

(121) Guzman, F.; Cain, M.; Larscheid, P.; Hagen, T.; Cook, J. M.; Schweri, M.; Skolnick, P.; Paul, S. M. Biomimetic approach to potential benzodiazepine receptor agonists and antagonists. *J. Med. Chem.* **1984**, *27*, 564–570.

(122) Braestrup, C.; Nielsen, M.; Olsen C. E. Urinary and brain *β*-carboline-3-carboxylates as potent inhibitors of brain benzodiazepine receptors. *Proc. Natl. Acad. Sci. USA* **1980**, *77*, 2288–2292.

(123) Dorey, G.; Poissonnet, G.; Potier, M.-C.; de Carvalho, L. P.; Venault, P.; Chapouthier, G.; Rossier, J.; Potier, P.; Dodd, R. H. Synthesis and benzodiazepine receptor affinities of rigid analogues of 3-carboxy-*β*-carbolines: demonstration that the benzodiazepine receptor recognizes preferentially the s-cis conformation of the 3-carboxy group. *J. Med. Chem.* **1989**, *32*, 1799–1804.

(124) Cain, M.; Weber; R. W.; Guzman, F.; Cook, J. M.; Barker, S. A.; Rice, K. C.; Crawley, J. N.; Paul, S. M.; Skolnick, P. β-Carbolines: synthesis and neurochemical and pharmacological actions on brain benzodiazepine receptors. *J. Med. Chem.* **1982**, *25*, 1081–1091.

(125) Dodd, R. H.; Ouannès, C.; Prado de Carvalho, L.; Valin, A.; Venault, P.; Chapouthier, G.; Rossier, J.; Potier, P. 3-Amino-*β*-carboline derivatives and the benzodiazepine receptor. Synthesis of a selective antagonist of the sedative action of diazepam. *J. Med. Chem.* **1985**, *28*, 824–828.

(126) Hagen, T. J.; Skolnick, P.; Cook, J. M. Synthesis of 6-substituted *β*-carbolines that behave as benzodiazepine receptor antagonists or inverse agonists. *J. Med. Chem.* **1987**, *30*, 750–753.

(127) Hollinshead, S. P.; Trudell, M. L.; Skolnick, P.; Cook, J. M. Structural requirements for agonist actions at the benzodiazepine receptor: studies with analogues of 6-(benzyloxy)-4-(methoxymethyl)-*β*-carboline-3-carboxylic acid ethyl ester. *J. Med. Chem.* **1990**, *33*, 1062–1069.

(128) Cox, E. D.; Diaz-Arauzo, H.; Huang, Q.; Reddy, M. S.; Ma, C.; Harris, B.; McKernan, R.; Skolnick, P.; Cook, J. M. Synthesis and evaluation of analogues of the partial agonist 6-(propyloxy)-4-(methoxymethyl)-*β*-carboline-3-carboxylic acid ethyl ester (6-PBC) and the full agonist 6-(benzyloxy)-4-(methoxymethyl)-*β*-carboline-3-carboxylic acid ethyl ester (Zk 93423) at wild type and recombinant $GABA_A$ receptors. *J. Med. Chem.* **1998**, *41*, 2537–2552.

(129) Olesen, P. H.; Seidelmann, D.; Hansen, J. B. Oxazolo[4,5-*g*]-β-carbolines and pyrazino[2,3-*g*]-β-carbolines. Synthesis of modulators of the $GABA_A$/chloride channel complex. *Heterocycles* **1998**, *48*, 31–40.

(130) Petersen, E. N.; Jensen, L. H.; Honoré, T.; Braestrup, C.; Kehr, W.; Stephens, D. N.; Wachtel, H.; Seidelman, D.; Schmiechen, R. ZK 91296, a partial agonist at benzodiazepine receptors. *Psychopharmacology* **1984**, *83*, 240–248.

(131) Jensen, L. H.; Petersen, E. N.; Braestrup, C.; Honoré, T.; Kehr, W.; Stephens, D. N.; Schneider, H.; Seidelmann, D.; Schmiechen, R. Evaluation of the *β*-carboline ZK 93 426 as a benzodiazepine receptor antagonist. *Psychopharmacology* **1984**, *83*, 249–256.

(132) Wang, Q.; Han, Y.; Xue, H. Ligands of the $GABA_A$ receptor benzodiazepine binding site. *CNS Drug Rev.* **1999**, *5*, 125–144.

(133) Gardner, C. R. Functional in vivo correlates of the benzodiazepine agonist–inverse agonist continuum. *Prog. Neurobiol.* **1988**, *31*, 425–476.

(134) Gardner, C. R.; Tully, W. R.; Hedgecock, C. J. R. The rapidly expanding range of neuronal benzodiazepine receptor ligands. *Prog. Neurobiol.* **1993**, *40*, 1–61.

(135) Huang, Q.; He, X.; Ma, C.; Liu, R.; Yu, S.; Dayer, C. A.; Wenger, G. R.; McKernan, R.; Cook, J. M. Pharmacophore/receptor models for $GABA_A$/BzR subtypes (α1*β*3*γ*2, α5*β*3*γ*2, and α6*β*3*γ*2) via a comprehensive ligand-mapping approach. *J. Med. Chem.* **2000**, *43*, 71–95.

(136) Smith, A. J.; Alder, L.; Silk, J.; Adkins, J.; Fletcher, A. E.; Scales, T.; Kerby, J.; Marshall, G.; Wafford, K. A.; McKernan, R. M.; Atack, J. R. Effect of a subunit on allosteric modulation of ion channel function in stably expressed human recombinant γ-aminobutyric $acid_A$ receptors determined using ^{36}Cl ion flux. *Mol. Pharmacol.* **2001**, *59*, 1108–1118.

(137) Kelly, M. D.; Smith, A.; Banks, G.; Wingrove, P.; Whiting, P. W.; Atack, J.; Seabrook, G. R.; Maubach, K. A. Role of the histidine residue at position 105 in the human α5 containing $GABA_A$ receptor on the affinity and efficacy of benzodiazepine site ligands. *Br. J. Pharmacol.* **2002**, *135*, 248–256.

(138) Yin, W.; Majumder, S.; Clayton, T.; Petrou, S.; VanLinn, M. L.; Namjoshi, O. A.; Ma, C.; Cromer, B. A.; Roth, B. L.; Platt, D. M.; Cook, J. M. Design, synthesis, and subtype selectivity of 3,6-disubstituted β-carbolines at Bz/GABA(A)ergic receptors. SAR and studies

directed toward agents for treatment of alcohol abuse. *Bioorg. Med. Chem.* **2010**, *18*, 7548–7564.

(139) Yin, W.; Sarma, P. V. V. S.; Ma, J.; Han, D.; Chen, J. L.; Cook, J. M. Synthesis of bivalent ligands of β-carboline-3-carboxylates via a palladium-catalyzed homocoupling process. *Tetrahedron Lett.* **2005**, *46*, 6363–6368.

(140) Griebel, G.; Perrault, G.; Simiand, J.; Cohen, C.; Granger, P.; Depoortere, H.; Françon, D.; Avenet, P.; Schoemaker, H.; Evanno, Y.; Sevrin, M.; George, P.; Scatton, B. SL651498, a $GABA_A$ receptor agonist with subtype-selective efficacy, as a potential treatment for generalized anxiety disorder and muscle spasms. *CNS Drug Rev.* **2003**, *9*, 3–20.

(141) Trudell, M. L.; Basile, A. S.; Shannon, H. E.; Skolnick, P.; Cook, J. M. Synthesis of 7,12-dihydropyrido[3,4-*b*:5,4-*b'*]diindoles. A novel class of rigid, planar benzodiazepine receptor ligands. *J. Med. Chem.* **1987**, *30*, 456–458.

(142) Geldenhuys, W. J.; Van der Schyf C. J. Role of serotonin in Alzheimer's disease: a new therapeutic target? *CNS Drugs* **2011**, *25*, 765–781.

(143) Švob Štrac, D.; Pivac, N.; Mück-Šeler, D.; The serotonergic system and cognitive function. *Transl. Neurosci.* **2016**, *7*, 35−49.

(144) Grella, B.; Dukat, M.; Young, R.; Teitler, M.; Herrick-Davis, K.; Gauthier, C. B.; Glennon, R. A. Investigation of hallucinogenic and related β-carbolines. *Drug Alcohol Depend.* **1998**, *50*, 99–107.

(145) Glennon, R. A.; Dukat, M.; Grella, B.; Hong, S.-S.; Costantino, L.; Teitler, M.; Smith, C.; Egan, C.; Davis, K.; Mattson, M. V. Binding of β-carbolines and related agents at serotonin (5-HT_2 and 5-HT_{1A}), dopamine (D_2) and benzodiazepine receptors. *Drug Alcohol Depend.* **2000**, *60*, 121–132.

(146) Grella, B.; Teitler, M.; Smith, C.; Herrick-Davis, K.; Glennon, R. A. Binding of β-carbolines at 5-HT_2 serotonin receptors. *Bioorg. Med. Chem. Lett.* **2003**, *13*, 4421–4425.

(147) de la Fuente Revenga, M.; Pérez, C.; Morales-Garcia, J. A.; Alonso-Gil, S.; Pérez-Castillo, A.; Caignard, D.-H.; Yañez, M.; Gamo, A. M.; Rodriguez-Franco, M. I. Neurogenic potential assessment and pharmacological characterization of 6-methoxy-1,2,3,4-tetrahydro-*β*-carboline (pinoline) and melatonin−pinoline hybrids. *ACS Chem. Neurosci.* **2015**, *6*, 800–810.

(148) Audia, J. E.; Evrard, D. A.; Murdoch, G. R.; Droste, J. J.; Nissen, J. S.; Schenck, K. W.; Fludzinski, P.; Lucaites, V. L.; Nelson, D. L.; Cohen, M. L. Potent, selective tetrahydro-*β*-carboline antagonists of the serotonin 2B ($5HT_{2B}$) contractile receptor in the rat stomach fundus. *J. Med. Chem.* **1996**, *39*, 2773–2780.

(149) Millan, M. J.; Newman-Tancredi, A.; Audinot, V.; Cussac, D.; Lejeune, F.; Nicolas, J.-P.; Coge, F.; Galizzi, J.-P.; Boutin, J. A.; Rivet, J.-M.; Dekeyne, A.; Gobert, A. Agonist and antagonist actions of yohimbine as compared to fluparoxan at α_2-adrenergic receptors (AR)s, serotonin $(5\text{-HT})_{1A}$, 5-HT_{1B}, 5-HT_{1D} and dopamine D_2 and D_3 receptors. Significance for the modulation of frontocortical monoaminergic transmission and depressive states. *Synapse* **2000**, *35*, 79–95.

(150) Boksa, J.; Mokrosz, M. J.; Charakchieva-Minol, S.; Tatarczynska, E.; Klodzinska, A.; Wesolowska, A.; Misztal, S. 2-H- And 2-acyl-9-{ω-[4-(2-methoxyphenyl)piperazinyl]-alkyl}-1,2,3,4-tetrahydro-β-carbolines as ligands of 5-HT_{1A} and 5-HT_{2A} receptors. *Pol. J. Pharmacol.* **2001**, *53*, 501–508.

(151) Foley, C. A.; Al-Issa, Y. A.; Hiller, K. P.; Mulcahy, S. P. Synthesis and structure-activity relationships of 1-aryl-β-carbolines as affinity probes for the 5-hydroxytryptamine receptor. *ACS Omega* **2019**, *4*, 9807–9812.

(152) Yang, S.-S.; Zhang, R.; Wang, G.; Zhang, Y.-F. The development prospection of HDAC inhibitors as a potential therapeutic direction in Alzheimer's disease. *Transl. Neurodegener.* **2017**, *6*, 19.

(153) Xu, K.; Dai, X.-L.; Huang, H.-C.; Jiang, Z.-F. Targeting HDACs: a promising therapy for Alzheimer's Disease. *Oxid. Med. Cell. Longev.* **2011**, 143269.

(154) Ling, Y.; Xu, C.; Luo, L.; Cao, J.; Feng, J.; Xue, Y.; Zhu, Q.; Ju, C.; Li, F.; Zhang, Y.; Zhang, Y.; Ling, X. Novel *β*-carboline/hydroxamic acid hybrids targeting both histone deacetylase and DNA display high anticancer activity via regulation of the p53 signaling pathway. *J. Med. Chem.* **2015**, *58*, 9214–9227.

(155) Ling, Y.; Guo, J.; Yang, Q.; Zhu, P.; Miao, J.; Gao, W.; Peng, Y.; Yang, J.; Xu, K.; Xiong, B.; Liu, G.; Tao, J.; Luo, L.; Zhu, Q.; Zhang, Y. Development of novel β-carboline-based hydroxamate derivatives as HDAC inhibitors with antiproliferative and antimetastatic activities in human cancer cells. *Eur. J. Med. Chem.* **2018**, *144*, 398–409.

(156) Liu, J.; Wang, T.; Wang, X.; Luo, L.; Guo, J.; Peng, Y.; Xu, Q.; Miao, J.; Zhang, Y.; Ling, Y. Development of novel β-carboline-based hydroxamate derivatives as HDAC inhibitors with DNA damage and apoptosis inducing abilities. *Med. Chem. Commun.* **2017**, *8*, 1213–1219.

(157) Ling, Y.; Feng, J.; Luo, L.; Guo, J.; Peng, Y.; Wang, T.; Ge, X.; Xu, Q.; Wang, X.; Dai, H.; Zhang, Y. Design and synthesis of C3-substituted β-carboline-based histone deacetylase inhibitors with potent antitumor activities. *ChemMedChem* **2017**, *12*, 646–651.

(158) Butler, K. V.; Kalin, J.; Brochier, C.; Vistoli, G.; Langley, B.; Kozikowski, A. P. Rational design and Simple chemistry yield a superior, neuroprotective HDAC6 inhibitor, tubastatin A. *J. Am. Chem. Soc.* **2010**, *132*, 10842–10846.

(159) Kalin, J. H.; Butler, K. V.; Akimova, T.; Hancock, W. W.; Kozikowski, A. P. Second-generation histone deacetylase 6 inhibitors enhance the immunosuppressive effects of Foxp3+ T-regulatory cells. *J. Med. Chem.* **2012**, *55*, 639–651.

(160) Leonhardt, M.; Sellmer, A.; Krämer, O. H.; Dove, S.; Elz, S.; Kraus, B.; Beyer, M.; Mahboobi, S. Design and biological evaluation of tetrahydro-*β*-carboline derivatives as highly potent histone deacetylase 6 (HDAC6) inhibitors. *Eur. J. Med. Chem.* **2018**, *152*, 329–357.

(161) Grünstein, E.; Sellmer, A.; Mahboobi, S. Enantioselective synthesis and biological investigation of tetrahydro-β-carboline-based HDAC6 inhibitors with improved solubility. *Arch. Pharm. Chem. Life Sci.* **2019**, *352*, e1900026.

(162) He, S.; Dong, G.; Wang, Z.; Chen, W.; Huang, Y.; Li, Z.; Jiang, Y.; Liu, N.; Yao, J.; Miao, Z.; Zhang, W.; Sheng, C. Discovery of novel multiacting topoisomerase I/II and histone deacetylase inhibitors. *ACS Med. Chem. Lett.* **2015**, *6*, 239–243.

(163) Mehndiratta, S.; Hsieh, Y.-L.; Liu, Y.-M.; Wang, A. W.; Lee, H.-Y.; Liang, L.-Y.; Kumar, S.; Teng, C.-M.; Yang, C.-R.; Liou, J.-P. Indole-3-ethylsulfamoylphenylacrylamides: potent histone deacetylase inhibitors with anti-inflammatory activity. *Eur. J. Med. Chem.* **2014**, *85*, 468–479.

(164) Gong, C.-X.; Liu, F.; Iqbal, K.; Multifactorial hypothesis and multi-targets for Alzheimer's disease. *J. Alzheimers Dis.* **2018**, *64*, 107−117.

(165) Panek, D.; Wichur, T.; Godyń, Pasieka, A.; Malawska, B. Advances toward multifunctional cholinesterase and β-amyloid aggregation inhibitors. *Future Med. Chem.* **2017**, *9*, 1835–1854.

(166) He, Y.; Yao, P.-F.; Chen, S.; Huang, Z.; Huang, S.-L.; Tan, J.-T.; Li, D.; Gu, L.-Q.; Huang, Z.-S. Synthesis and evaluation of 7,8-dehydrorutaecarpine derivatives as potential

multifunctional agents for the treatment of Alzheimer's disease. *Eur. J. Med. Chem.* **2013**, *63*, 299–312.

(167) Wu, M.; Ma, J.; Ji, L.; Wang, M.; Han, J.; Li, Z. Design, synthesis, and biological evaluation of rutacecarpine derivatives as multitarget-directed ligands for the treatment of Alzheimer's disease. *Eur. J. Med. Chem.* **2019**, *177*, 198–211.

(168) Lan, J.-S.; Xie, S.-S.; Li, S.-Y.; Pan, L.-F.; Wang, X.-B.; Kong, L.-Y. Design, synthesis and evaluation of novel tacrine-(β-carboline) hybrids as multifunctional agents for the treatment of Alzheimer's disease. *Bioorg. Med. Chem.* **2014**, *22*, 6089–6104.

(169) Zhao, Y.; Ye, F.; Xu, J.; Liao, Q.; Chen, L.; Zhang, W.; Sun, H.; Liu, W.; Feng, F.; Qu, W. Design, synthesis and evaluation of novel bivalent β-carboline derivatives as multifunctional agents for the treatment of Alzheimer's disease. *Bioorg. Med. Chem.* **2018**, *26*, 3812–3824.

(170) Liao, Q.; Li, Q.; Zhao, Y.; Jiang, P.; Yan, Y.; Sun, H.; Liu, W.; Feng, F.; Qu, W. Design, synthesis and biological evaluation of novel carboline-cinnamic acid hybrids as multifunctional agents for treatment of Alzheimer's disease. *Bioorg. Chem.* **2020**, *99*, 103844.

(171) Jiaranaikulwanitch, J.; Govitrapong, P.; Fokin, V. V.; Vajragupta, O. From BACE1 inhibitor to multifunctionality tryptoline and tryptamine triazole derivatives for Alzheimer's disease. *Molecules* **2012**, *17*, 8312–8333.

(172) Jiaranaikulwanitch, J.; Tadtong, S.; Govitrapong, P.; Fokin, V. V.; Vajragupta, O. Neuritogenic activity of bi-functional bis-tryptoline triazole. *Bioorg. Med. Chem. Lett.* **2017**, *25*, 1195–1201.

(173) Prickaerts, J.; Sik, A.; van der Staay, F. J.; de Vente, J.; Blokland, A. Dissociable effects of acetylcholinesterase inhibitors and phosphodiesterase type 5 inhibitors on object

recognition memory: acquisition versus consolidation. *Psychopharmacology* **2005**, *177*, 381–390.

(174) Mao, F.; Wang, H.; Ni, W.; Zheng, X.; Wang, M.; Bao, K.; Ling, D.; Li, X.; Xu, Y.; Zhang, H.; Li, J. Design, synthesis, and biological evaluation of orally available first-generation dual-target selective inhibitors of acetylcholinesterase (AChE) and phosphodiesterase 5 (PDE5) for the treatment of Alzheimer's disease. *ACS Chem. Neurosci.* **2018**, *9*, 328–345.

(175) Ni, W.; Wang, H.; Li, X.; Zheng, X.; Wang, M.; Zhang, J.; Gong, Q.; Ling, D.; Mao, F.; Zhang, H.; Li, J. Novel tadalafil derivatives ameliorates scopolamine-induced cognitive impairment in mice via inhibition of acetylcholinesterase (AChE) and phosphodiesterase 5 (PDE5). *ACS Chem. Neurosci.* **2018**, *9*, 1625–1636.

(176) Otto, R.; Penzis, R.; Gaube, F.; Adolph, O.; Föhr, K. J.; Warncke, P.; Robaa, D.; Appenroth, D.; Fleck, C.; Enzensperger, C.; Lehmann, J.; Winckler, T. Evaluation of homobivalent carbolines as designed multiple ligands for the treatment of neurodegenerative disorders. *J. Med. Chem.* **2015**, *58*, 6710−6715.

(177) Sanchez-Arias, J. A.; Rabal, O.; Cuadrado-Tejedor, M.; de Miguel, I.; Pérez-Gonzalez, M.; Ugarte, A.; Saez, E.; Espelosin, M.; Ursua, S.; Haizhong, T.; Wei, W.; Musheng, X.; Garcia-Osta, A.; Oyarzabal, J. Impact of scaffold exploration on novel dual-acting histone deacetylases and phosphodiesterase 5 inhibitors for the treatment of Alzheimer's disease. *ACS Chem. Neurosci.* **2017**, *8*, 638–661.

(178) Rabal, O.; Sanchez-Arias, J. A.; Cuadrado-Tejedor, M.; de Miguel, I.; Pérez-Gonzalez, M.; Garcia-Barroso, C.; Ugarte, A.; Estella-Hermoso de Mendoza, A.; Saez, E.; Espelosin, M.; Ursua, S.; Haizhong, T.; Wei, W.; Musheng, X.; Garcia-Osta, A.; Oyarzabal, J. Discovery

of *in vivo* chemical probes for treating Alzheimer's disease: dual phosphodiesterase 5 (PDE5) and class I histone deacetylase selective inhibitors. *ACS Chem. Neurosci*. **2019**, *10*, 1765–1782.

(179) ElHady, A. K.; Shih, S.-P.; Chen, Y.-C.; Liu, Y.-C.; Ahmed, N. S.; Keeton, A. B.; Piazza, G. A.; Engel, M.; Abadi, A. H.; Abdel-Halim, M. Extending the use of tadalafil scaffold: Development of novel selective phosphodiesterase 5 inhibitors and histone deacetylase inhibitors. *Bioorg. Chem.* **2020**, *98*, 103742.

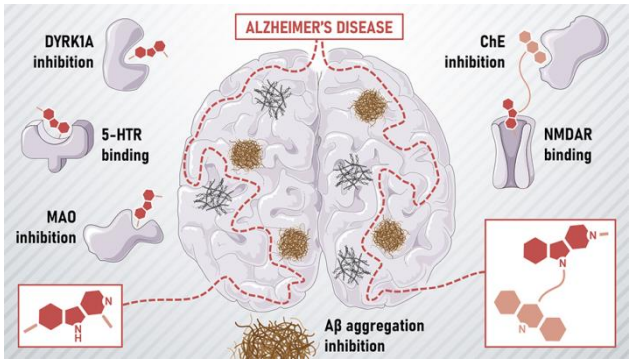

For Table of Contents Only